Journal of Geophysical Research: Solid Earth

Supporting Information for

Whole-mantle tomography of Southeast Asia: New insight into plumes and slabs

Genti Toyokuni[1], Dapeng Zhao[1], and Kenkichi Kurata[1]

[1]Department of Geophysics, Graduate School of Science, Tohoku University, Sendai 980-8578, Japan

Contents of this file

- Figures S1 to S62
- Tables S1 to S3

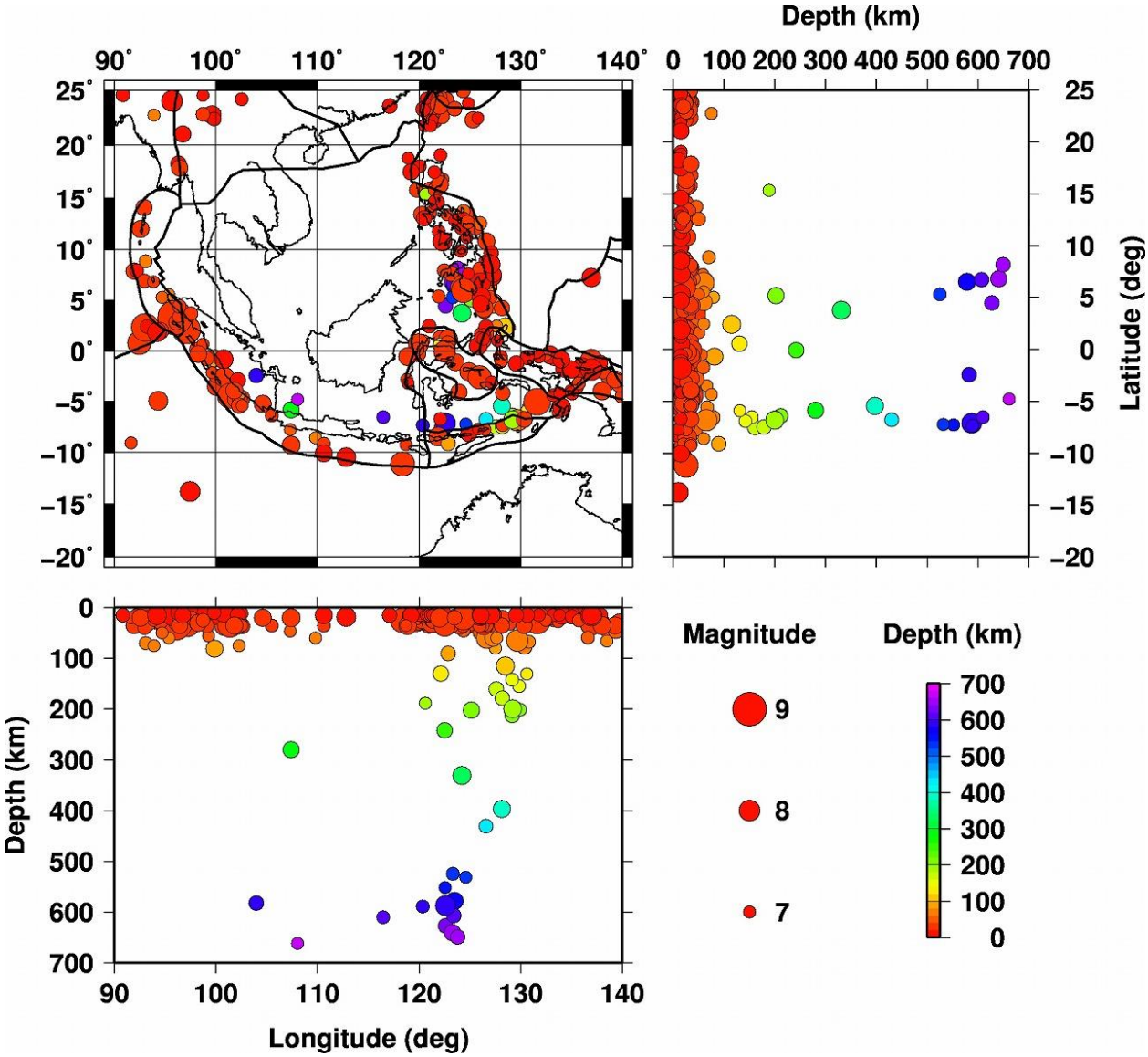

Figure S1. Hypocenter distribution of 287 large earthquakes (M ≥ 7) that occurred from January 1, 1900 to January 5, 2022 (https://earthquake.usgs.gov/). The circle size and color indicate the magnitude and focal depth, respectively, whose scales are shown in the lower right.

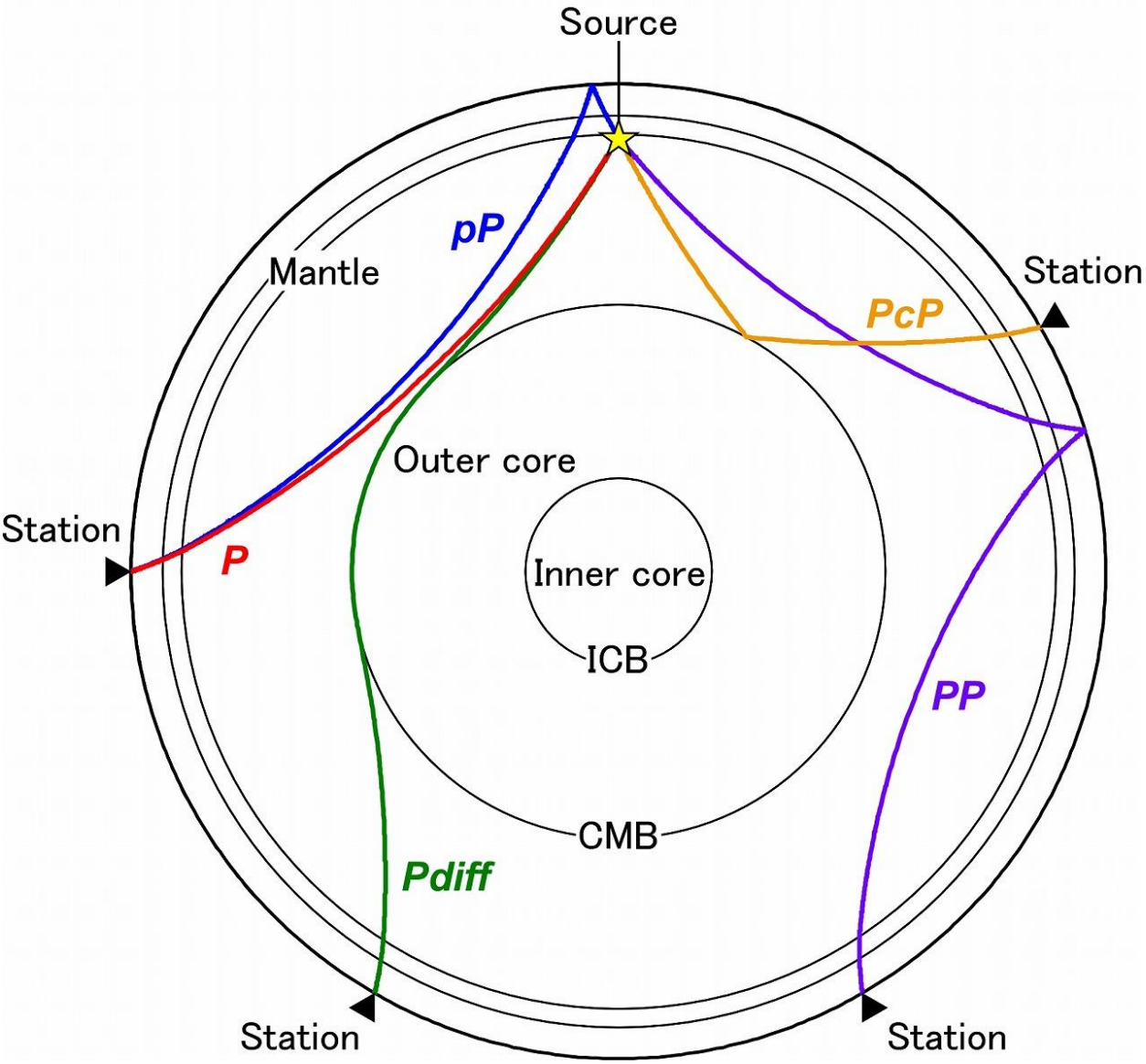

Figure S2. Schematic illustration of ray paths of P, pP, PP, PcP, and Pdiff waves. The star denotes a hypocenter. The reverse triangles denote seismic stations.

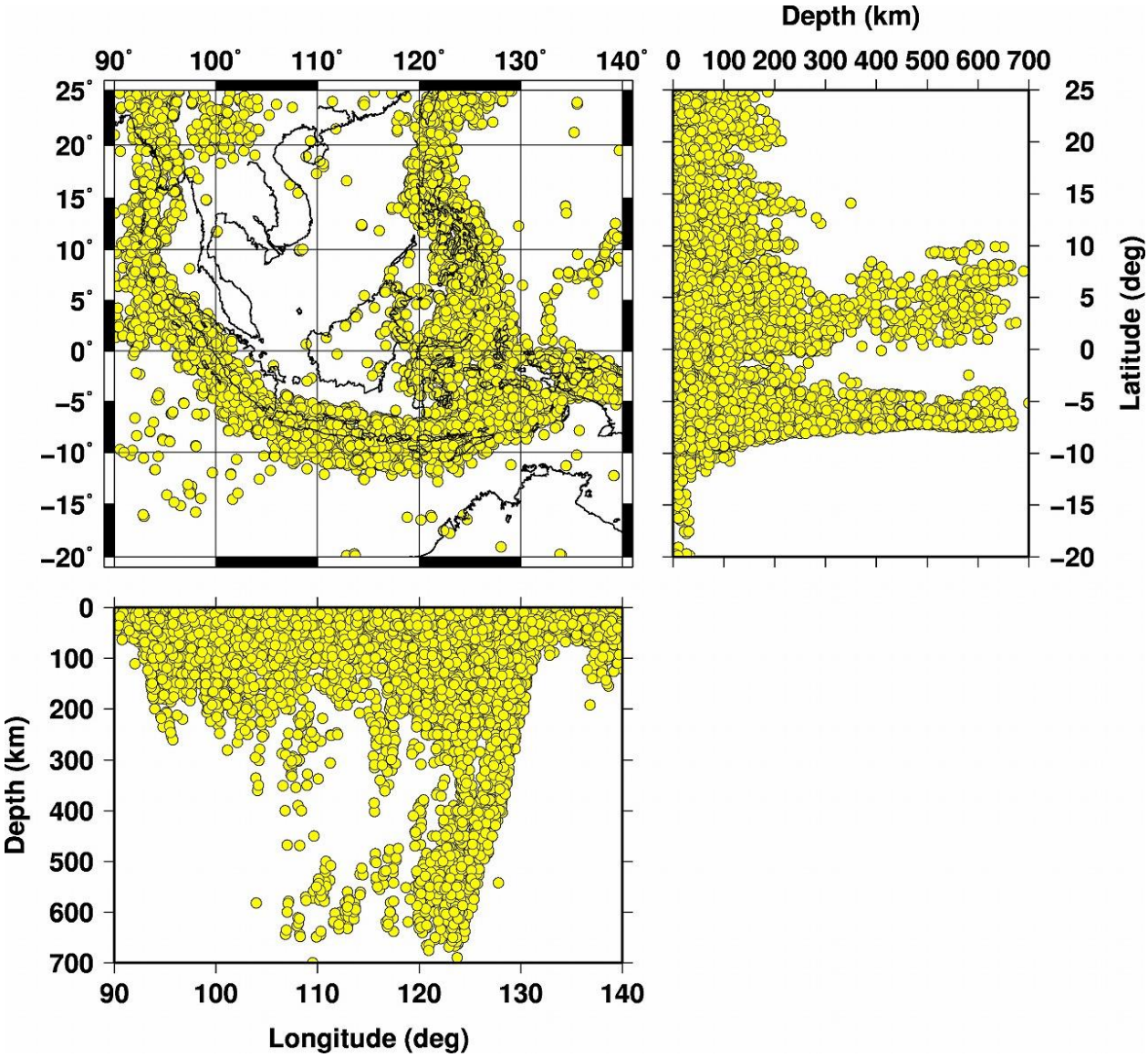

Figure S3. Distribution of 11,344 earthquakes inside the study volume, which are used in the tomographic inversion.

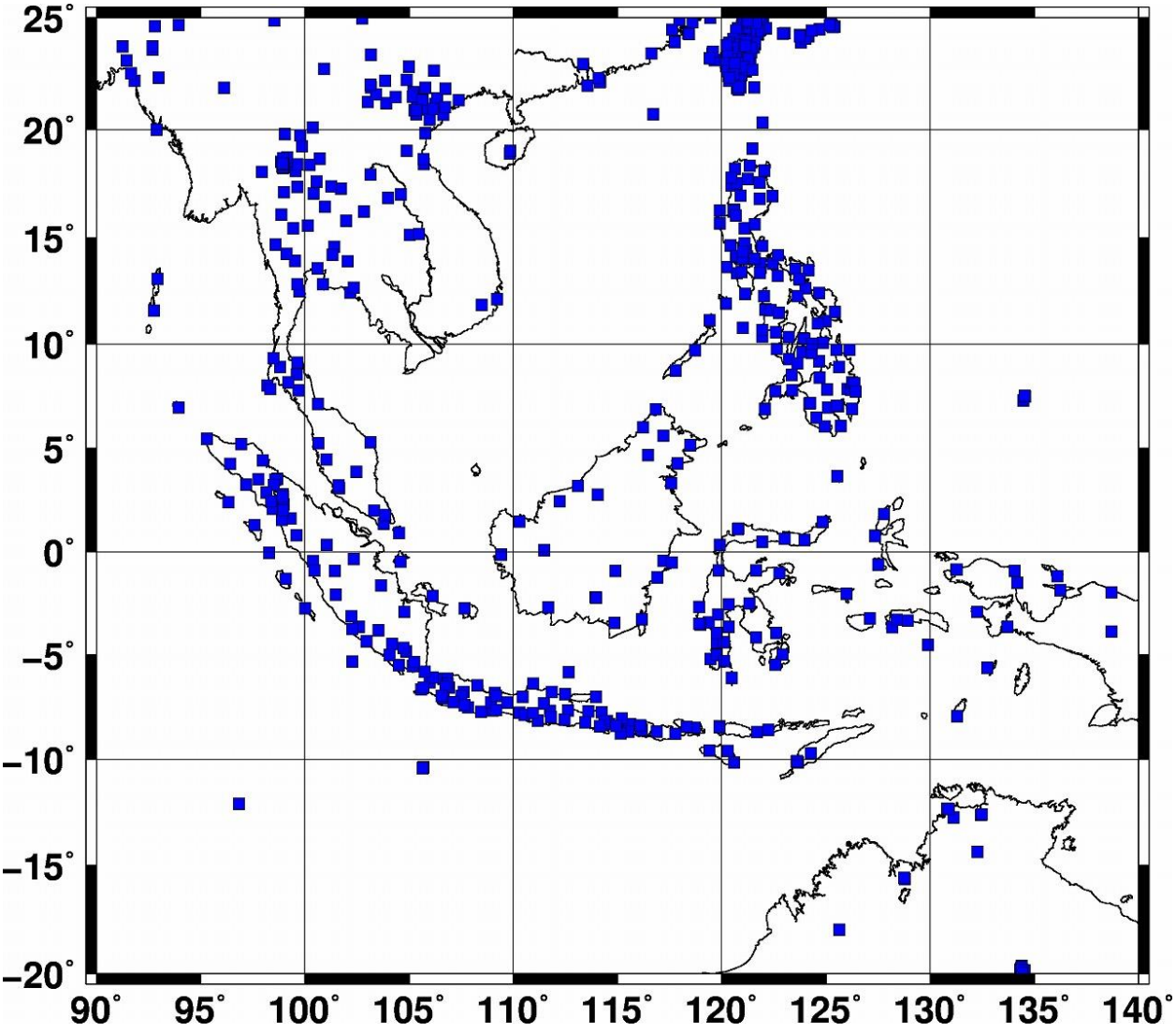

Figure S4. Distribution of 656 seismic stations inside the study region used in the tomographic inversion.

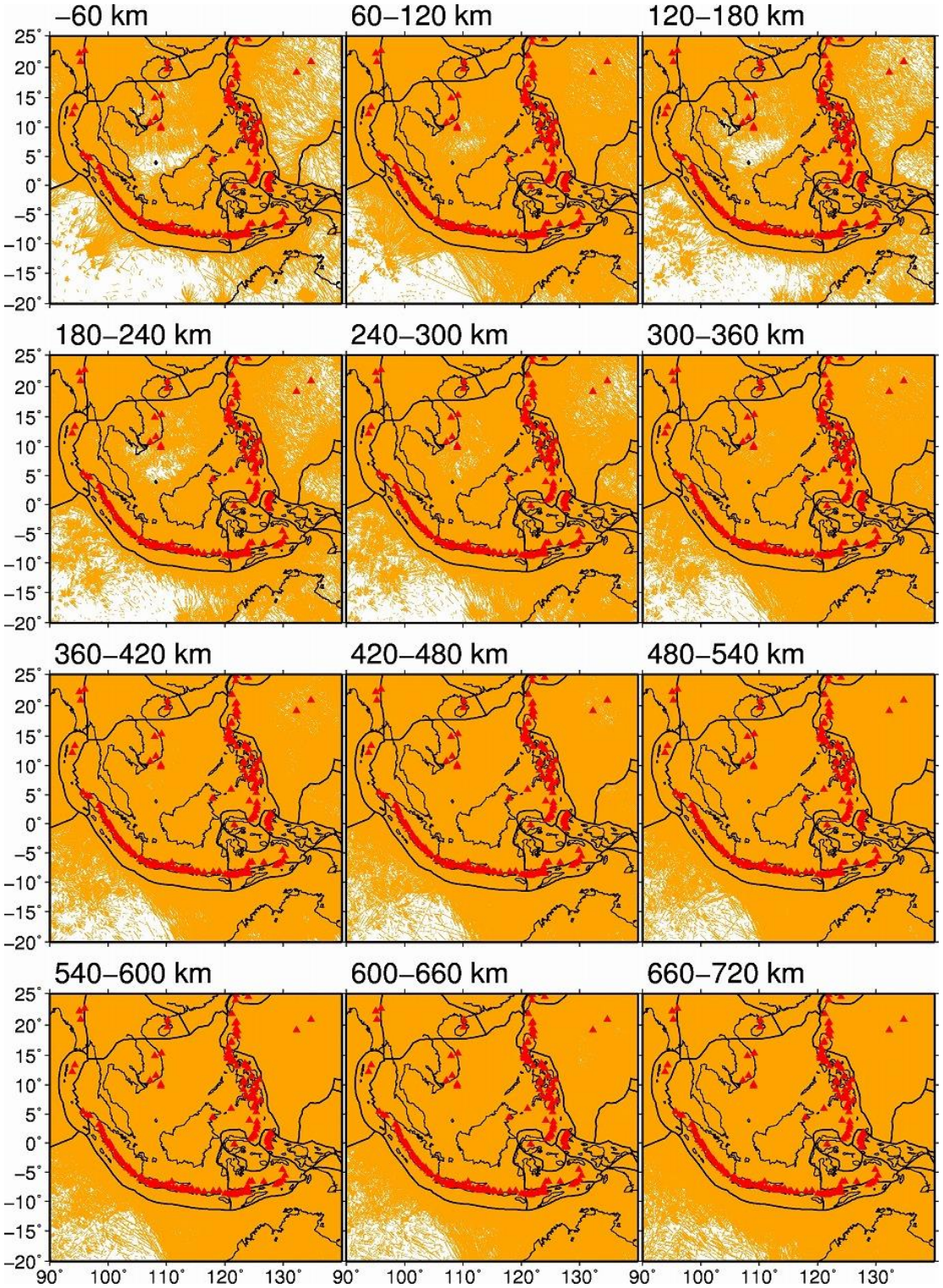

Figure S5. Distribution of seismic rays throughout the study volume. The layer depth range is shown at the upper-left corner of each panel.

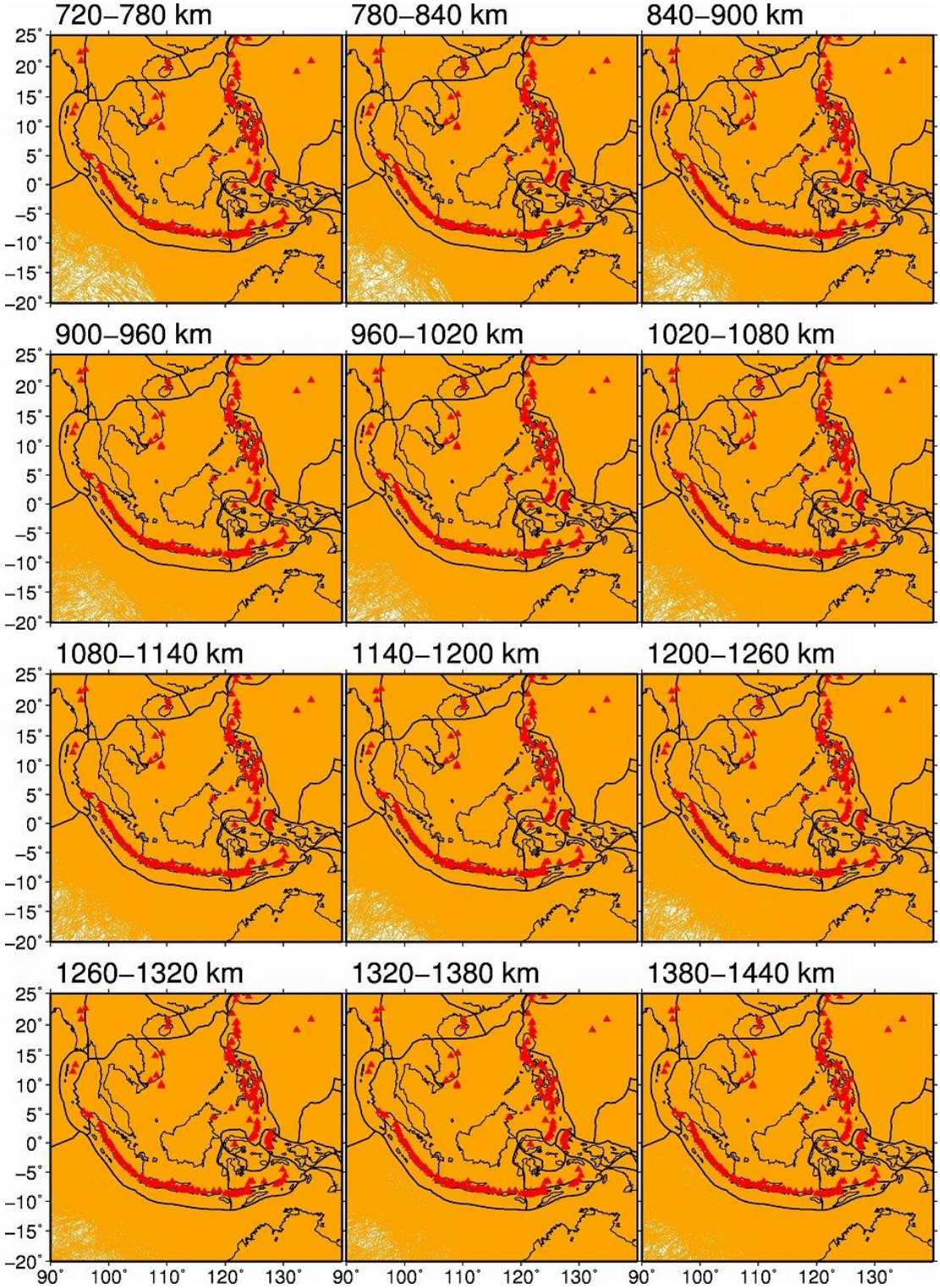

Figure S5. (continued).

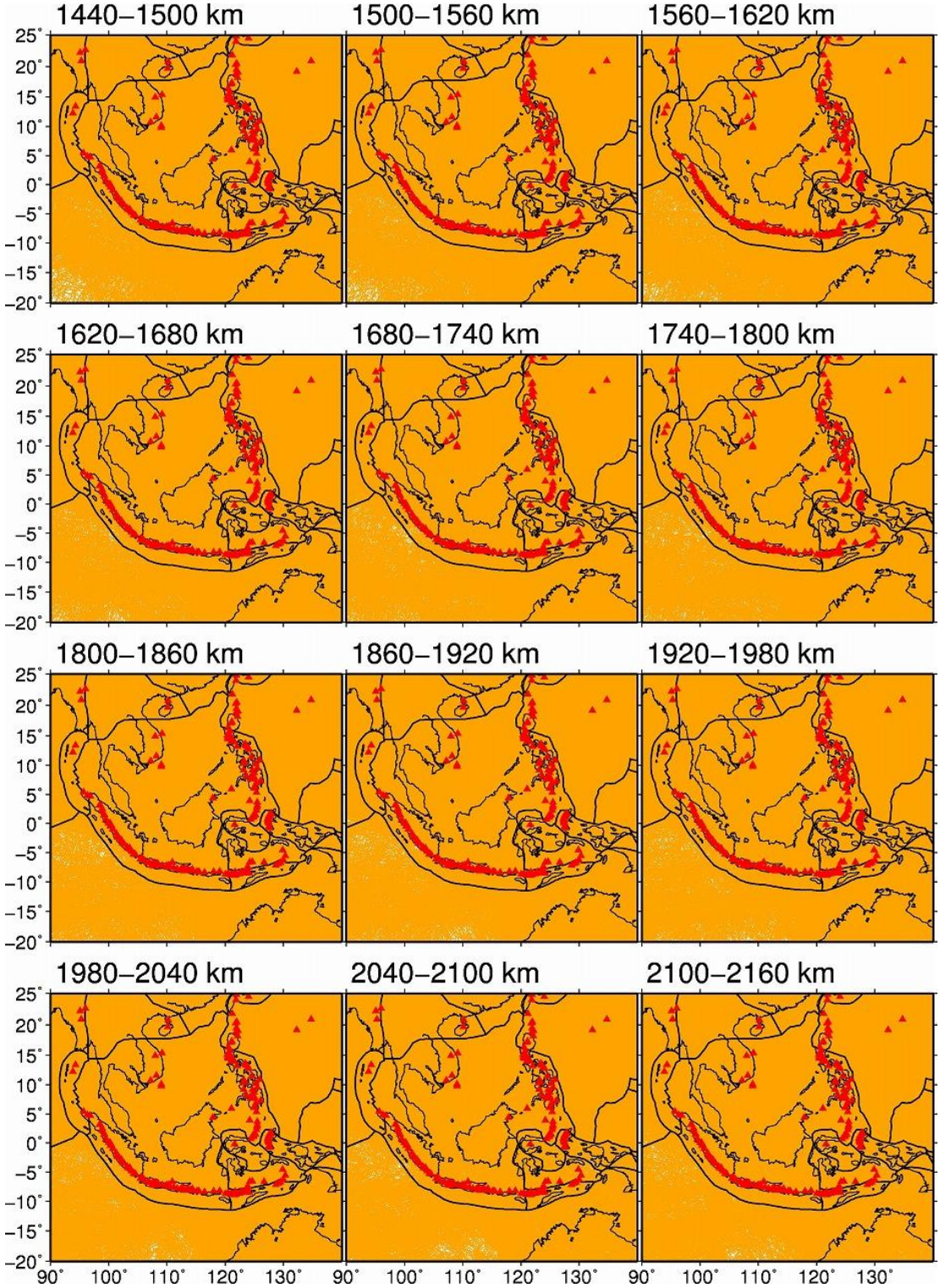

Figure S5. (continued).

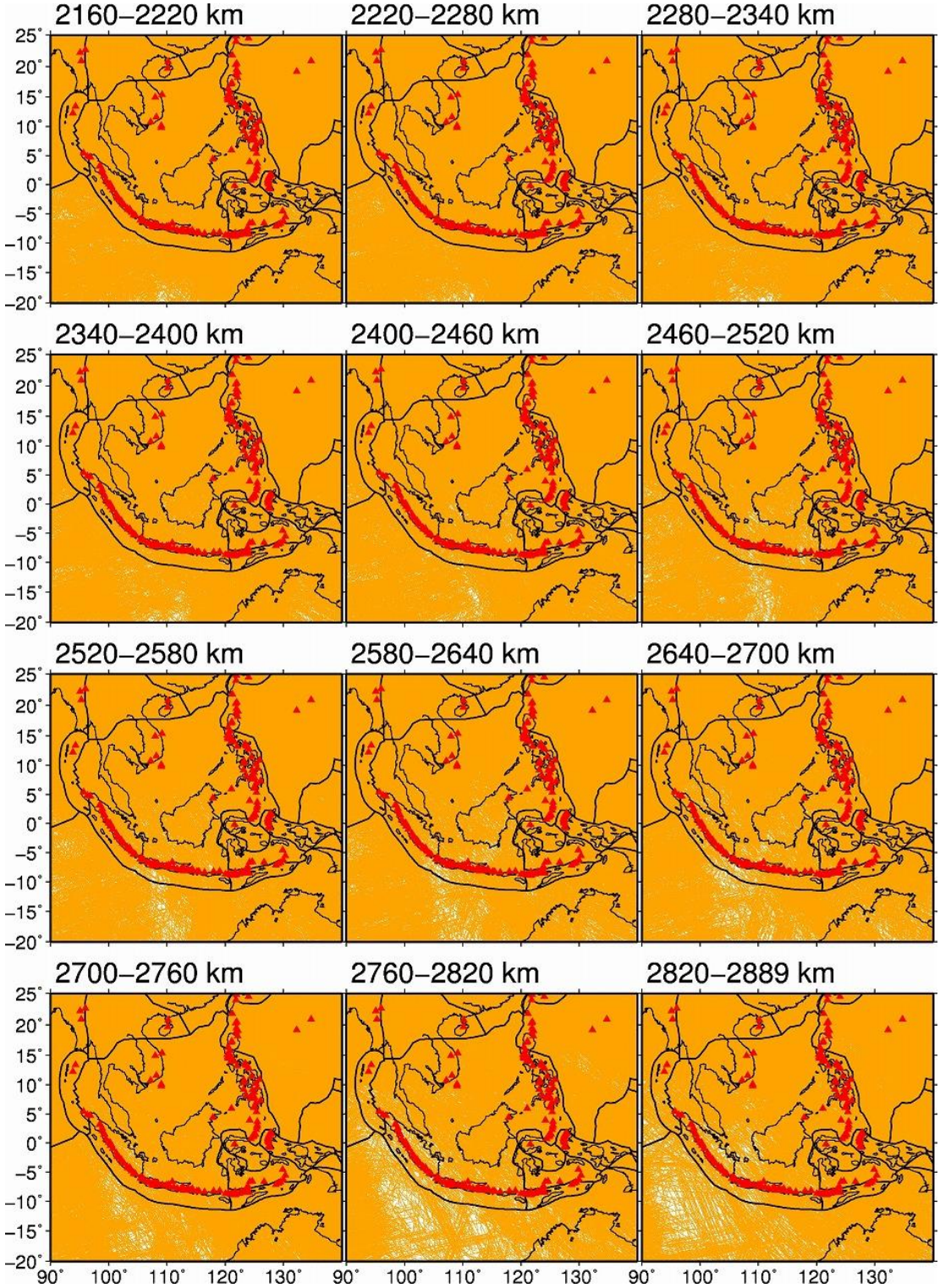

Figure S5. (continued).

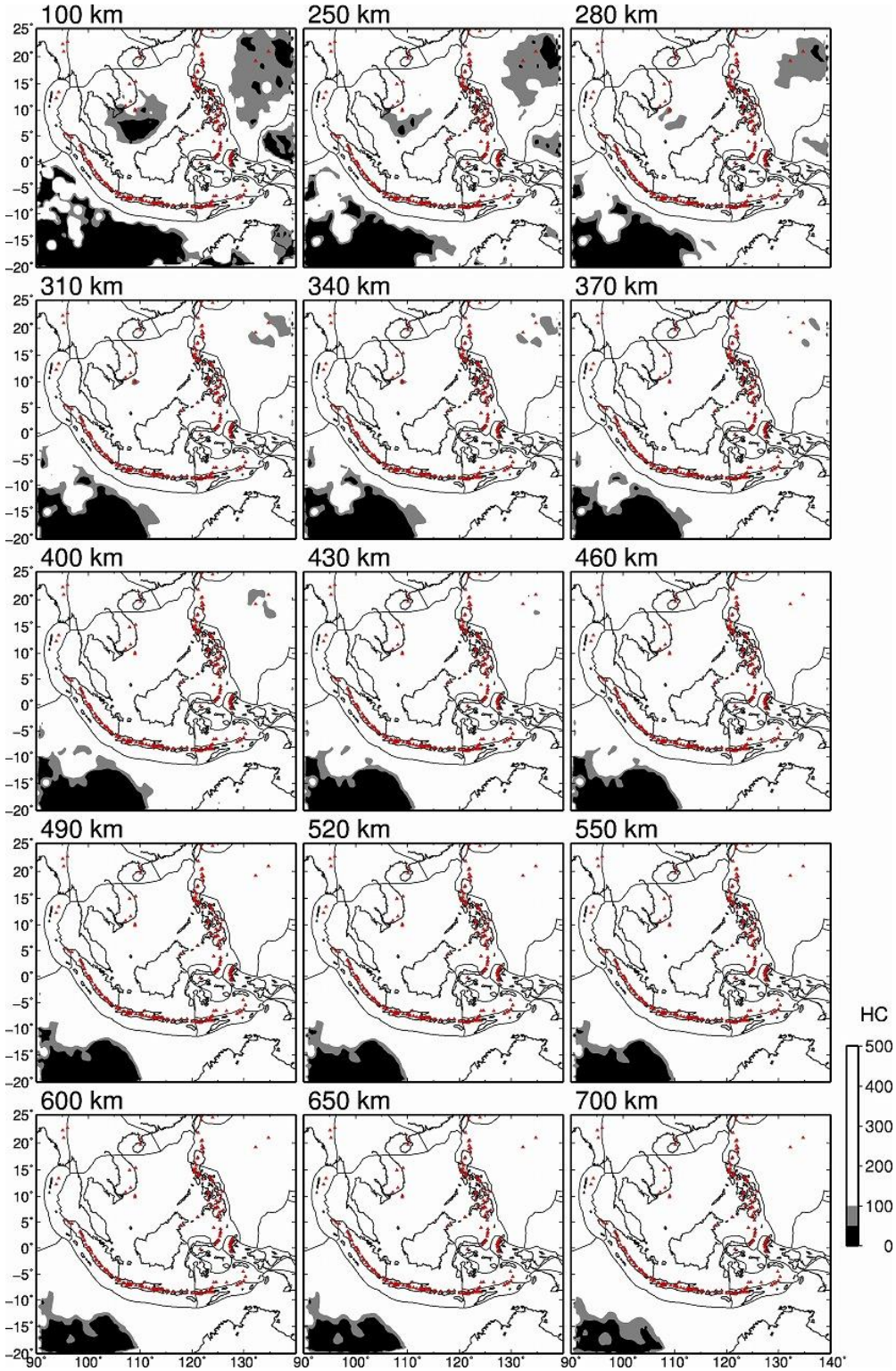
100 km
250 km
280 km
310 km
340 km
370 km
400 km
430 km
460 km
490 km
520 km
550 km
600 km
650 km
700 km
HC
500
400
300
200
100
0

Figure S6.

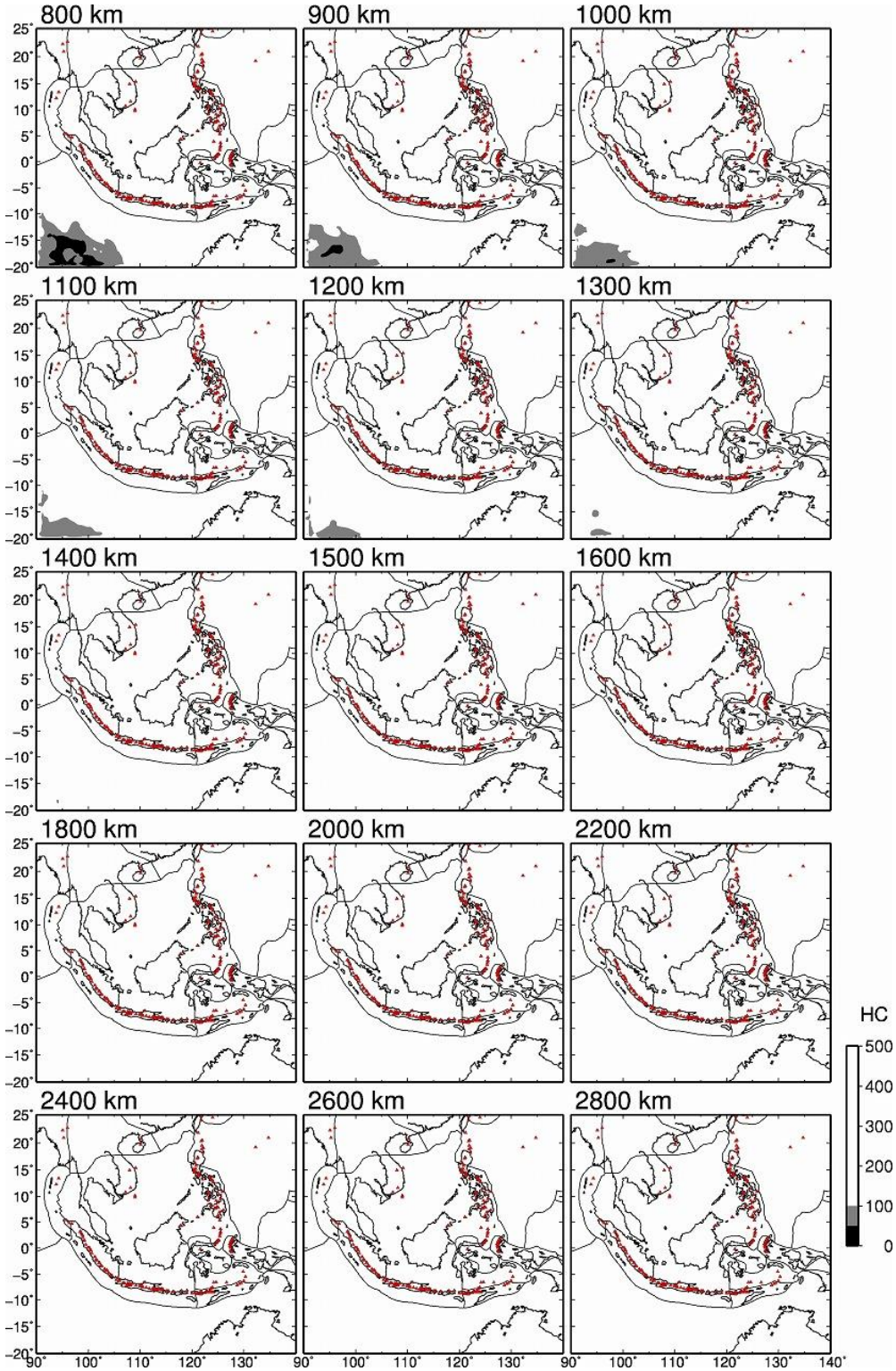

Figure S6. (continued).

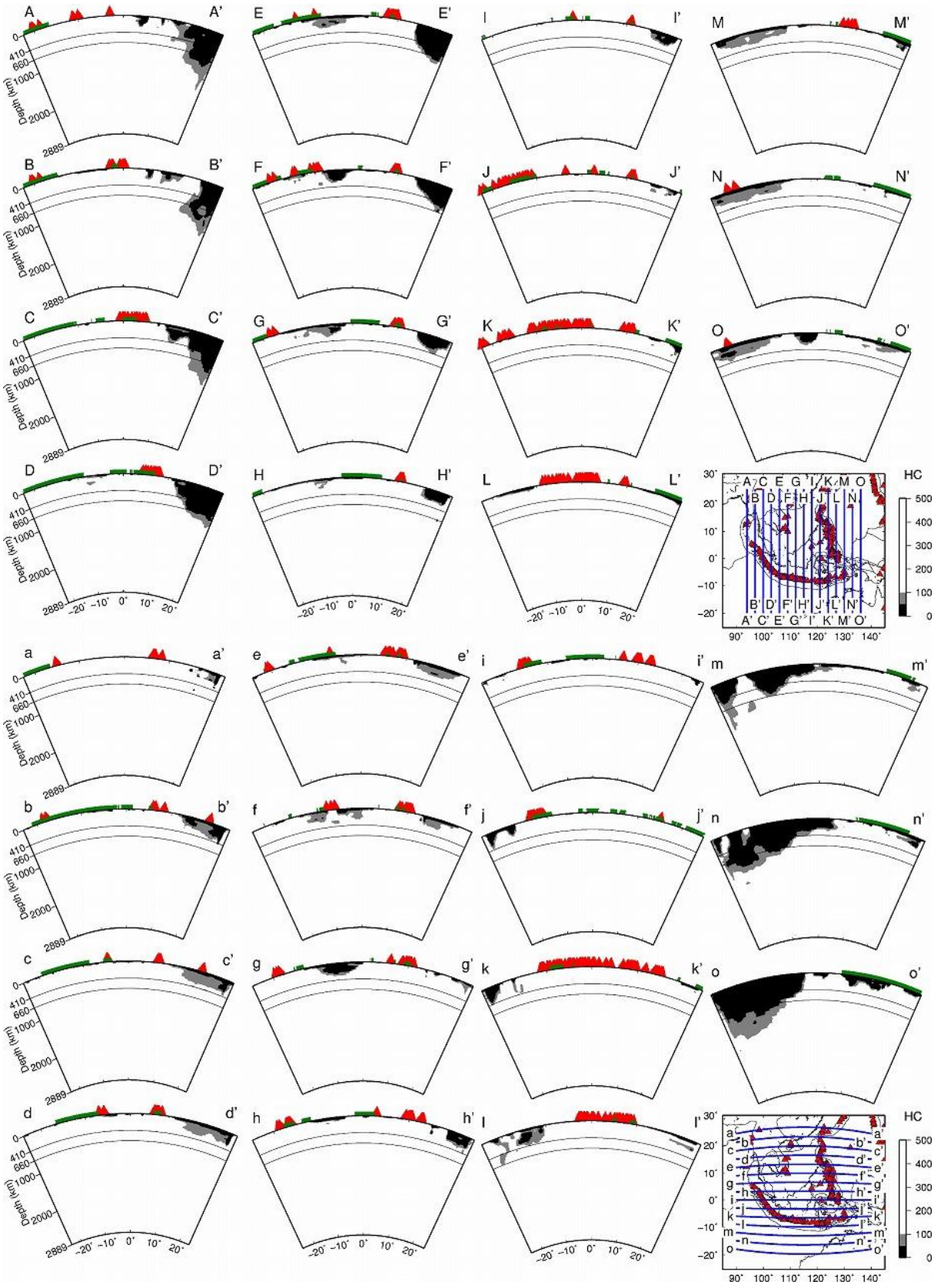
A A'
B B'
C C'
D D'
E E'
F F'
G G'
H H'
I I'
J J'
K K'
L L'
M M'
N N'
O O'
a a'
b b'
c c'
d d'
e e'
f f'
g g'
h h'
i i'
j j'
k k'
l l'
m m'
n n'
o o'
Depth (km)
0
410
660
1000
2000
2889
-20° -10° 0° 10° 20°
HC
500
400
300
200
100
0
90° 100° 110° 120° 130° 140°
30°
20°
10°
0°
-10°
-20°

Figure S7.

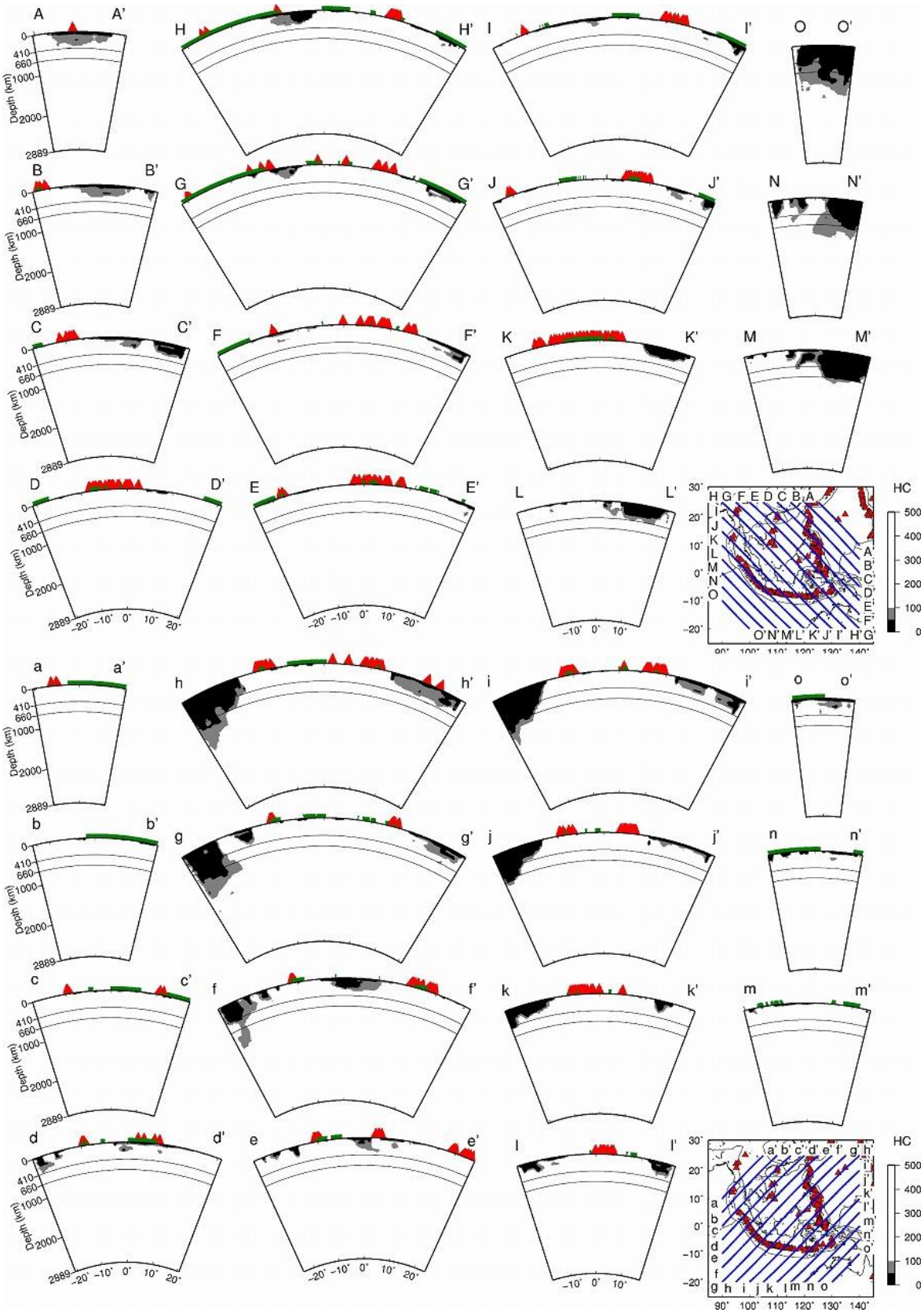
A A' H H' I I' O O'
B B' G G' J J' N N'
C C' F F' K K' M M'
D D' E E' L L'
a a' h h' i i' o o'
b b' g g' j j' n n'
c c' f f' k k' m m'
d d' e e' l l'
Depth (km)
0
410
660
1000
2000
2889
HC
500
400
300
200
100
0

55 **Figure S8.**

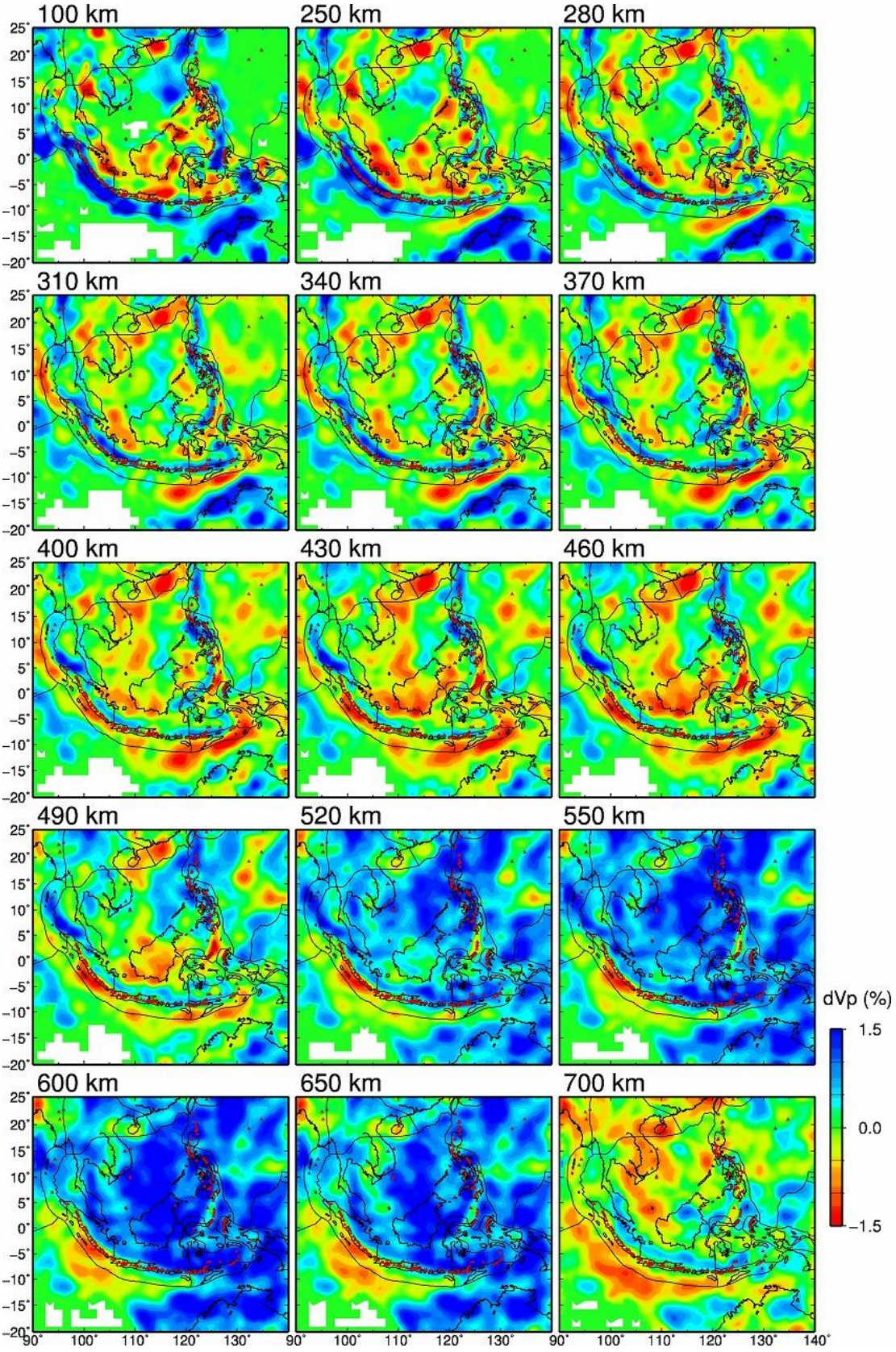
100 km
250 km
280 km
310 km
340 km
370 km
400 km
430 km
460 km
490 km
520 km
550 km
600 km
650 km
700 km
dVp (%)
1.5
0.0
−1.5

Figure S9.

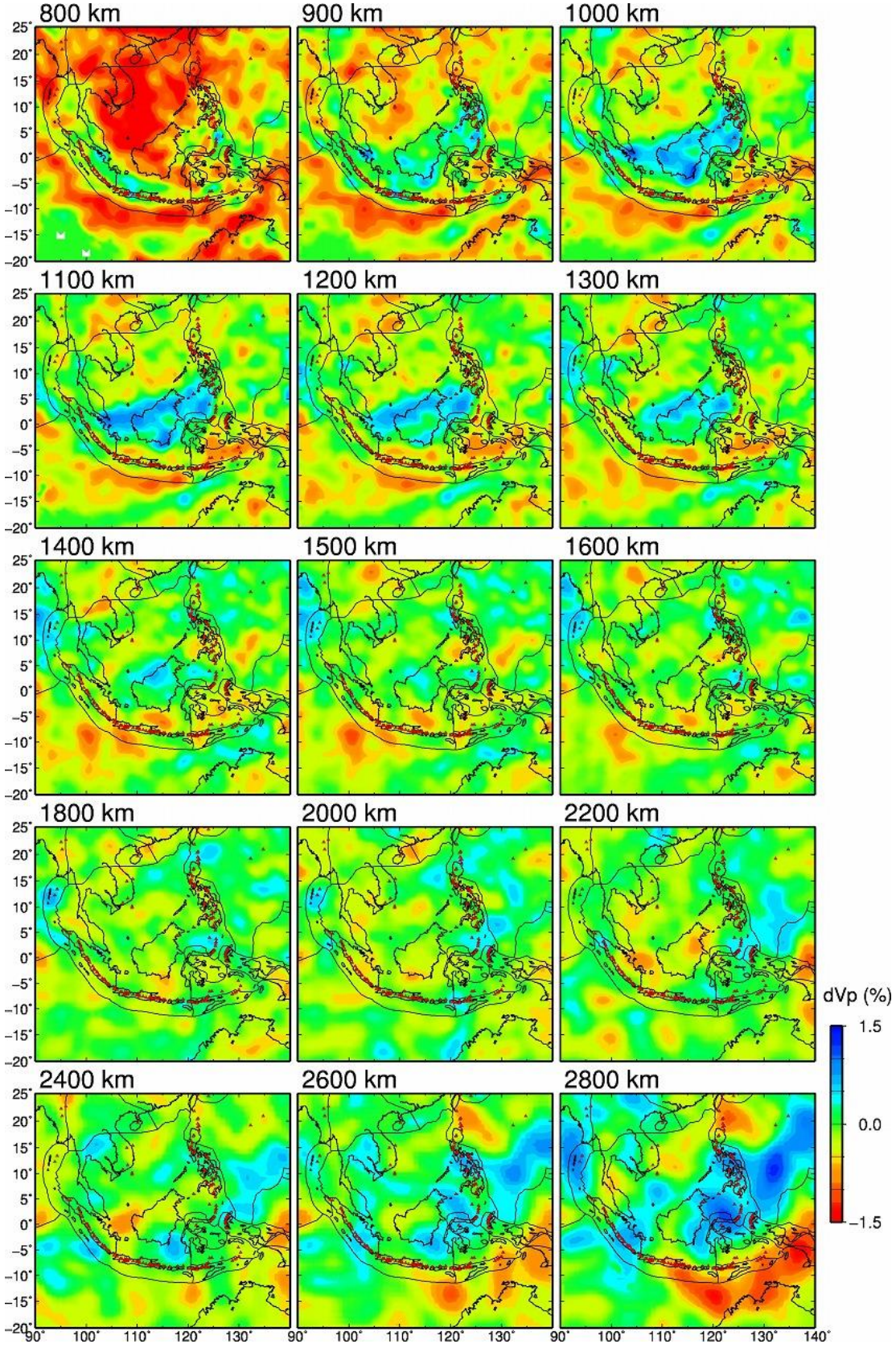

Figure S9. (continued).

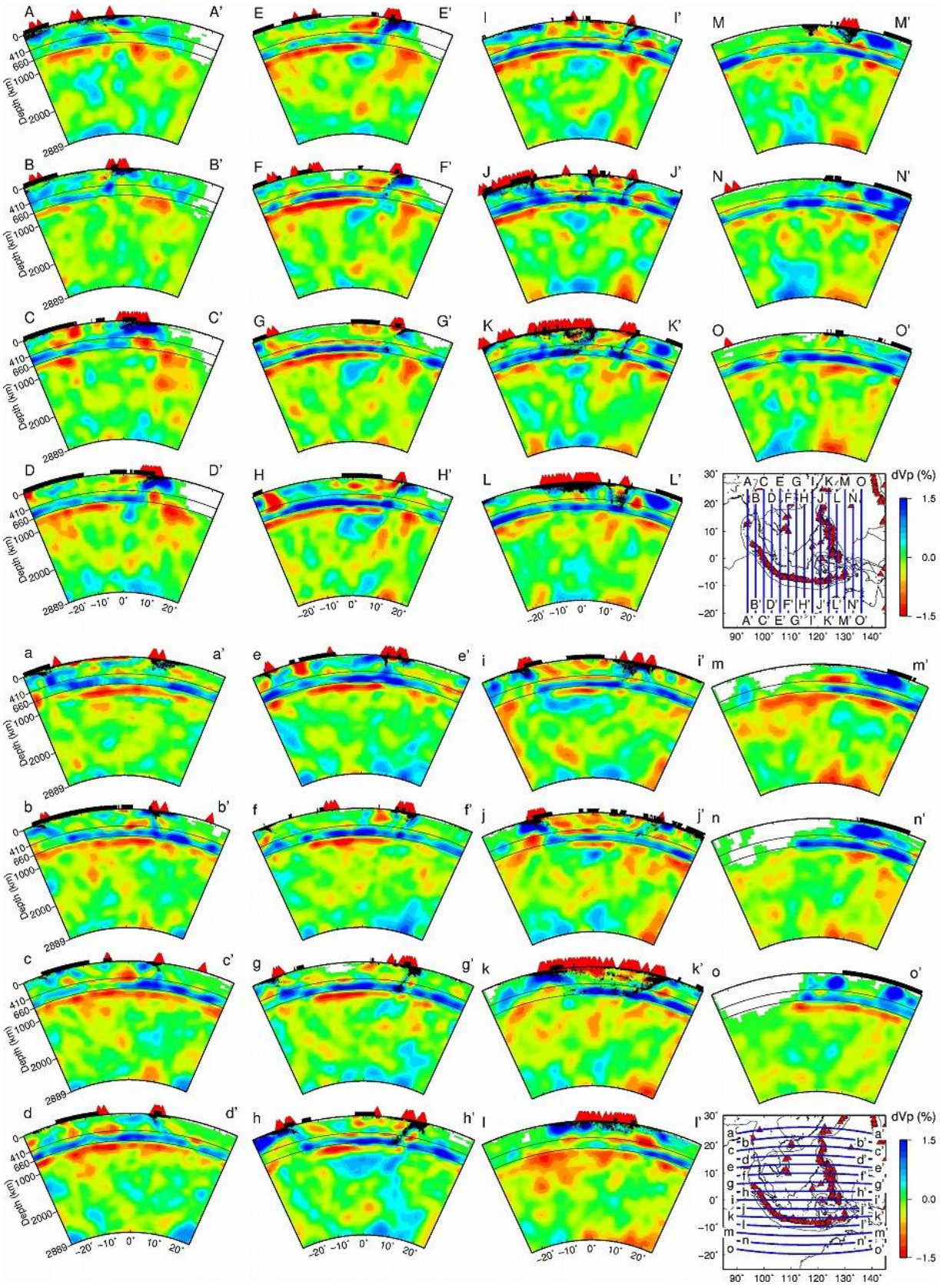

58 **Figure S10.**

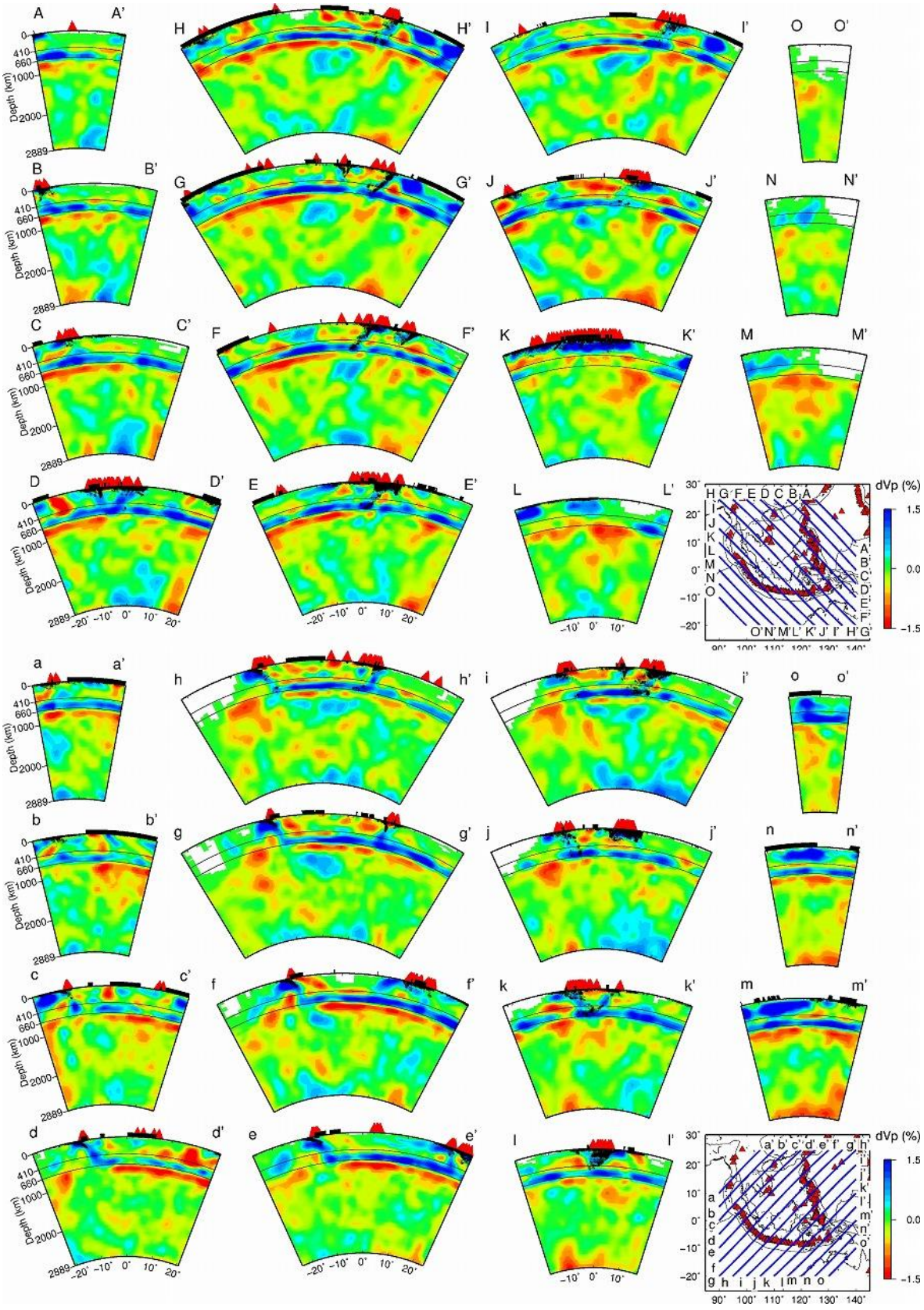

59 **Figure S11.**

Figure S6. Map view images of the ray hit count. The layer depth is shown at the lower-right corner of each map. The color scale is shown on the right. The areas in black color with hit count < 50 are masked in the resulting tomographic images.

Figure S7. Vertical cross-sections of the ray hit count along **(top)** 15 profiles in the N-S direction, and **(bottom)** 15 profiles in the E-W direction. Locations of the profiles are shown on the inset map. The 410-km and the 660-km discontinuities are shown in black solid lines. The thick green lines on the surface denote land areas. The red triangles denote active volcanoes. The thin black lines on the inset map denote the plate boundaries.

Figure S8. The same as Figure S7 but along **(top)** 15 profiles in the NW-SE direction, and **(bottom)** 15 profiles in the NE-SW direction.

Figure S9. The same as Figures 5 and 6 but before subtracting the average velocity anomalies at each depth (Figure 4) from the velocity anomalies obtained using IASP91 (Kennett & Engdahl, 1991).

Figure S10. The same as Figures 7 but before subtracting the average velocity anomalies at each depth (Figure 4) from the velocity anomalies obtained using IASP91 (Kennett & Engdahl, 1991).

Figure S11. The same as Figures 8 but before subtracting the average velocity anomalies at each depth (Figure 4) from the velocity anomalies obtained using IASP91 (Kennett & Engdahl, 1991).

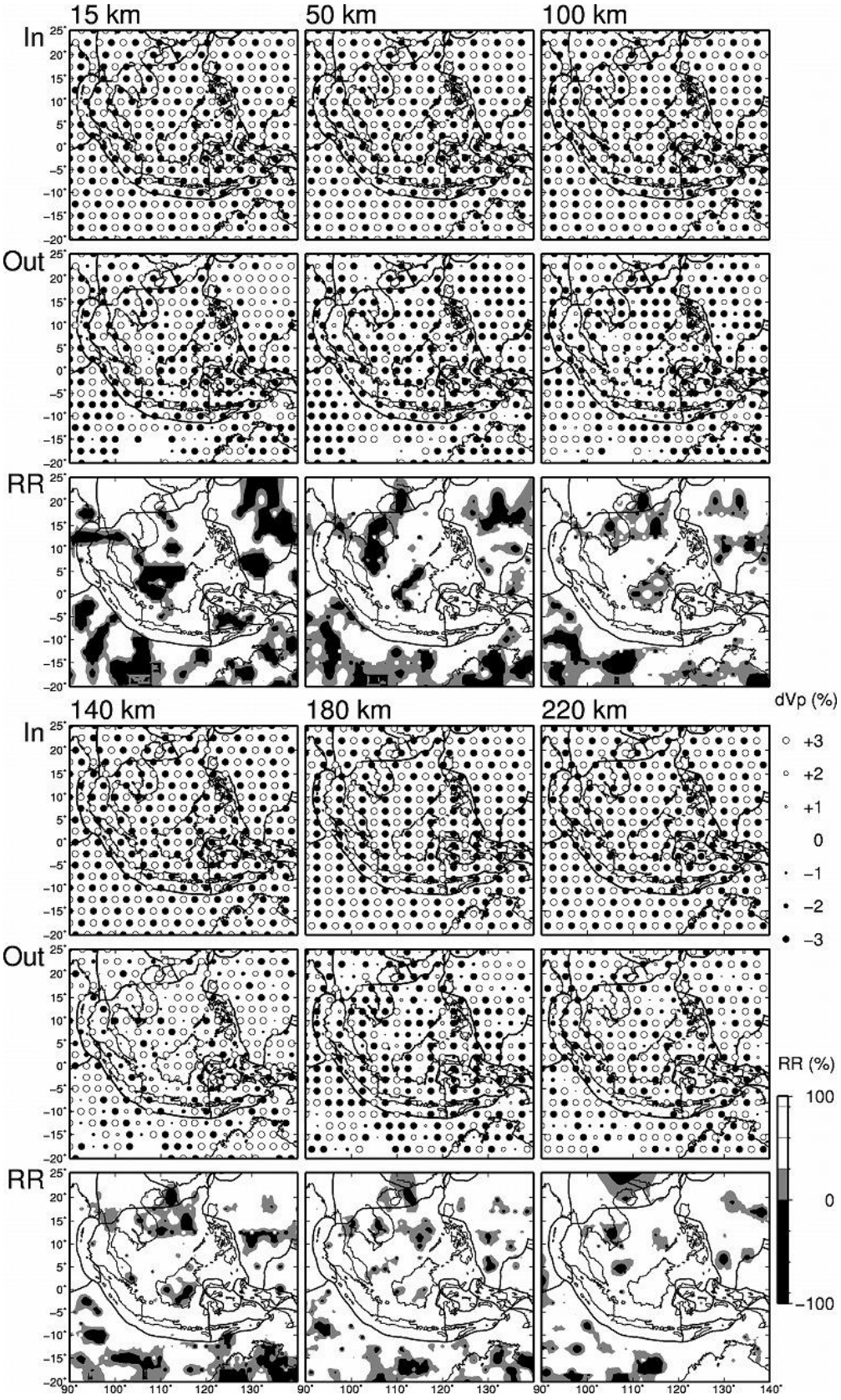
15 km
50 km
100 km
In
Out
RR
140 km
180 km
220 km
dVp (%)
+3
+2
+1
0
−1
−2
−3
RR (%)
100
0
−100

Figure S12.

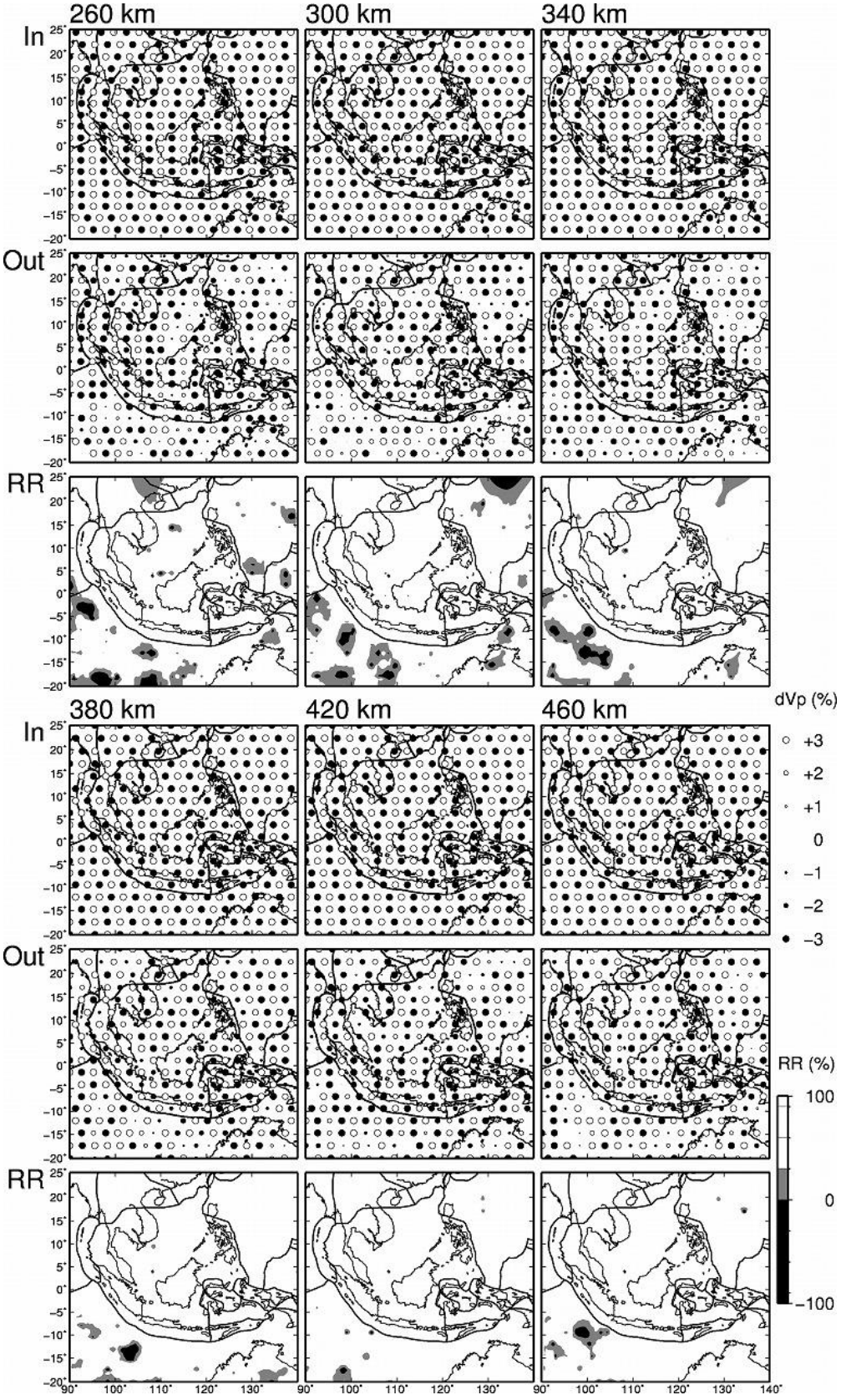

Figure S12. (continued).

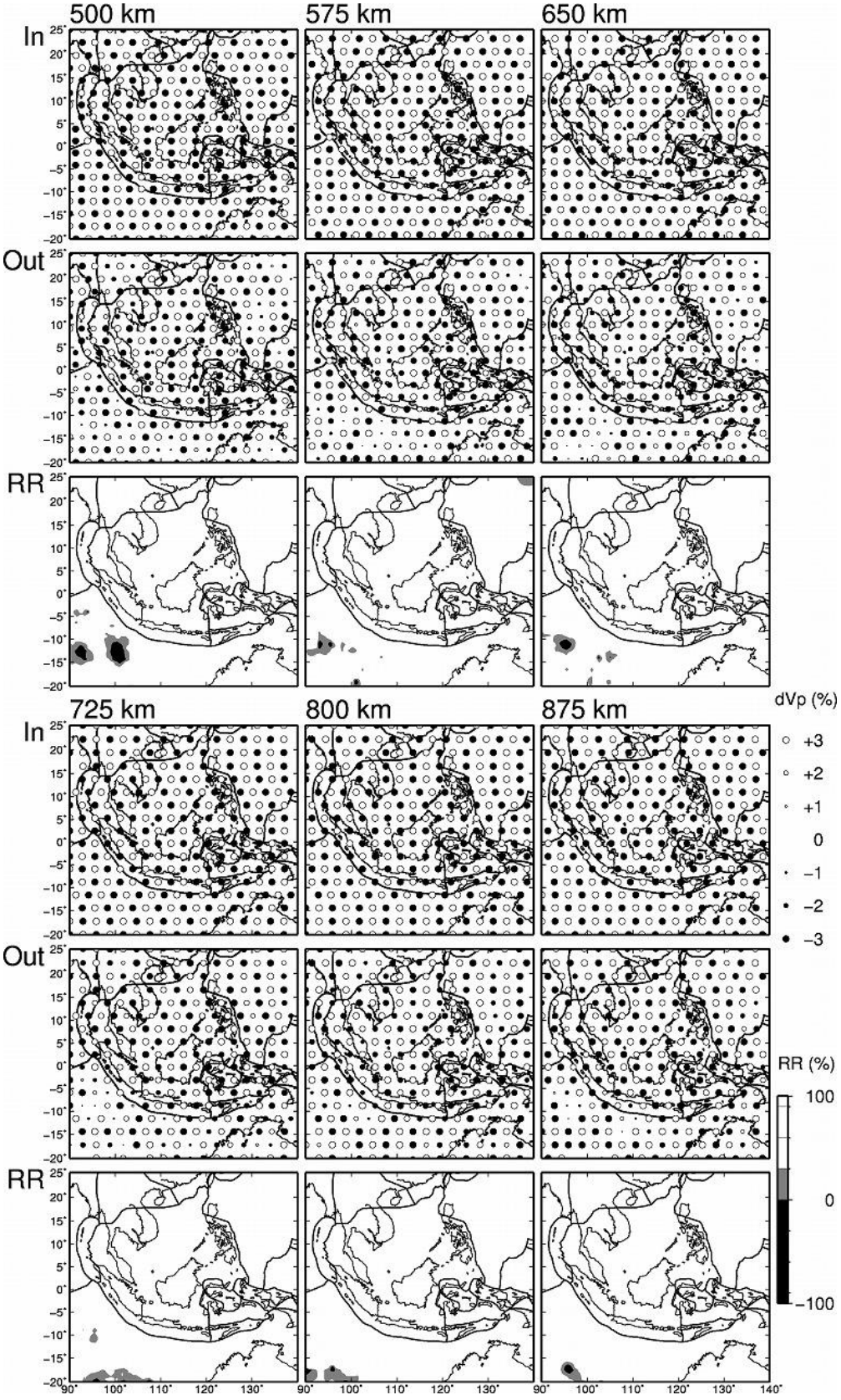

Figure S12. (continued).

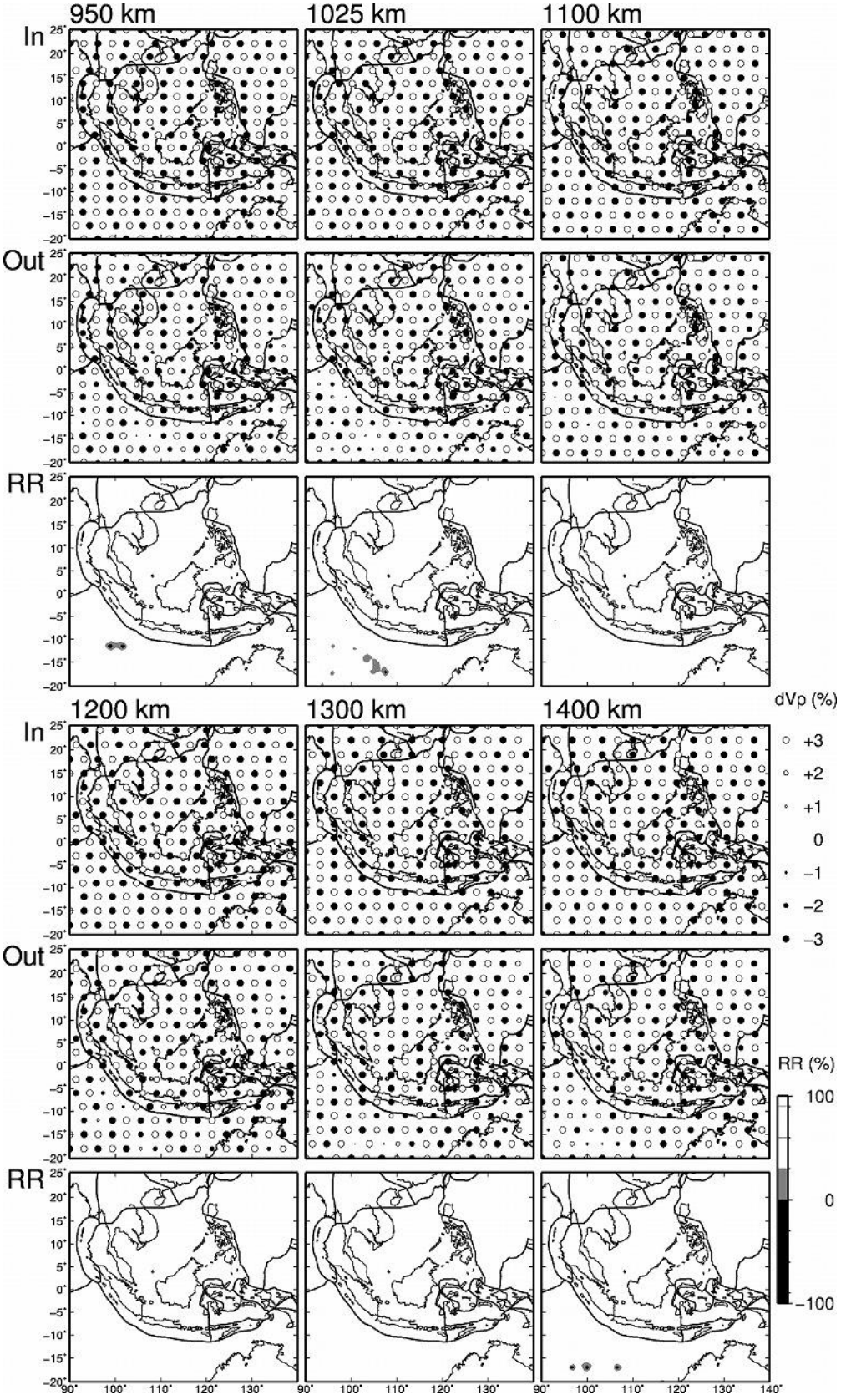

Figure S12. (continued).

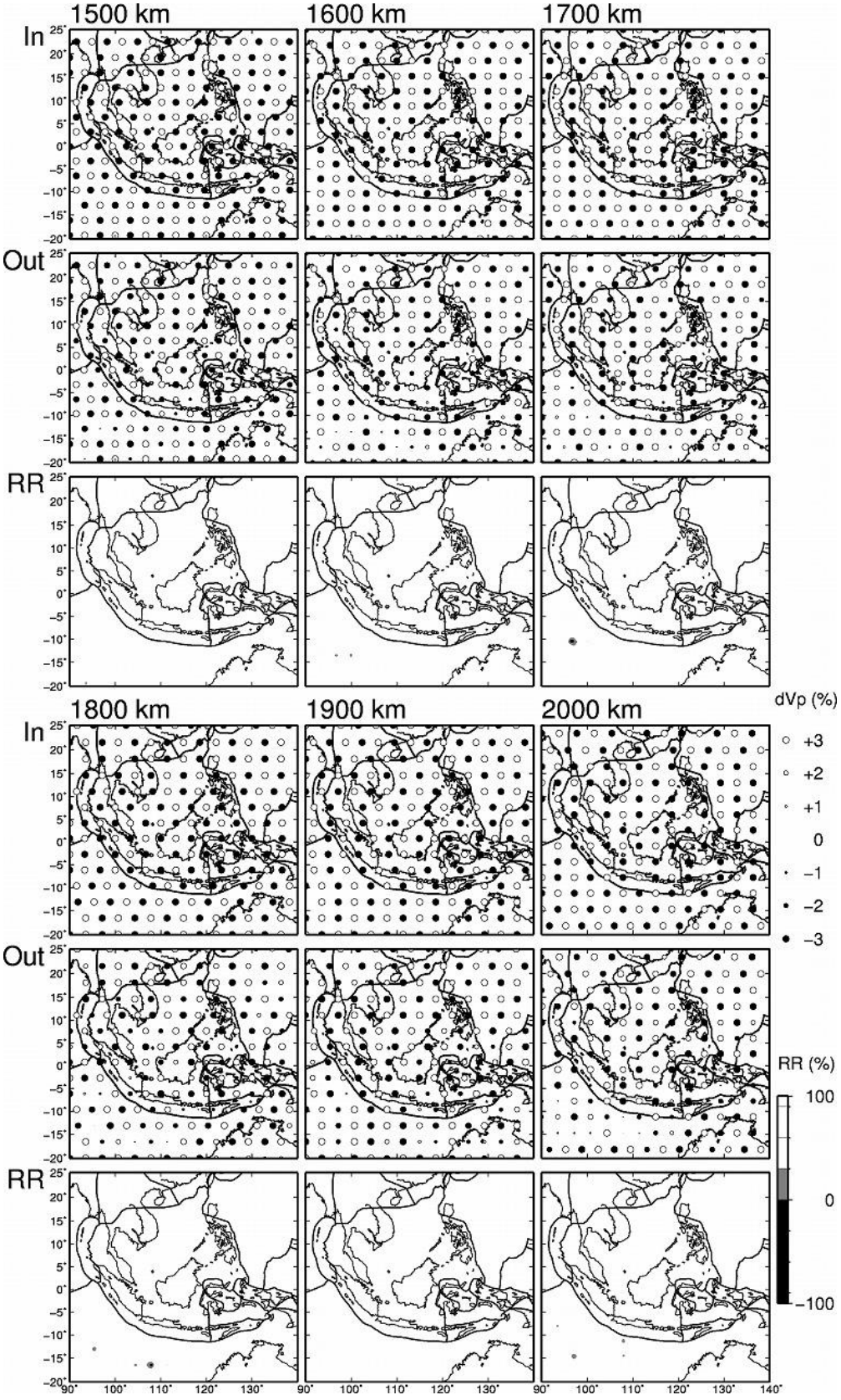

Figure S12. (continued).

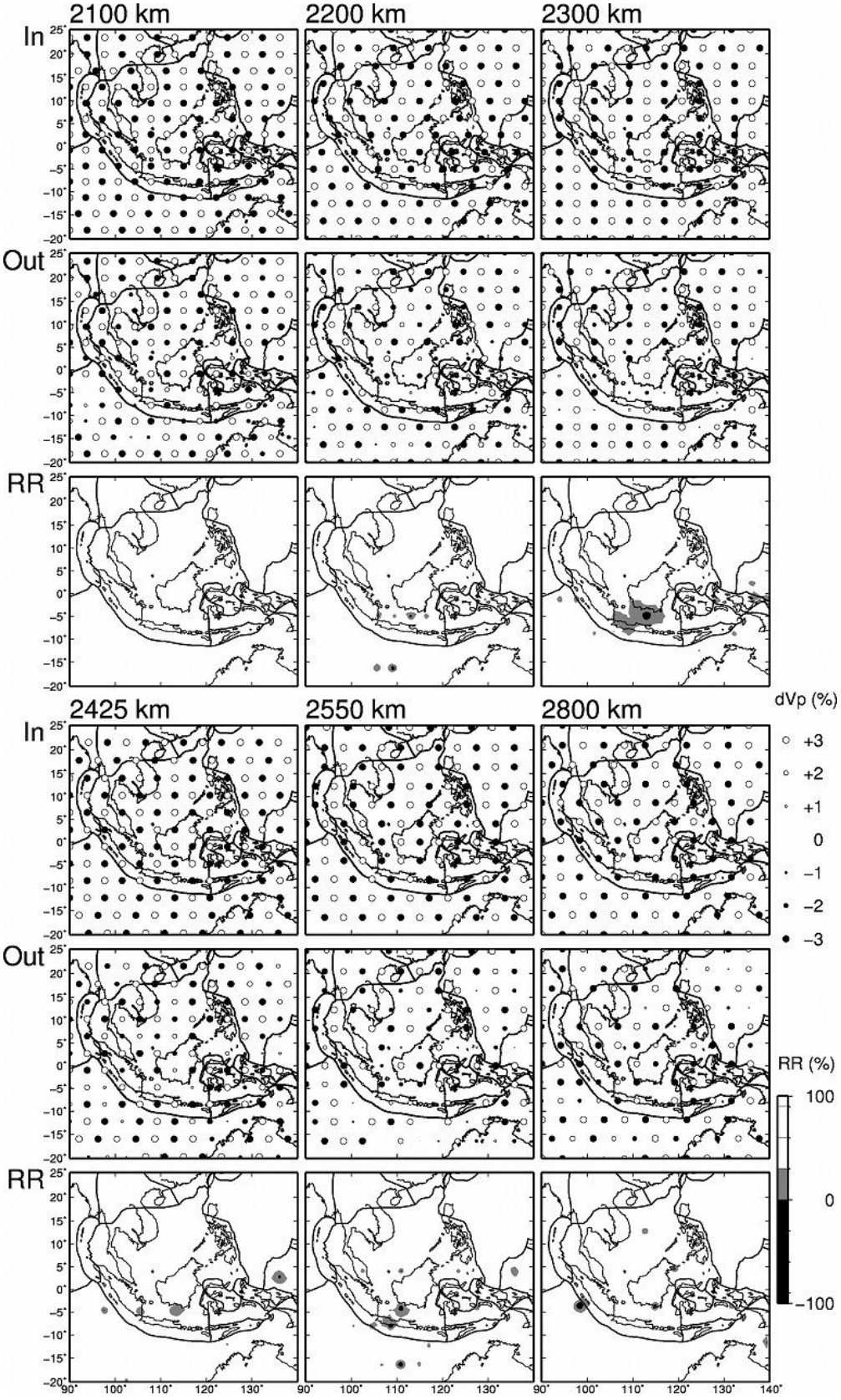

Figure S12. (continued).

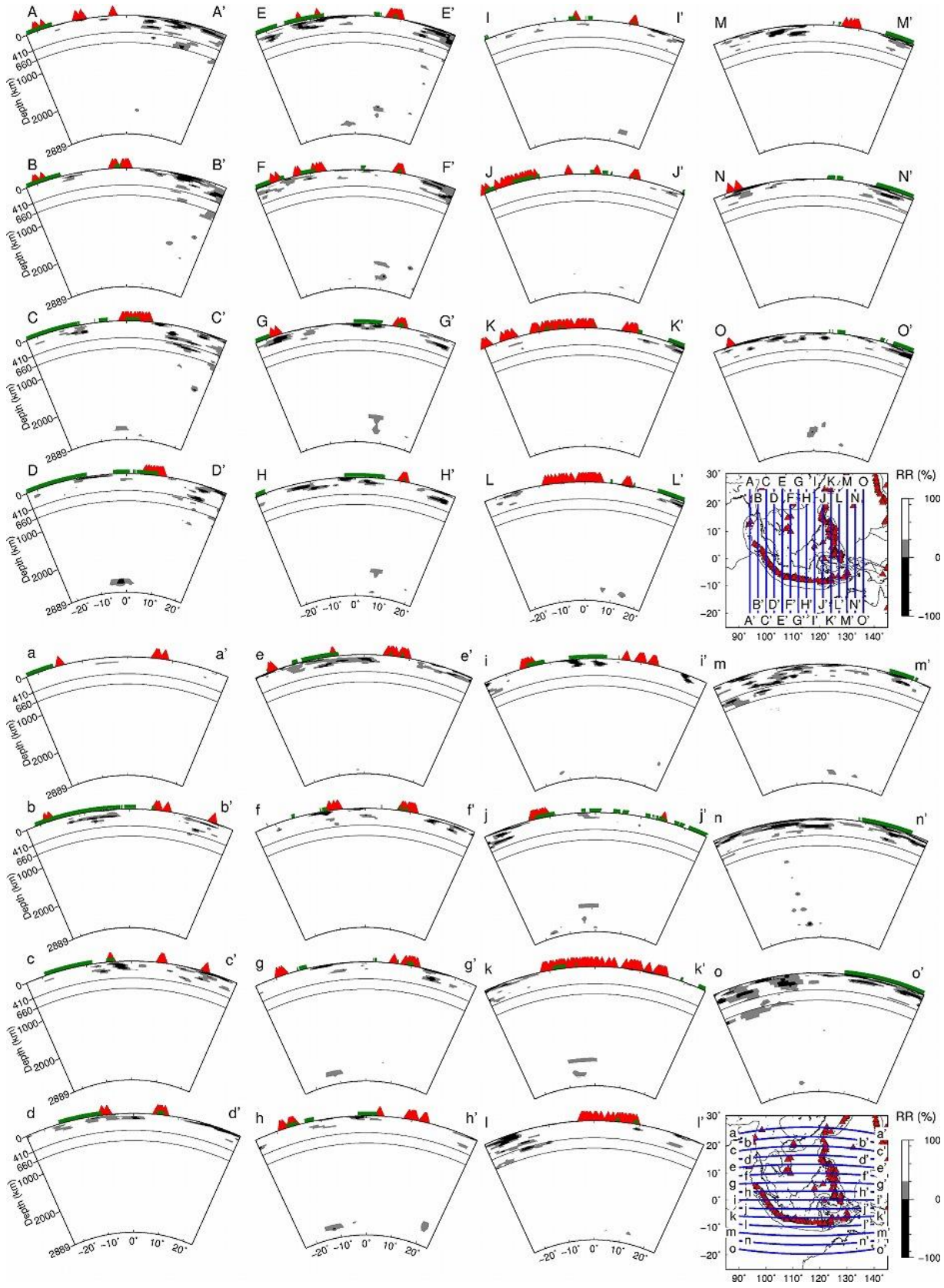

89 **Figure S13.**

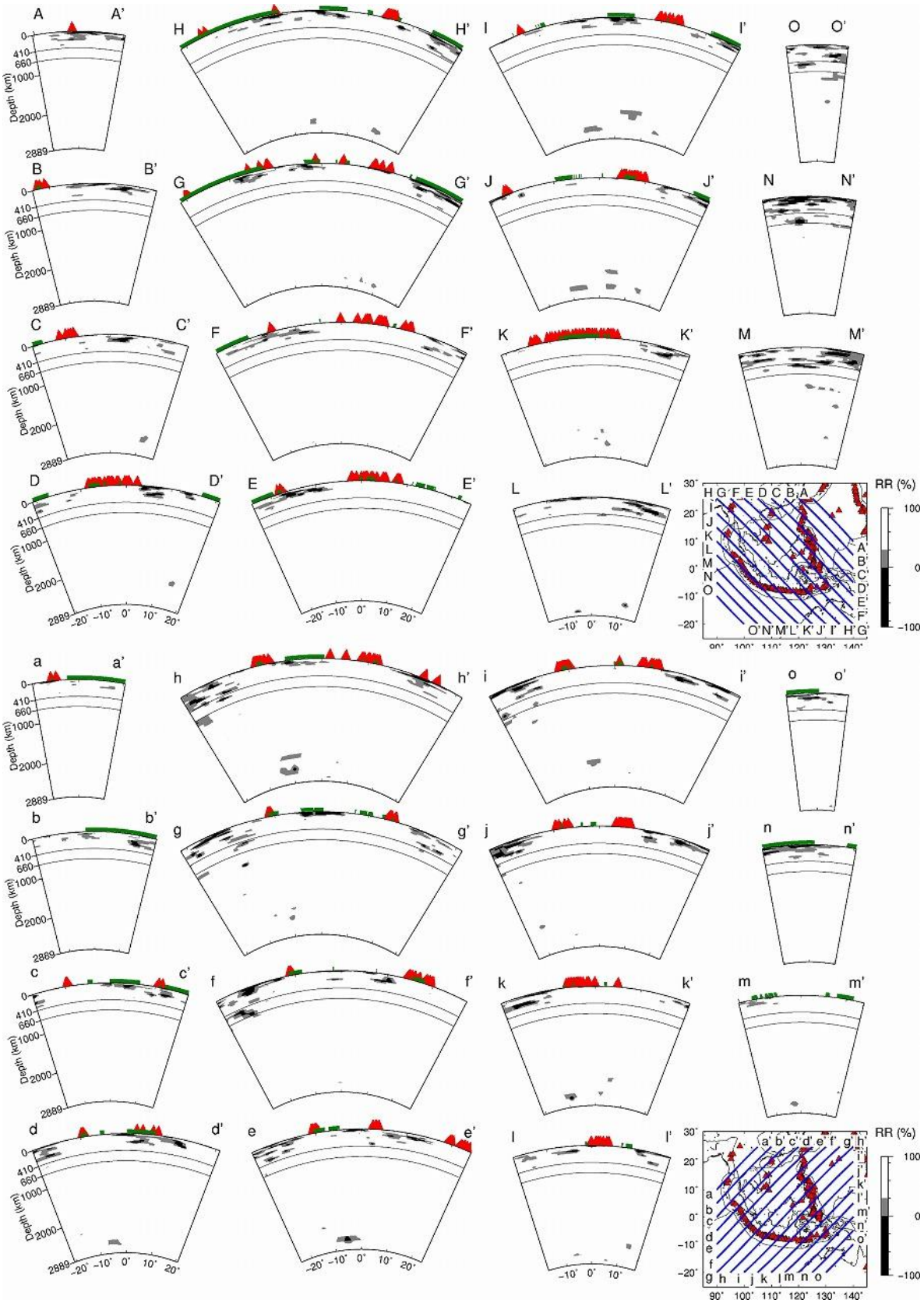
A A' H H' I I' O O'
B B' G G' J J' N N'
C C' F F' K K' M M'
D D' E E' L L'
a a' h h' i i' o o'
b b' g g' j j' n n'
c c' f f' k k' m m'
d d' e e' l l'
Depth (km)
0
410
660
1000
2000
2889
RR (%)
100
0
−100

Figure S14.

Figure S12. Map views showing the input model (top panels), output results (middle panels) and the recovery rate (bottom panels) of the checkerboard resolution test with a lateral grid interval of 278 km (CRT1). The layer depth is shown at the upper-left corner of the top panels. The open and solid circles denote high and low Vp perturbations, respectively, whose scale is shown on the right. The color scale of the recovery rate (in %) is also shown on the right.

Figure S13. Vertical cross-sections of the recovery rate along **(top)** 15 profiles in the N-S direction, and **(bottom)** 15 profiles in the E-W direction, obtained by the checkerboard resolution test with a lateral grid interval of 278 km inside the study region (CRT1). Locations of the profiles are shown on the inset map. Other labels are the same as those in Figure S7.

Figure S14. The same as Figure S13 but along **(top)** 15 profiles in the NW-SE direction, and **(bottom)** 15 profiles in the NE-SW direction.

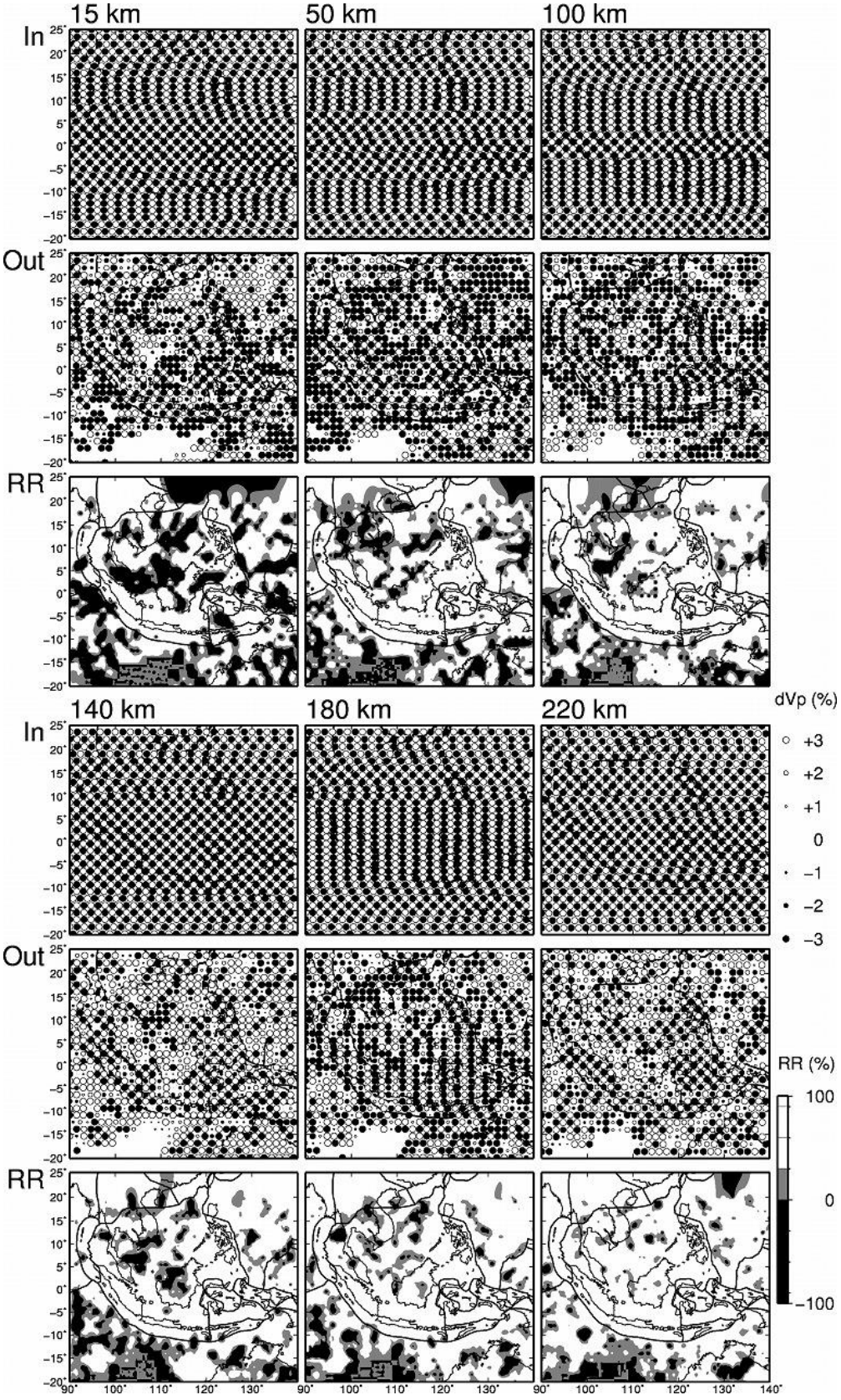
15 km
50 km
100 km
In
Out
RR
140 km
180 km
220 km
dVp (%)
+3
+2
+1
0
−1
−2
−3
RR (%)
100
0
−100

Figure S15.

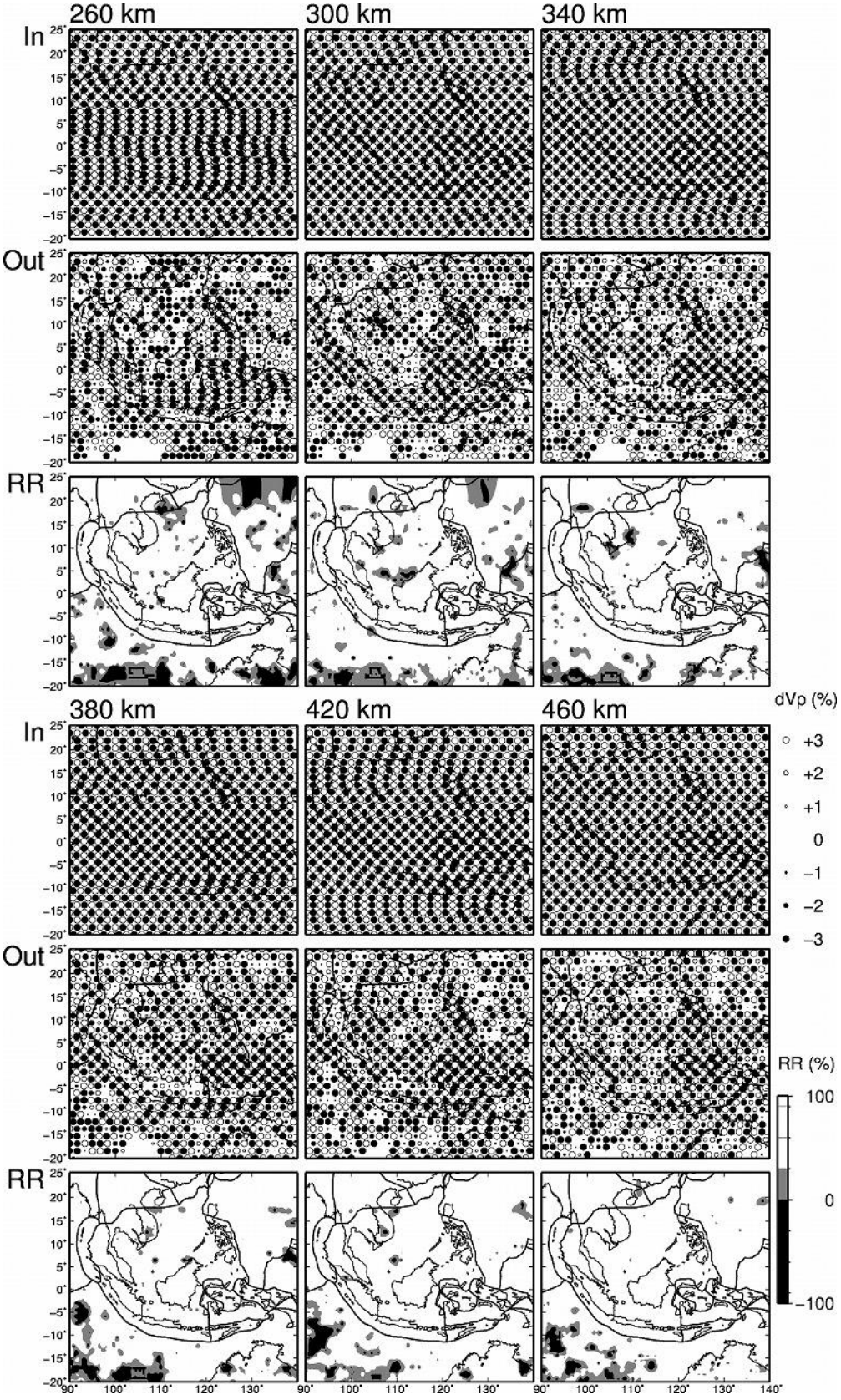

Figure S15. (continued).

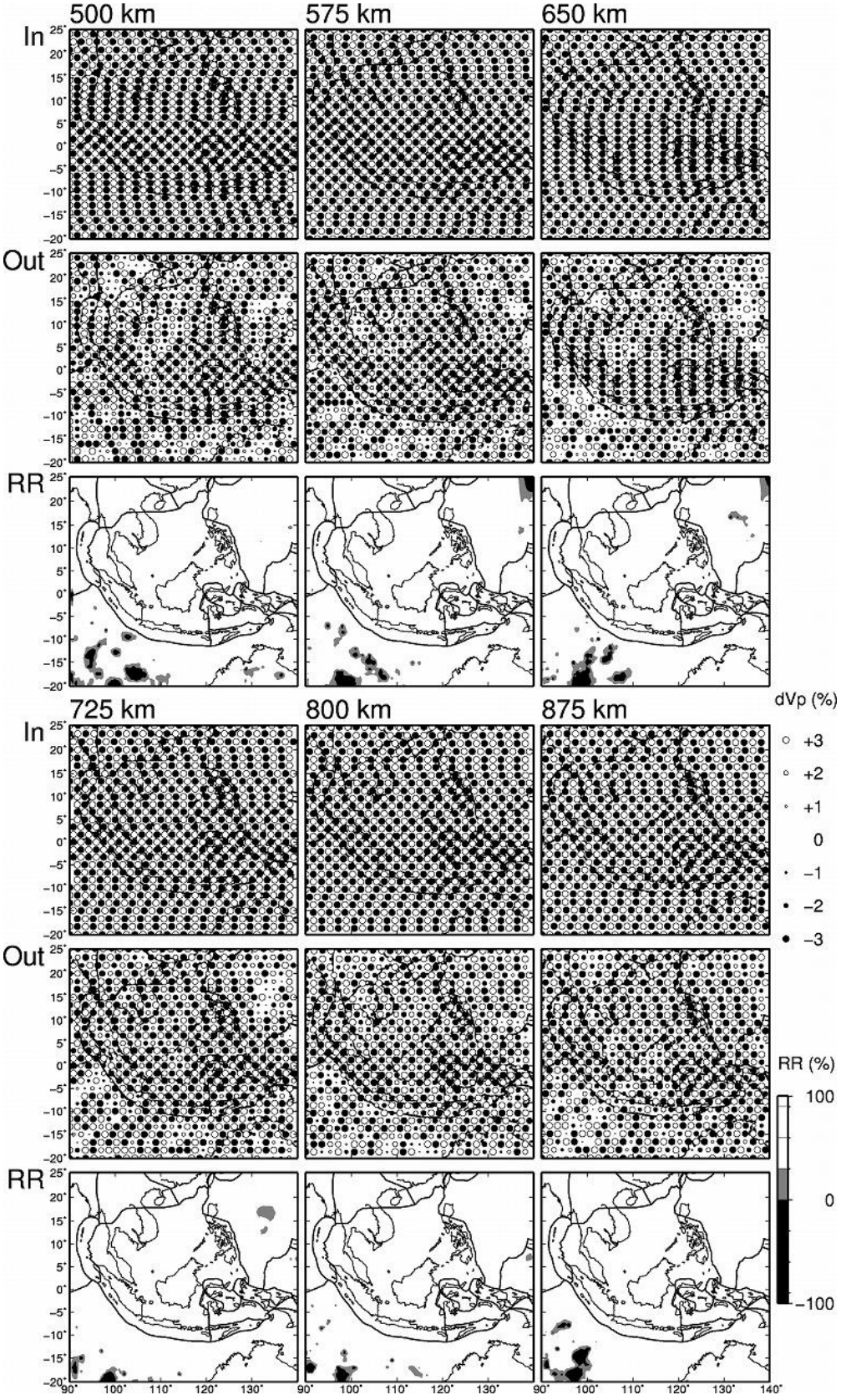

Figure S15. (continued).

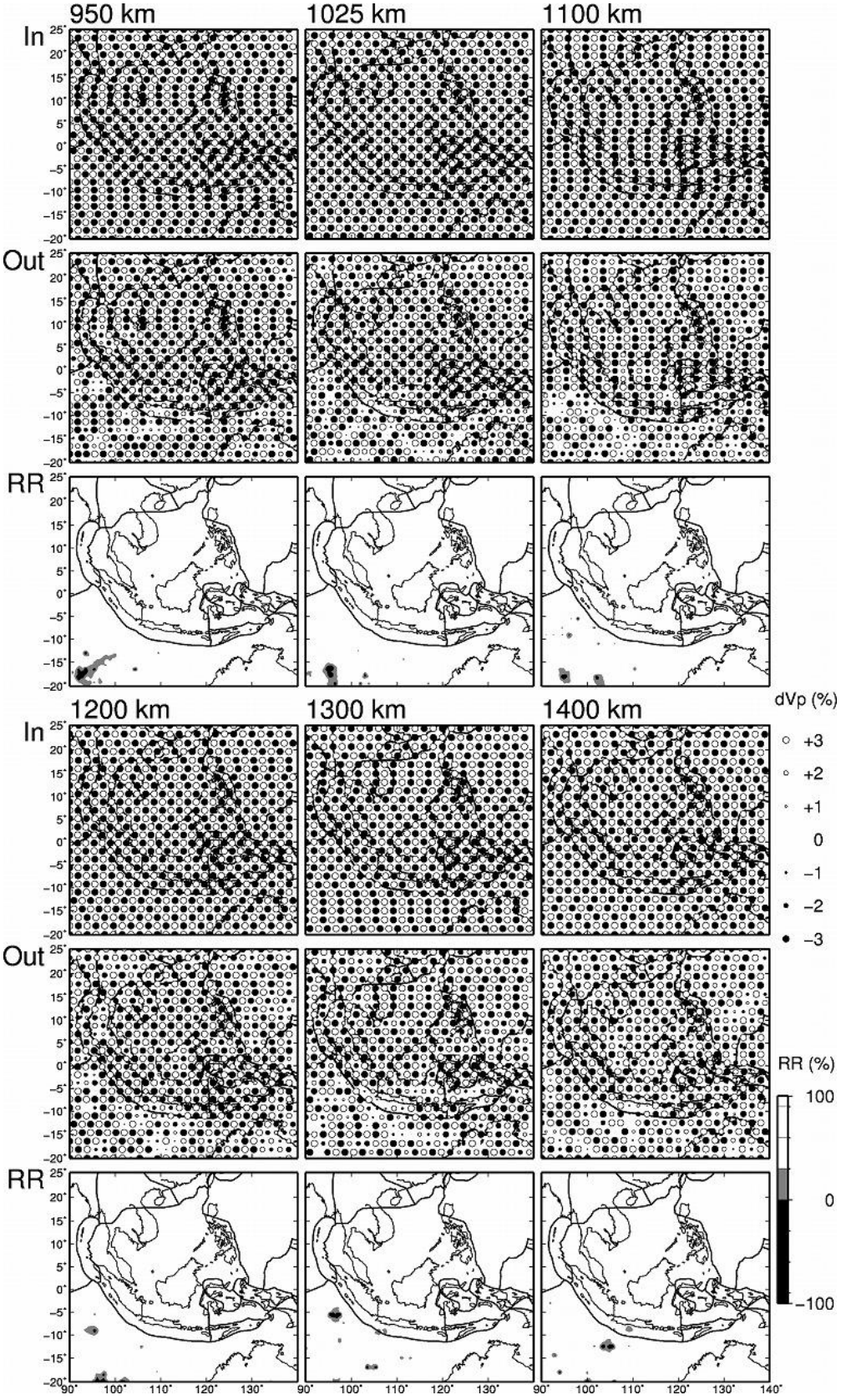

Figure S15. (continued).

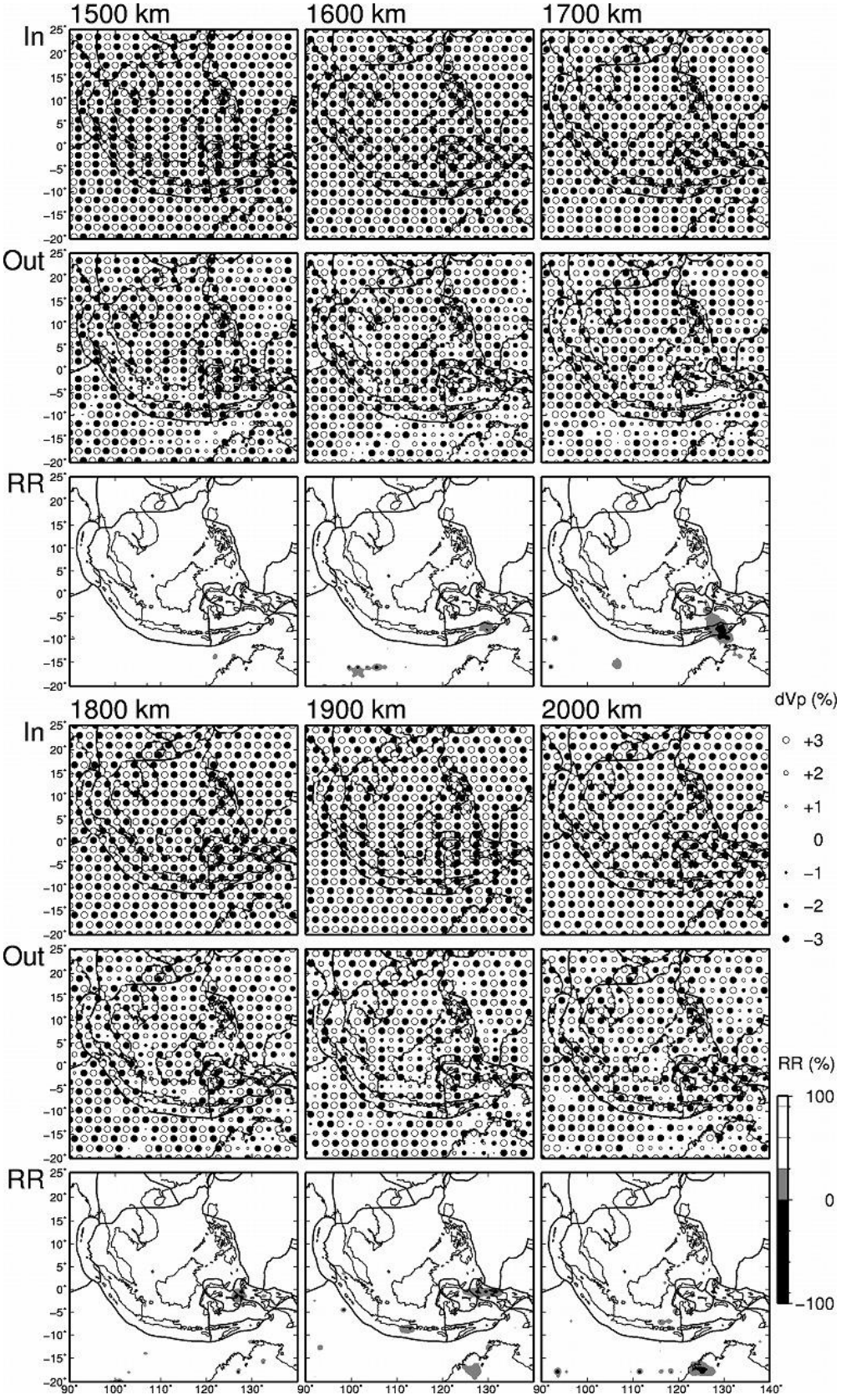

Figure S15. (continued).

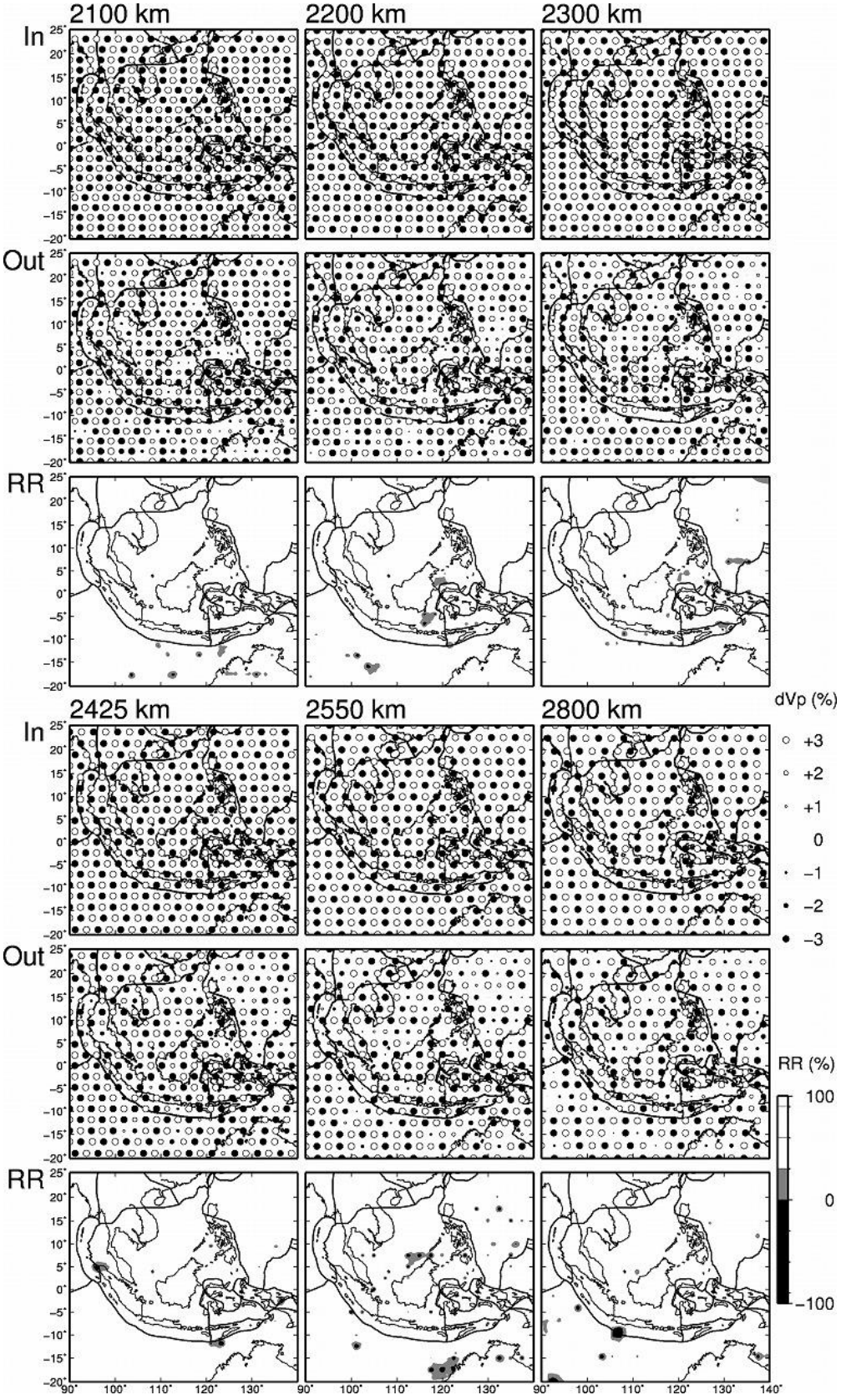

Figure S15. (continued).

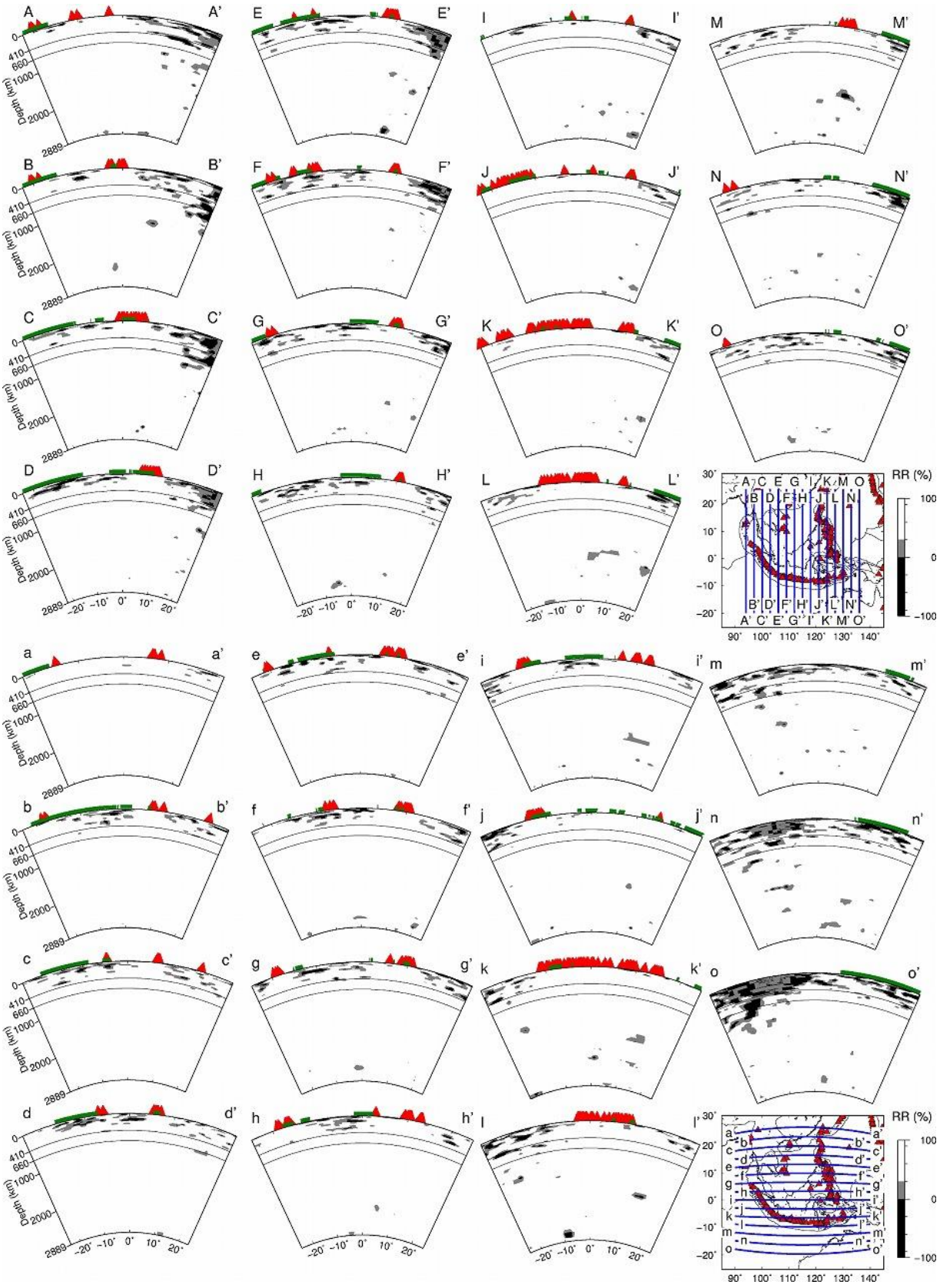
Depth (km)
0
410
660
1000
2000
2889
RR (%)
100
0
−100
30°
20°
10°
0°
−10°
−20°
90° 100° 110° 120° 130° 140°
−20° −10° 0° 10° 20°

Figure S16.

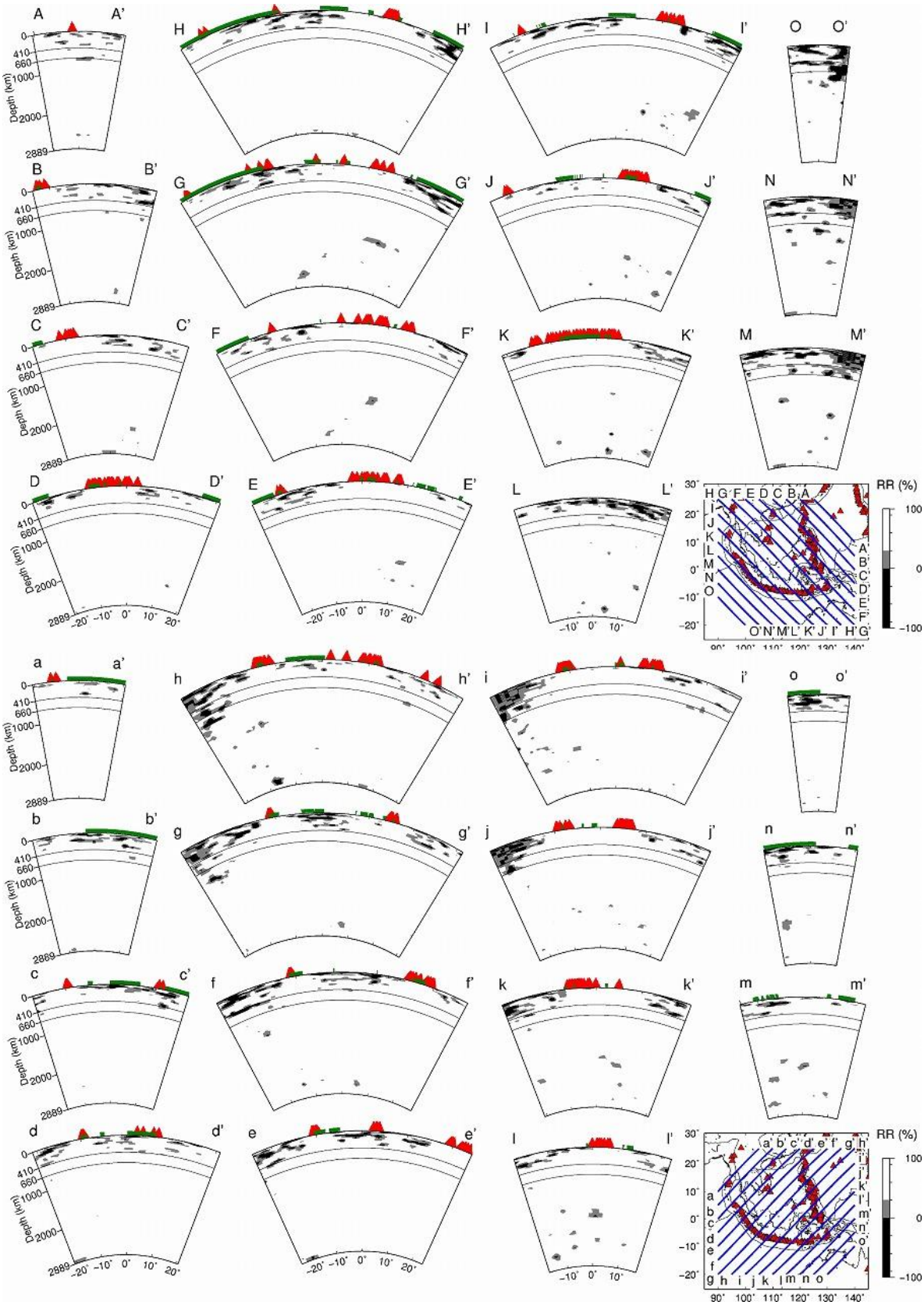
A
A'
H
H'
I
I'
O
O'
B
B'
G
G'
J
J'
N
N'
C
C'
F
F'
K
K'
M
M'
D
D'
E
E'
L
L'
Depth (km)
0
410
660
1000
2000
2889
RR (%)
100
0
−100
a
a'
h
h'
i
i'
o
o'
b
b'
g
g'
j
j'
n
n'
c
c'
f
f'
k
k'
m
m'
d
d'
e
e'
l
l'

Figure S17.

Figure S15. The same as Figure S12 but for the checkerboard resolution test with a lateral grid interval of 167 km inside the study region (CRT2).

Figure S16. The same as Figure S13 but for the checkerboard resolution test with a lateral grid interval of 167 km inside the study region (CRT2).

Figure S17. The same as Figure S14 but for the checkerboard resolution test with a lateral grid interval of 167 km inside the study region (CRT2).

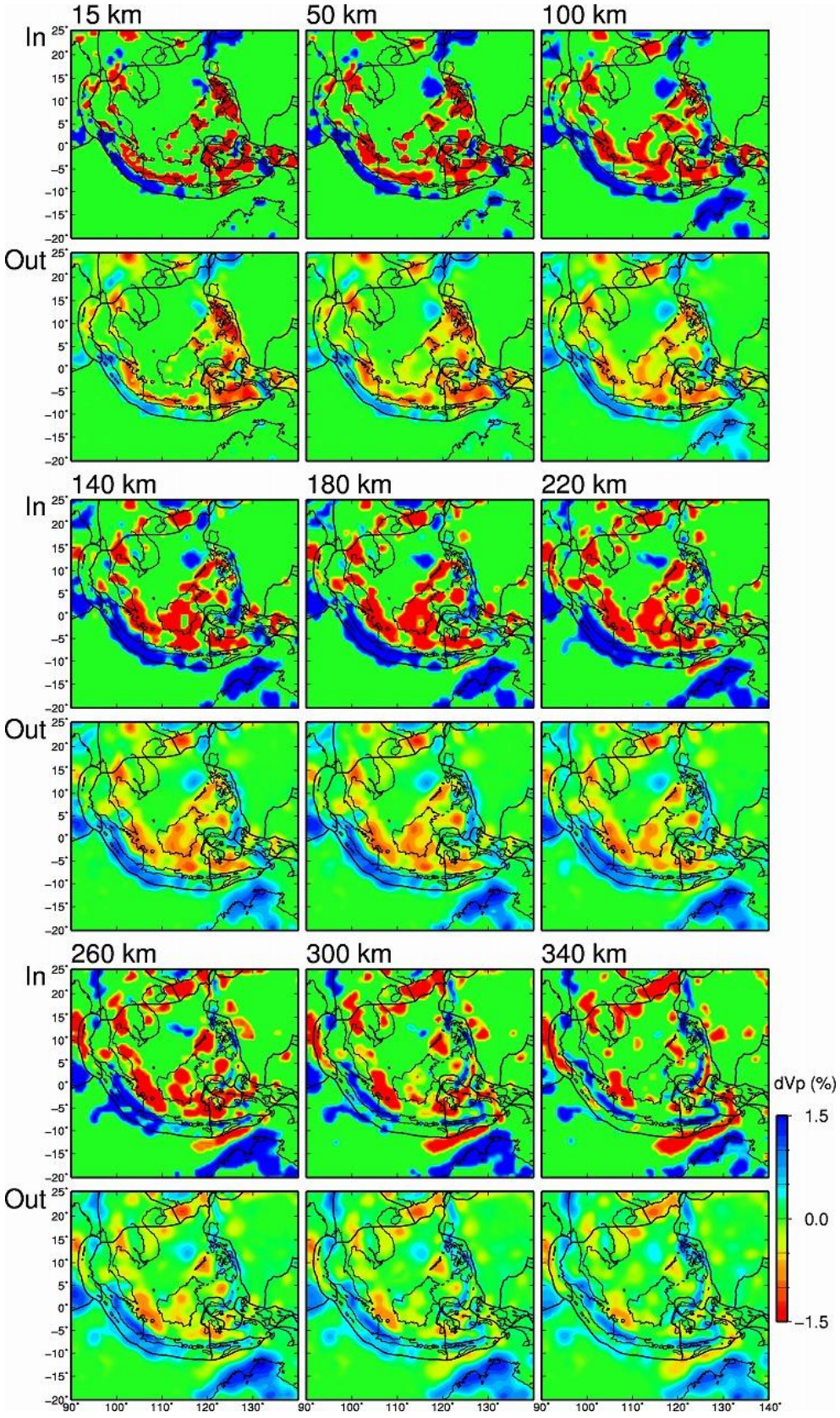
15 km
50 km
100 km
In
Out
140 km
180 km
220 km
In
Out
260 km
300 km
340 km
In
Out
dVp (%)
1.5
0.0
−1.5

Figure S18.

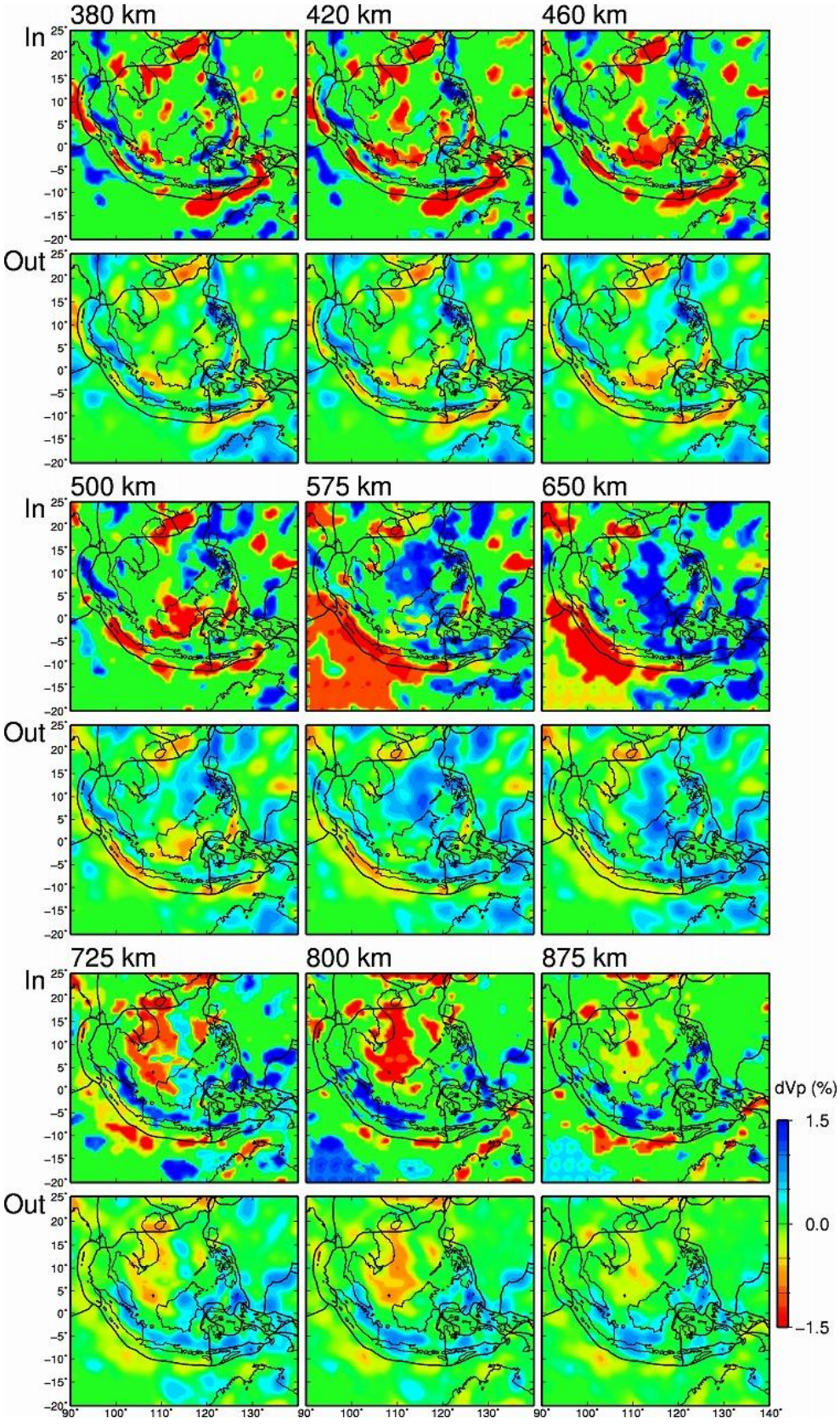

Figure S18. (continued).

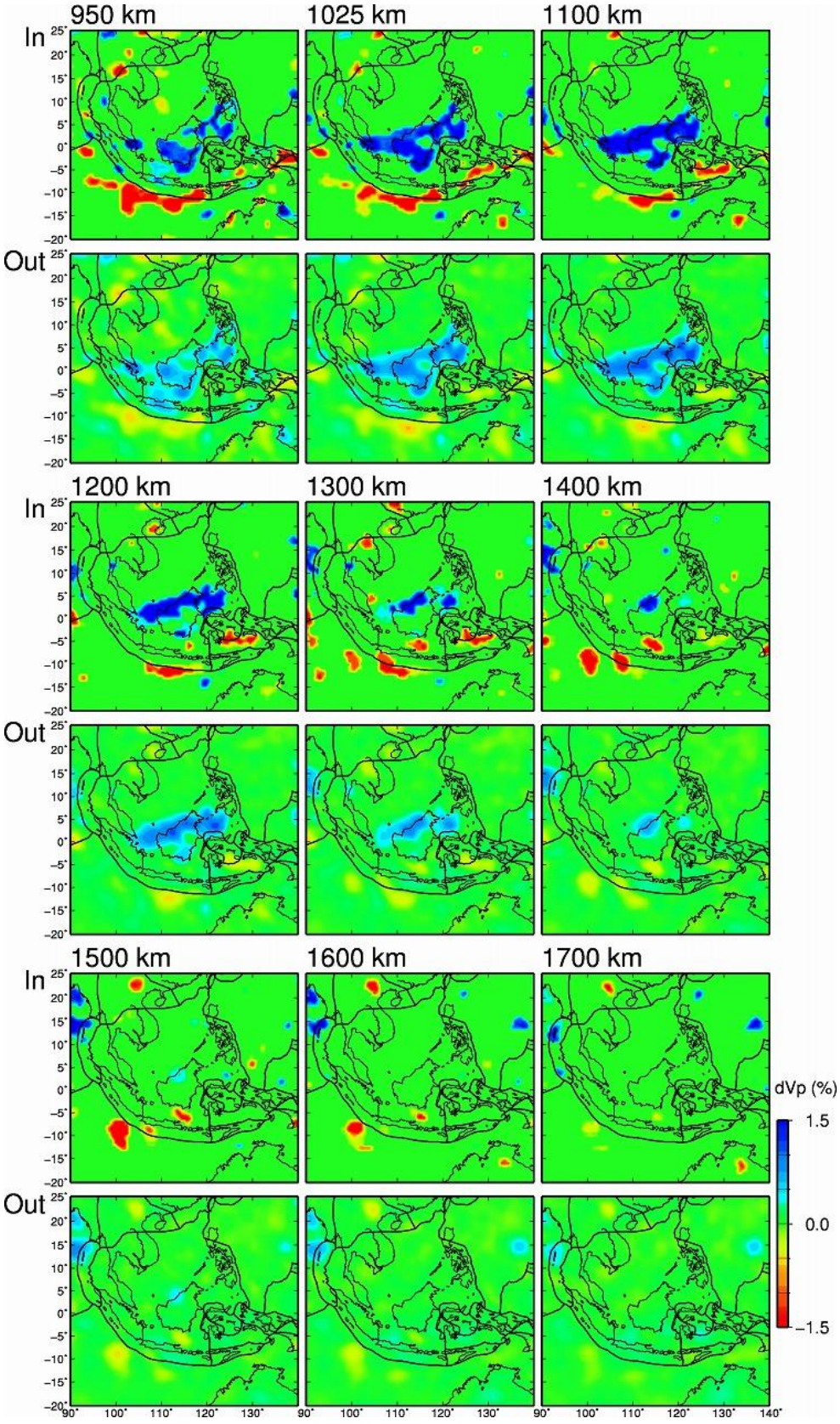

Figure S18. (continued).

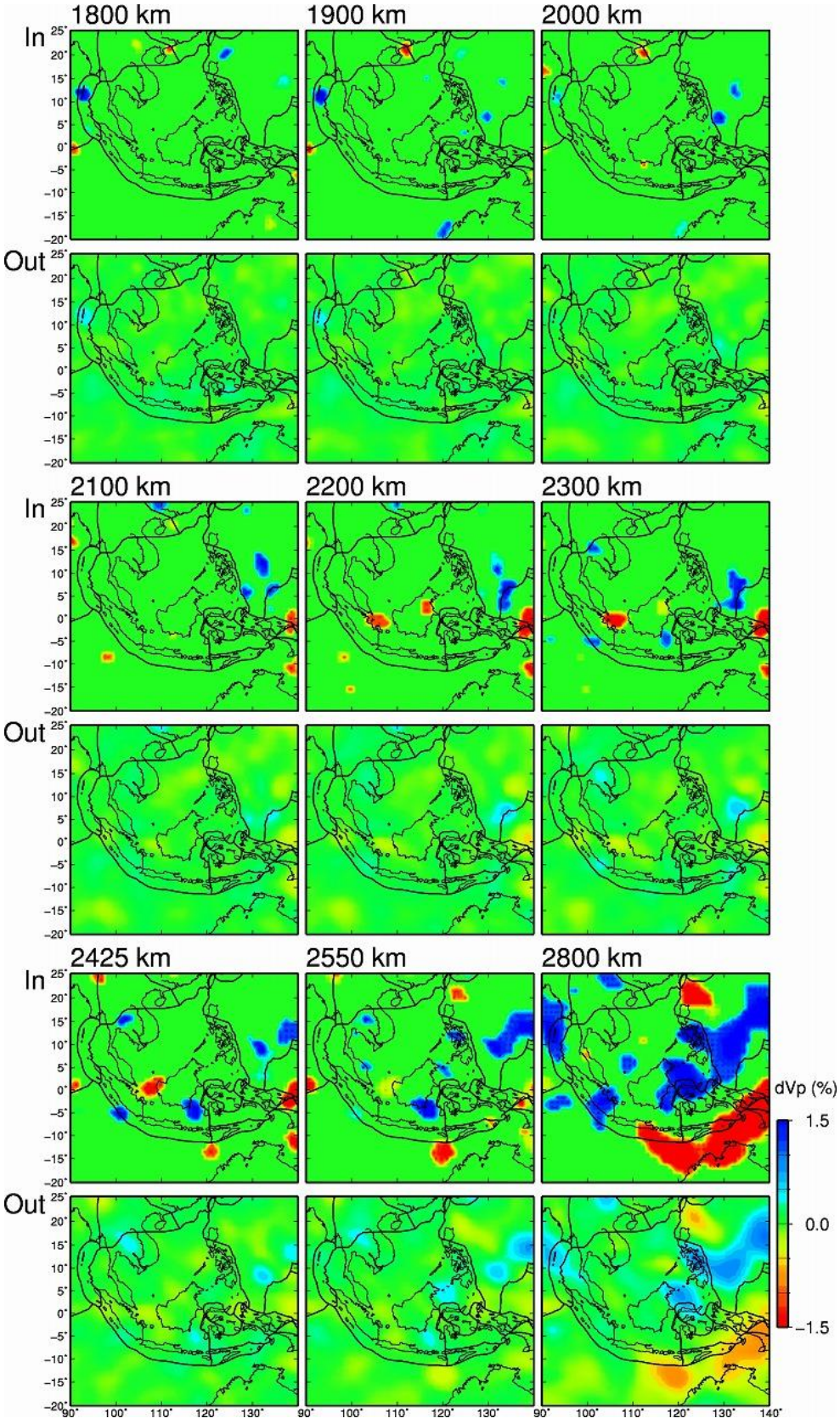

Figure S18. (continued).

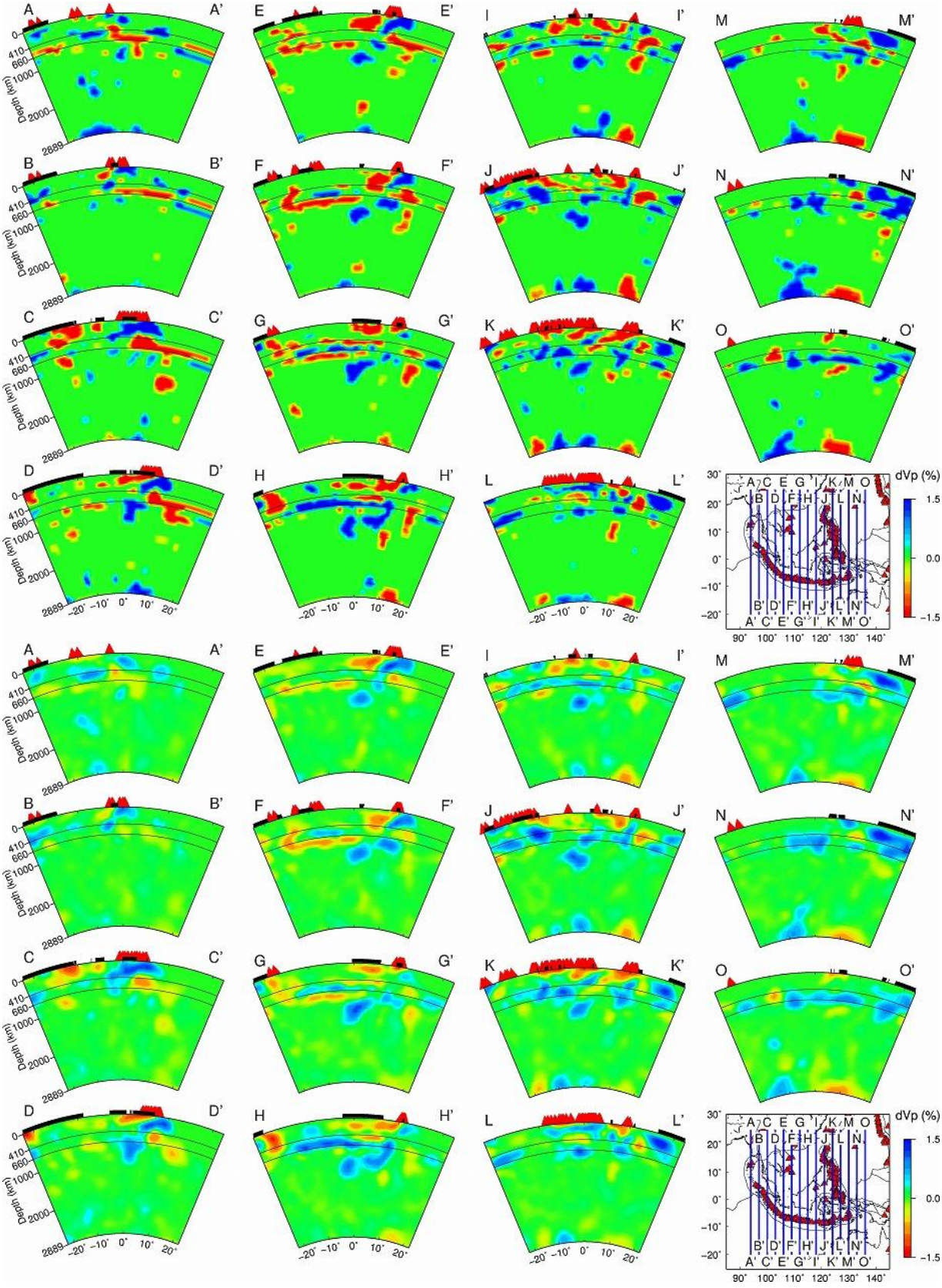

149 **Figure S19.**

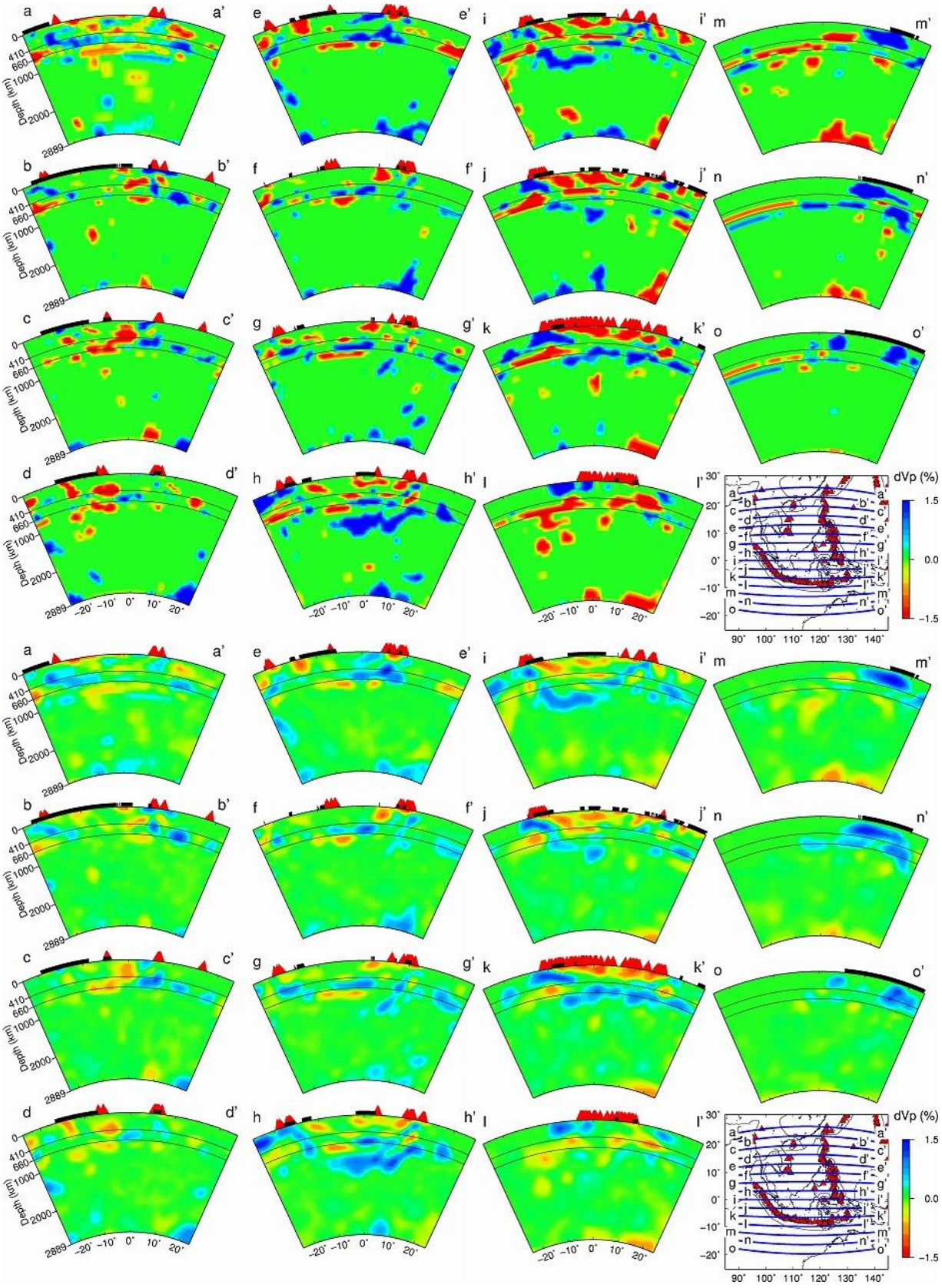

Figure S20.

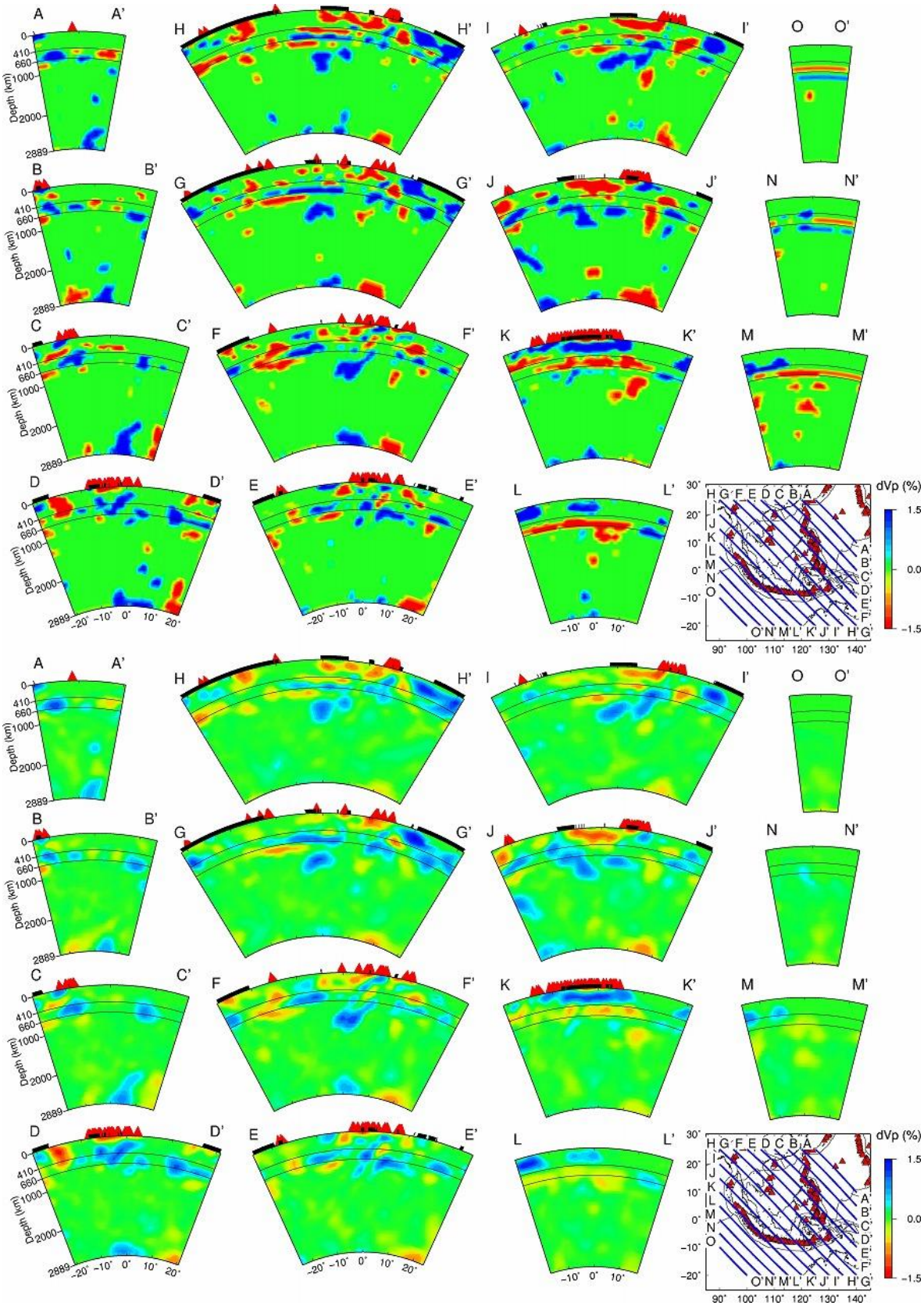

151 **Figure S21.**

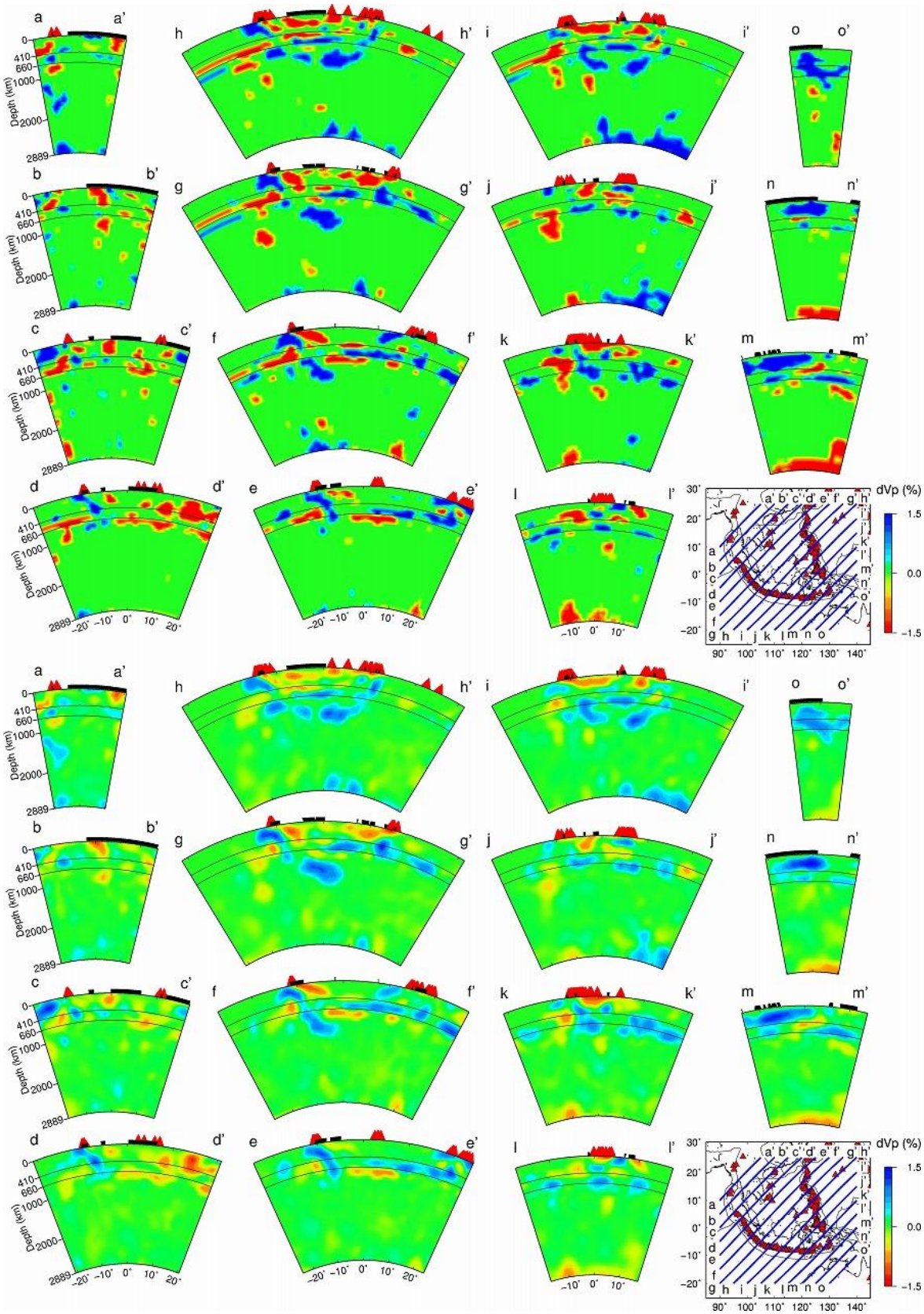
a a' h h' i i' o o'
b b' g g' j j' n n'
c c' f f' k k' m m'
d d' e e' l l'
Depth (km)
0
410
660
1000
2000
2889
dVp (%)
1.5
0.0
-1.5

Figure S22.

Figure S18. Map views showing the input model (upper panels) and output results (lower panels) of the restoring resolution test (RRT). The layer depth is shown above the upper panels. The blue and red colors denote high and low Vp perturbations, respectively, whose scale (in %) is shown on the right.

Figure S19. Vertical cross-sections showing **(top)** the input model and **(bottom)** output results of the restoring resolution test (RRT) along 15 profiles in the N-S direction. Locations of the profiles are shown on the inset map. The 410-km and the 660-km discontinuities are shown in black solid lines. The thick black lines on the surface denote land areas. The red triangles denote active volcanoes. The thin black lines on the inset map denote the plate boundaries.

Figure S20. The same as Figure S19 but along 15 profiles in the E-W direction.

Figure S21. The same as Figure S19 but along 15 profiles in the NW-SE direction.

Figure S22. The same as Figure S19 but along 15 profiles in the NE-SW direction.

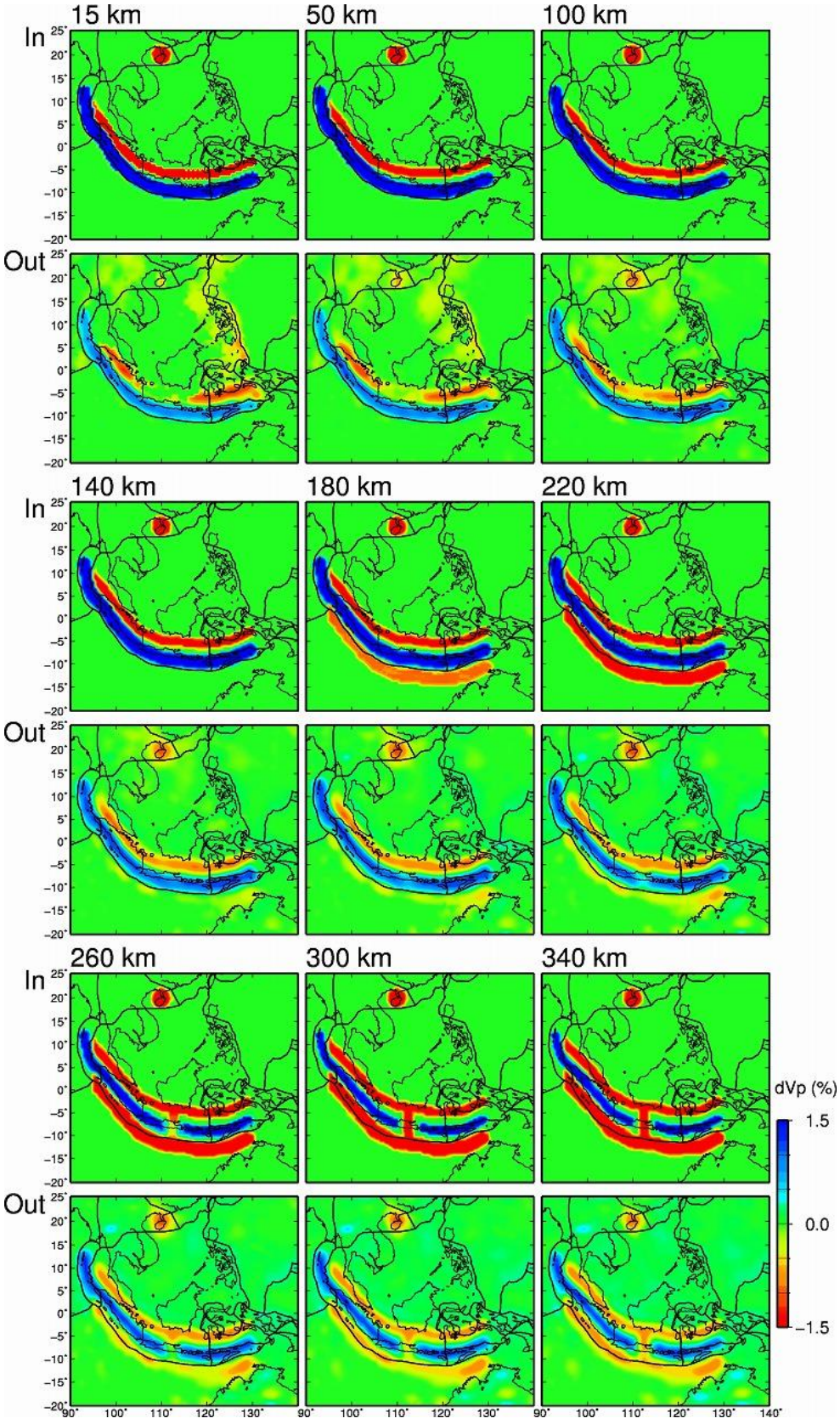
15 km
50 km
100 km
In
Out
140 km
180 km
220 km
In
Out
260 km
300 km
340 km
In
Out
dVp (%)
1.5
0.0
−1.5

Figure S23.

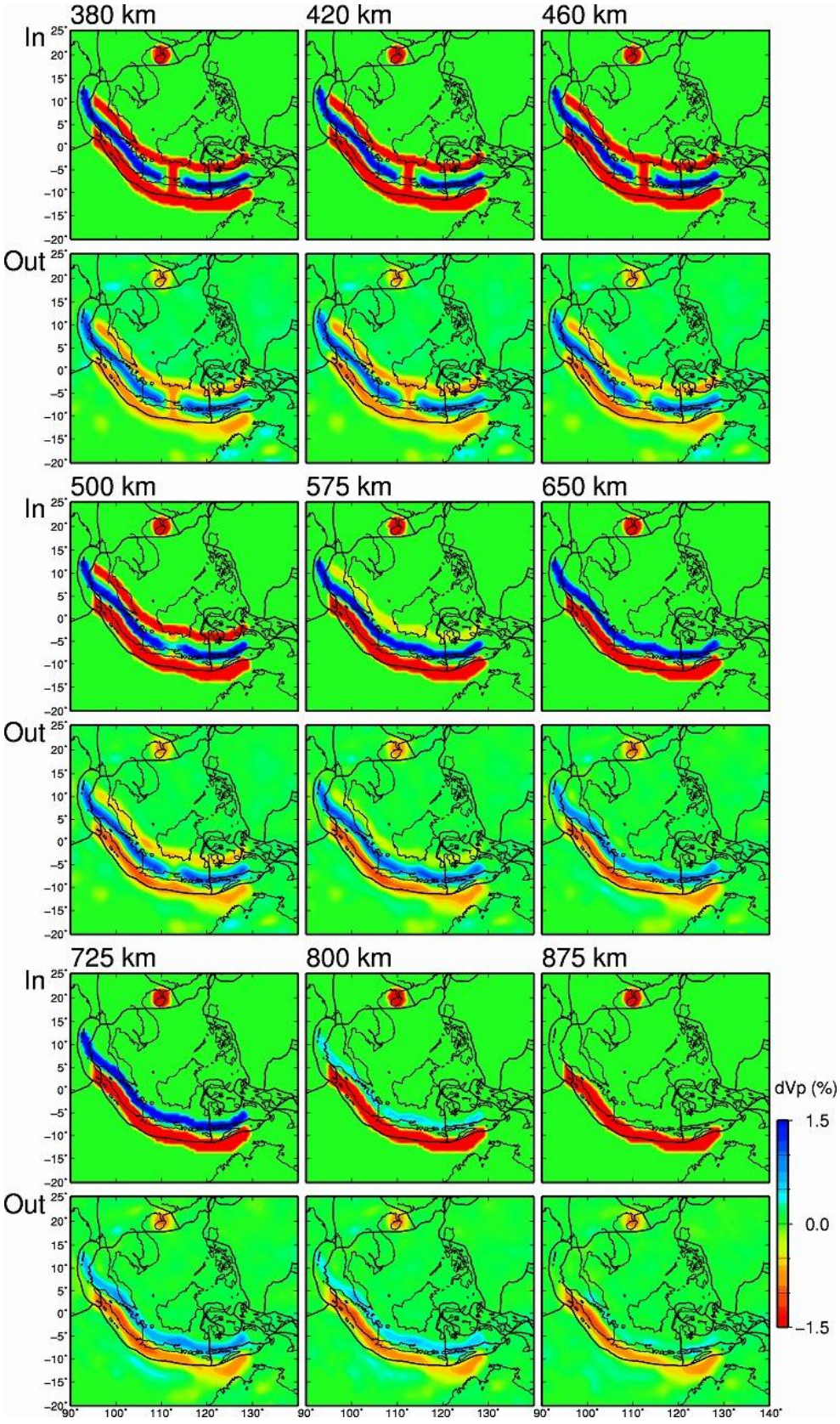

177 **Figure S23.** (continued).

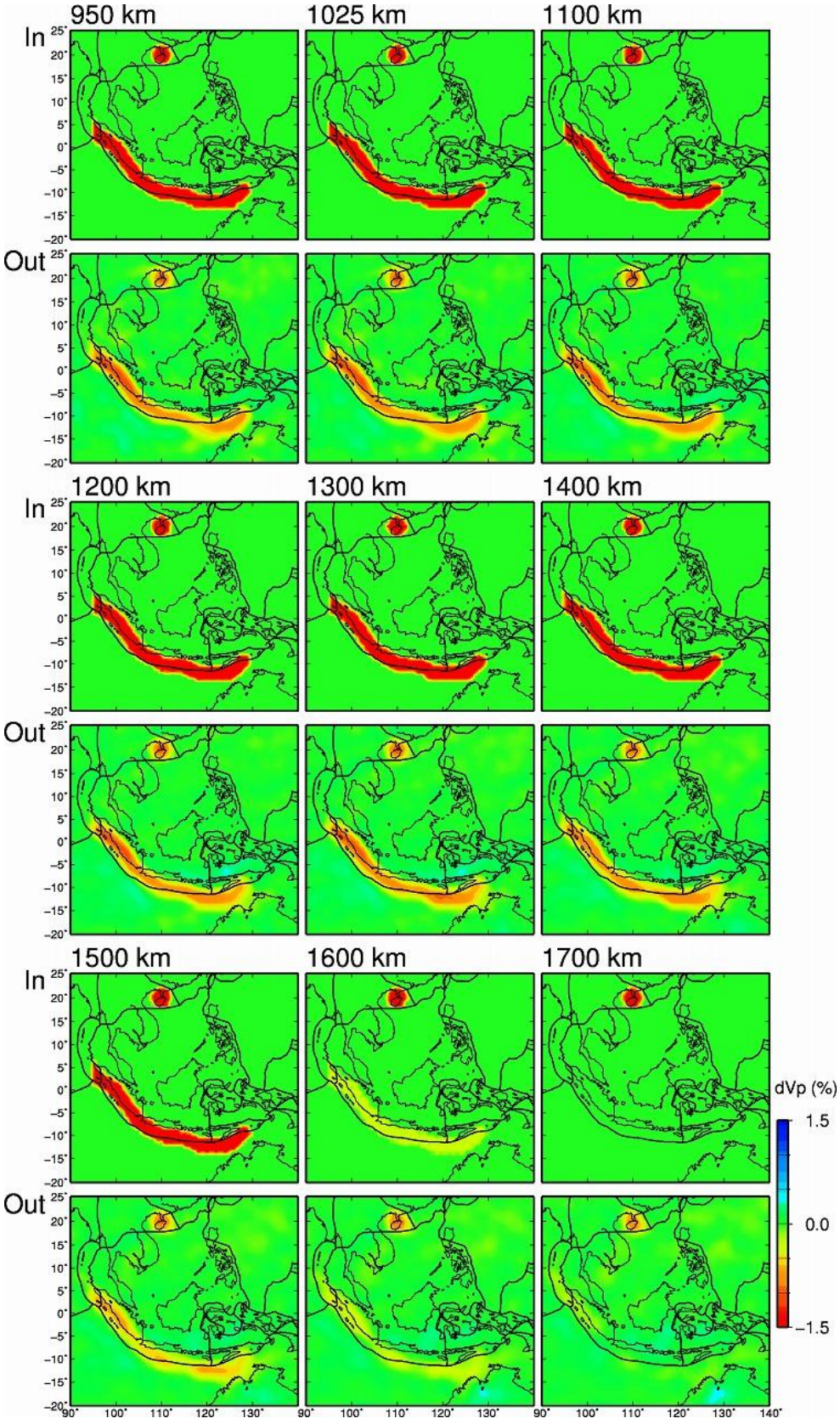

Figure S23. (continued).

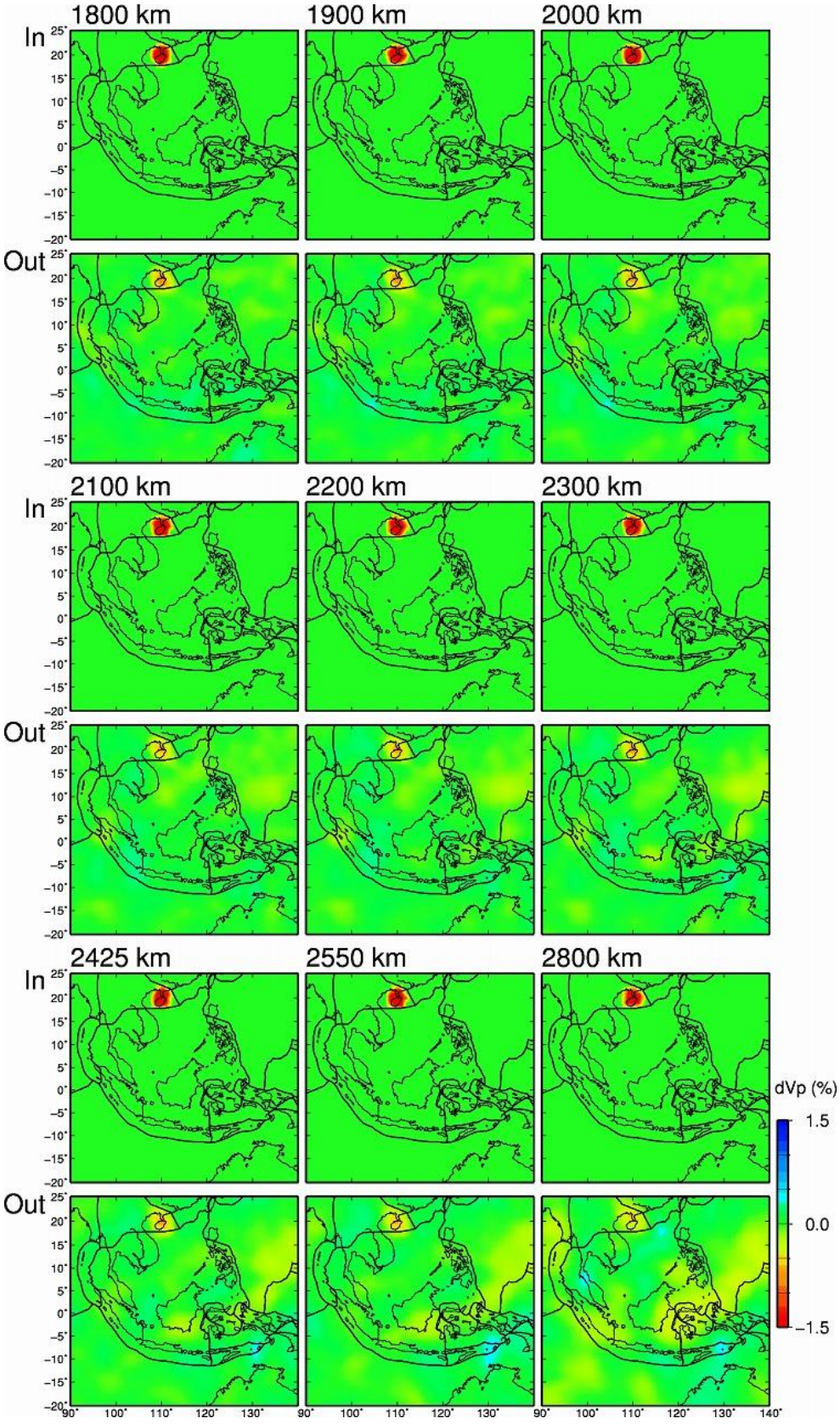

Figure S23. (continued).

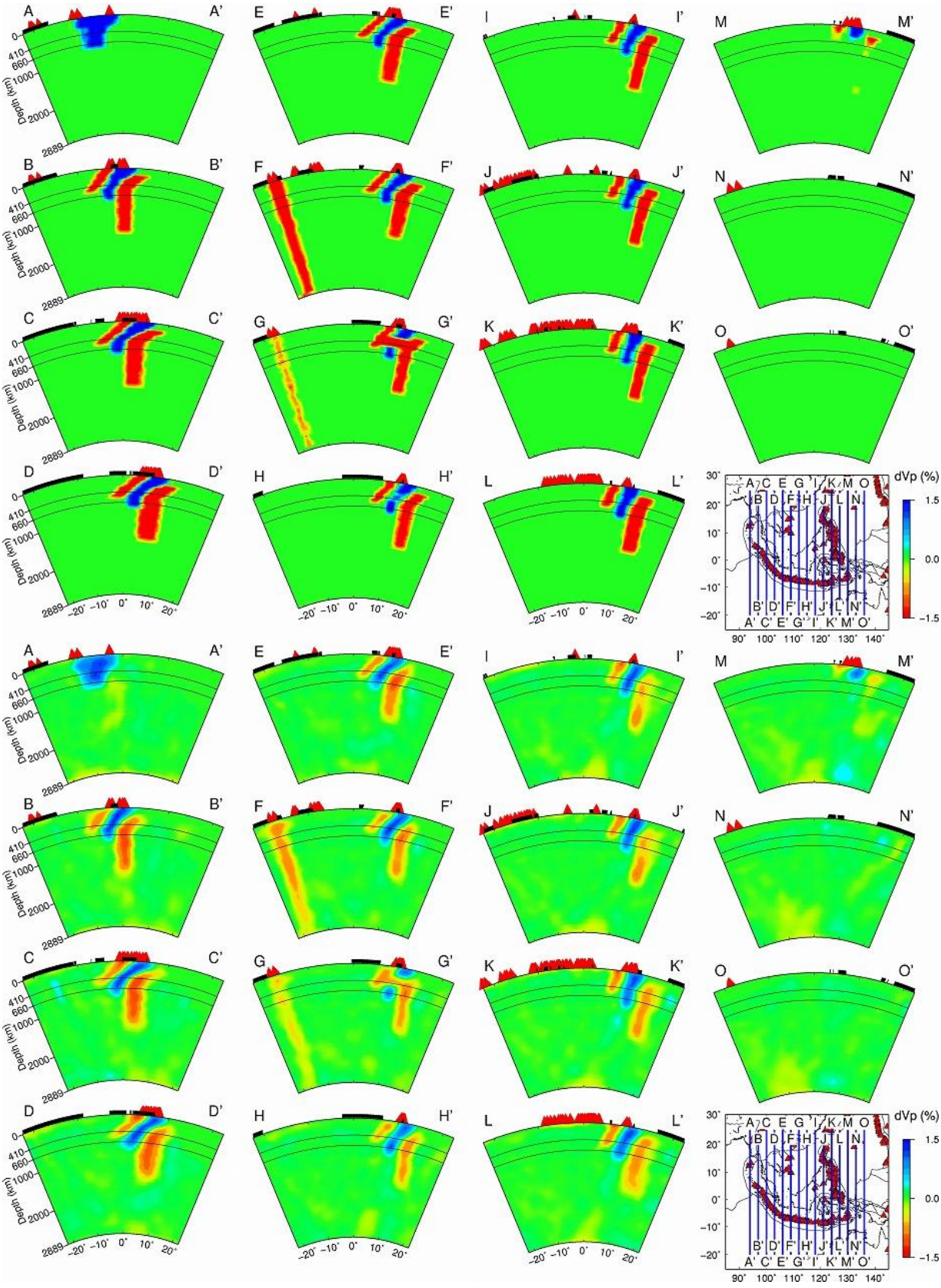
A A'
E E'
I I'
M M'
B B'
F F'
J J'
N N'
C C'
G G'
K K'
O O'
D D'
H H'
L L'
Depth (km)
0
410
660
1000
2000
2889
−20° −10° 0° 10° 20°
dVp (%)
1.5
0.0
−1.5
30°
20°
10°
0°
−10°
−20°
90° 100° 110° 120° 130° 140°

Figure S24.

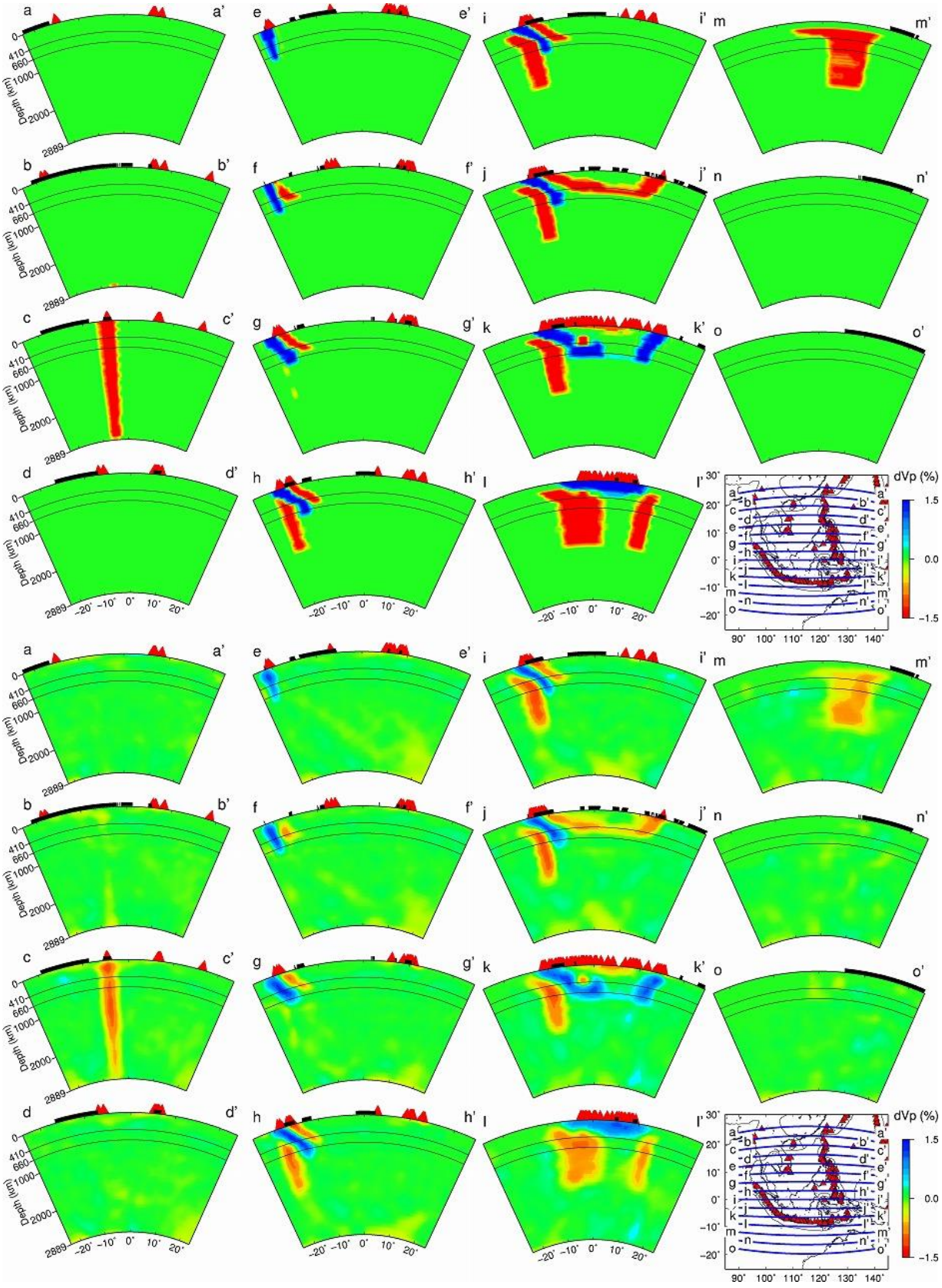

Figure S25.

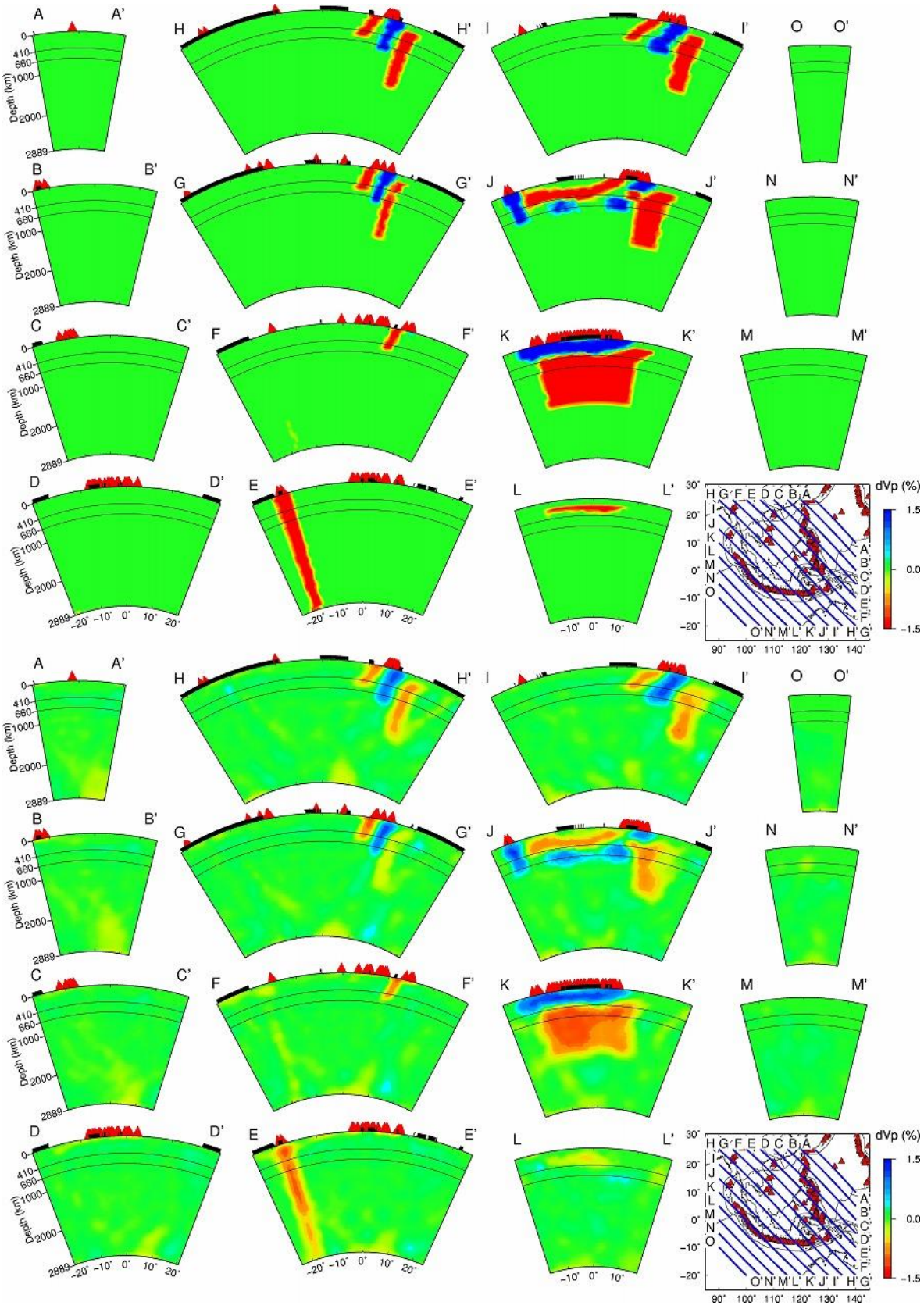
A
A'
H
H'
I
I'
O
O'
B
B'
G
G'
J
J'
N
N'
C
C'
F
F'
K
K'
M
M'
D
D'
E
E'
L
L'
Depth (km)
0
410
660
1000
2000
2889
dVp (%)
1.5
0.0
-1.5

Figure S26.

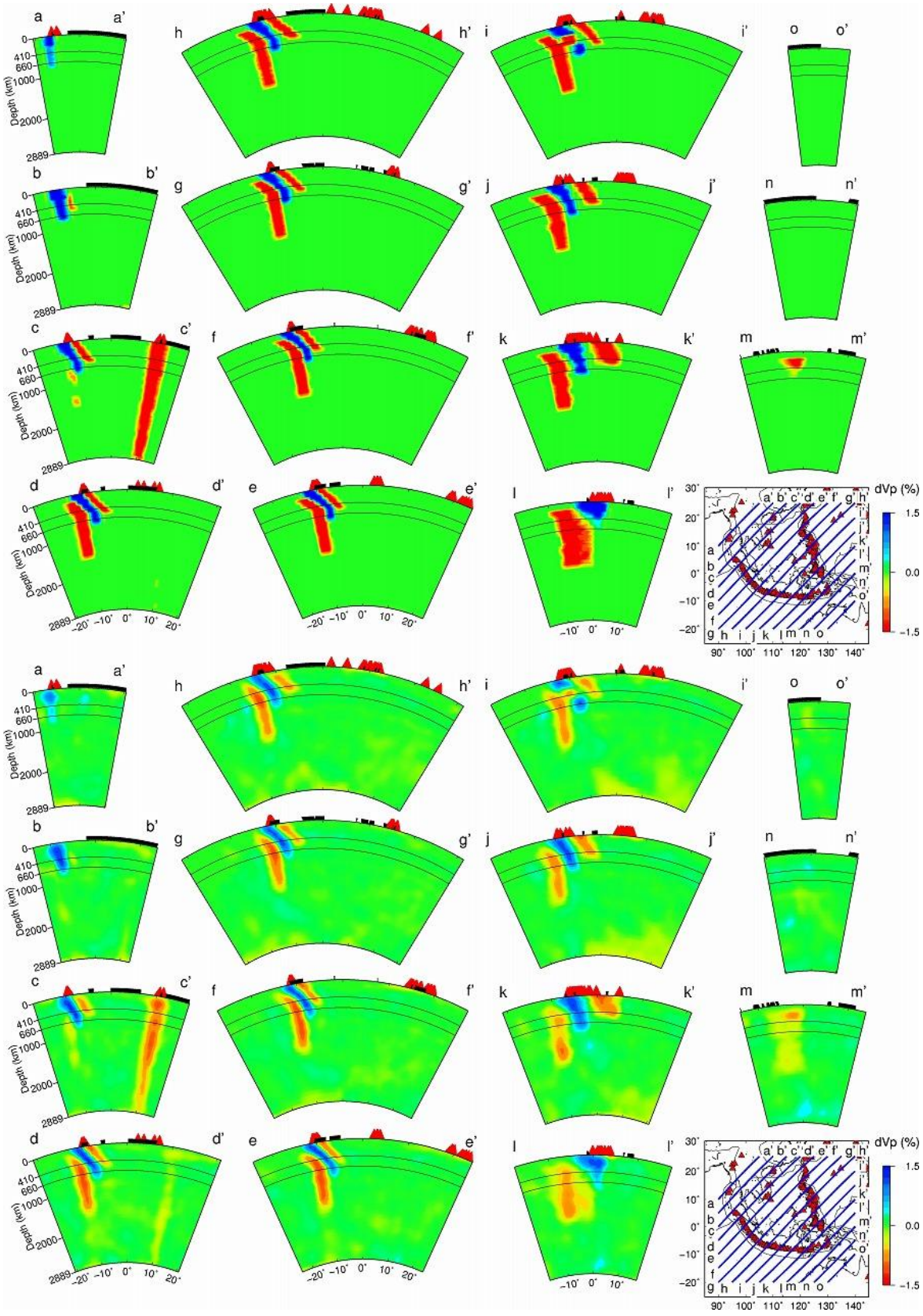

Figure S27.

Figure S23. The same as Figure S18 but for the synthetic resolution test with (1) high-Vp subducting Australian slab, (2) low-Vp hot mantle upwelling in the mantle wedge, (3) low-Vp subslab hot mantle upwelling (SHMU), (4) a hole in the Australian slab at depths of 260−460 km and latitudes 110°−115°, (5) a low-Vp bridge connecting (2) and (3) through the slab hole, and (6) low-Vp whole-mantle Hainan plume (SRT1).

Figure S24. Vertical cross-sections showing **(top)** the input model and **(bottom)** output results of the SRT1 along 15 profiles in the N-S direction. Locations of the profiles are shown on the inset map. The 410-km and the 660-km discontinuities are shown in black solid lines. The thick black lines on the surface denote land areas. The red triangles denote active volcanoes. The thin black lines on the inset map denote the plate boundaries.

Figure S25. The same as Figure S24 but along 15 profiles in the E-W direction.

Figure S26. The same as Figure S24 but along 15 profiles in the NW-SE direction.

Figure S27. The same as Figure S24 but along 15 profiles in the NE-SW direction.

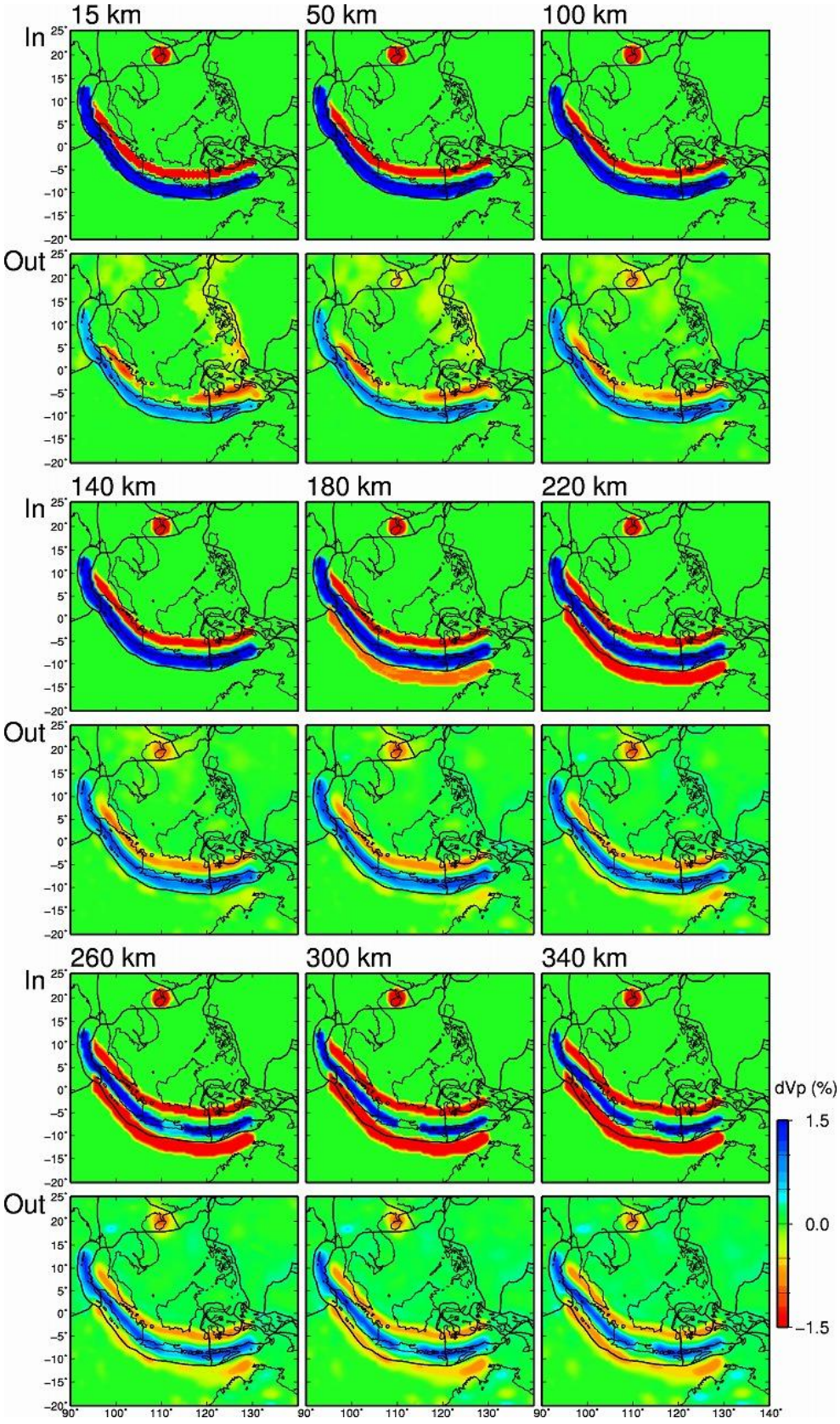
15 km
50 km
100 km
In
Out
140 km
180 km
220 km
In
Out
260 km
300 km
340 km
In
Out
dVp (%)
1.5
0.0
−1.5

Figure S28.

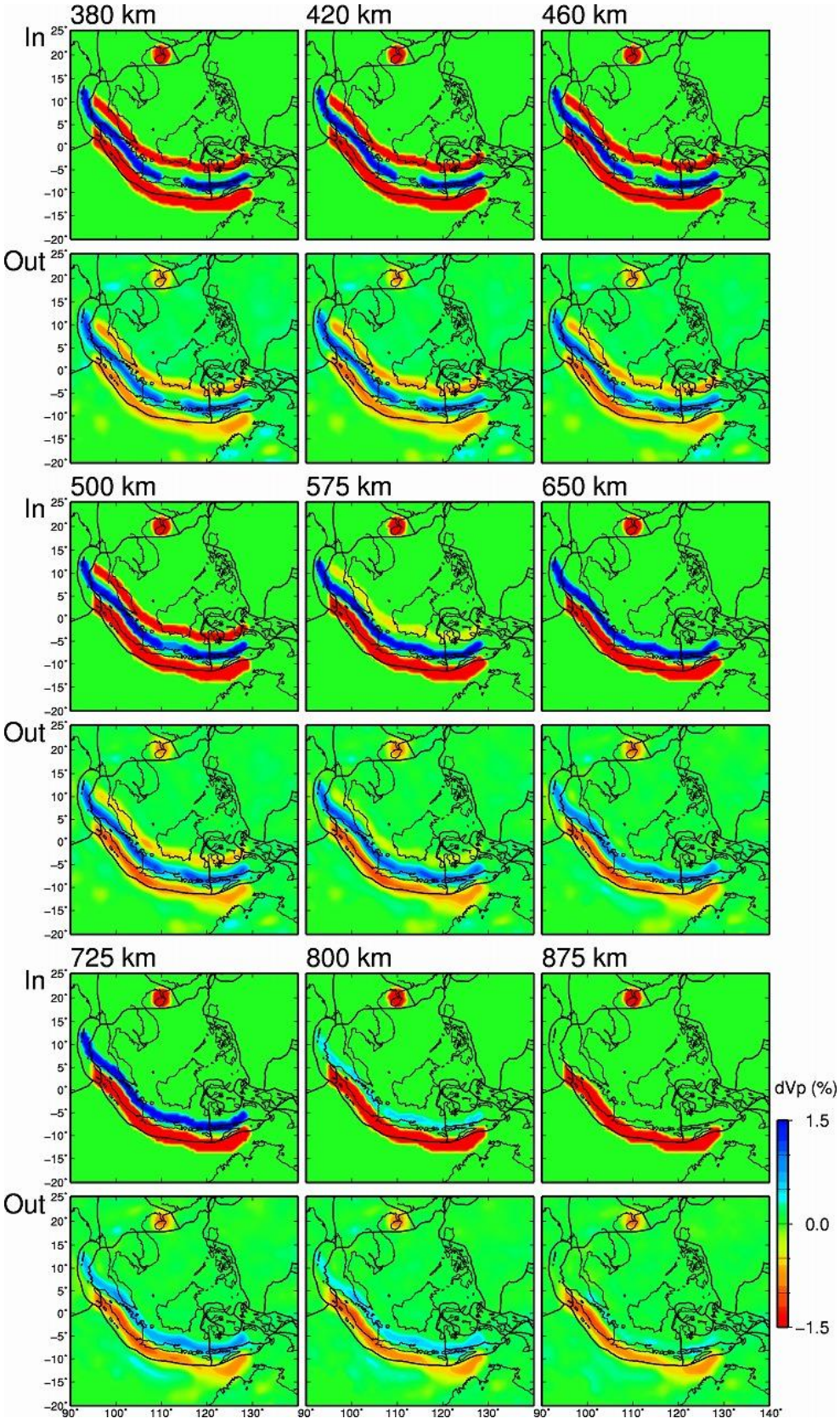

Figure S28. (continued).

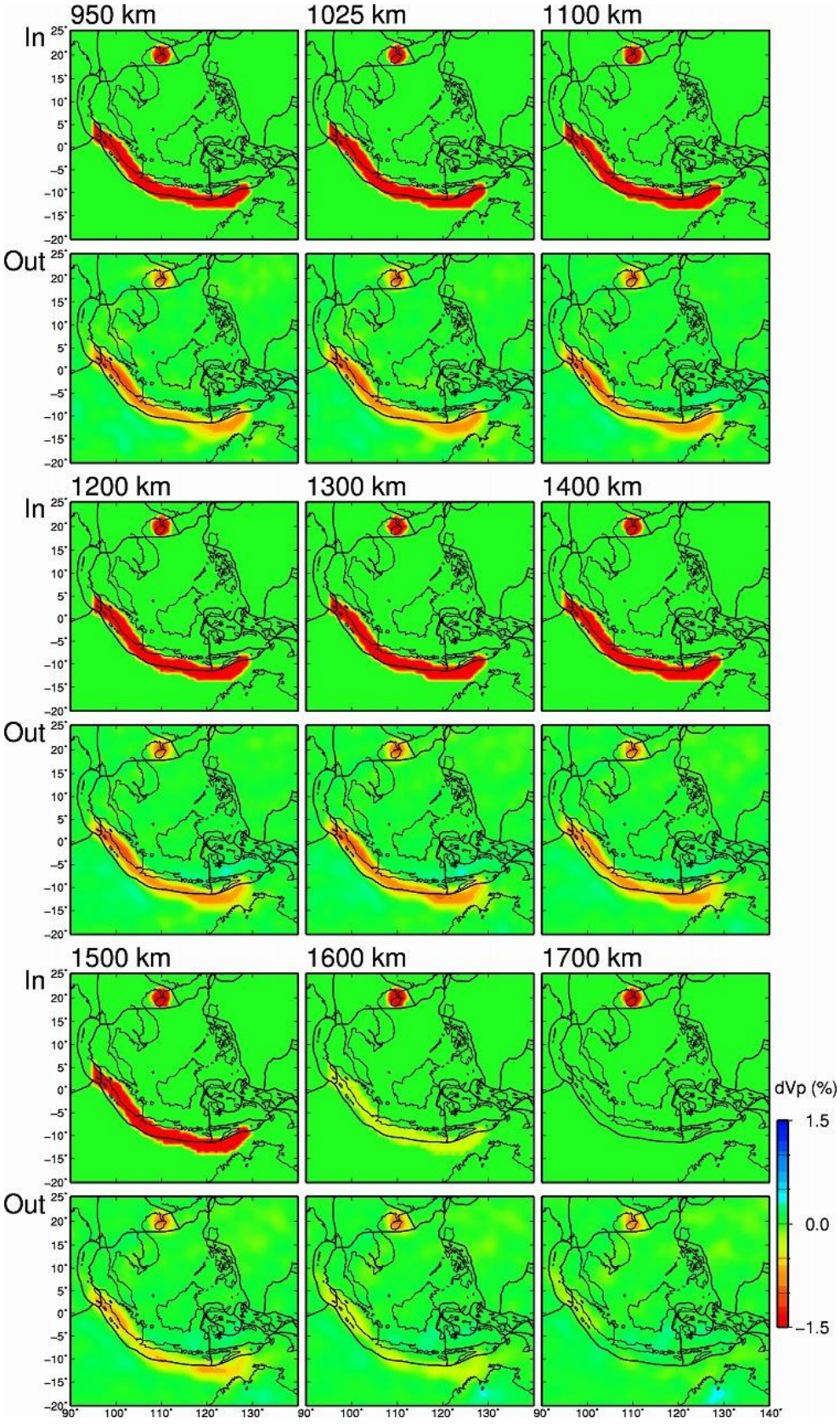

Figure S28. (continued).

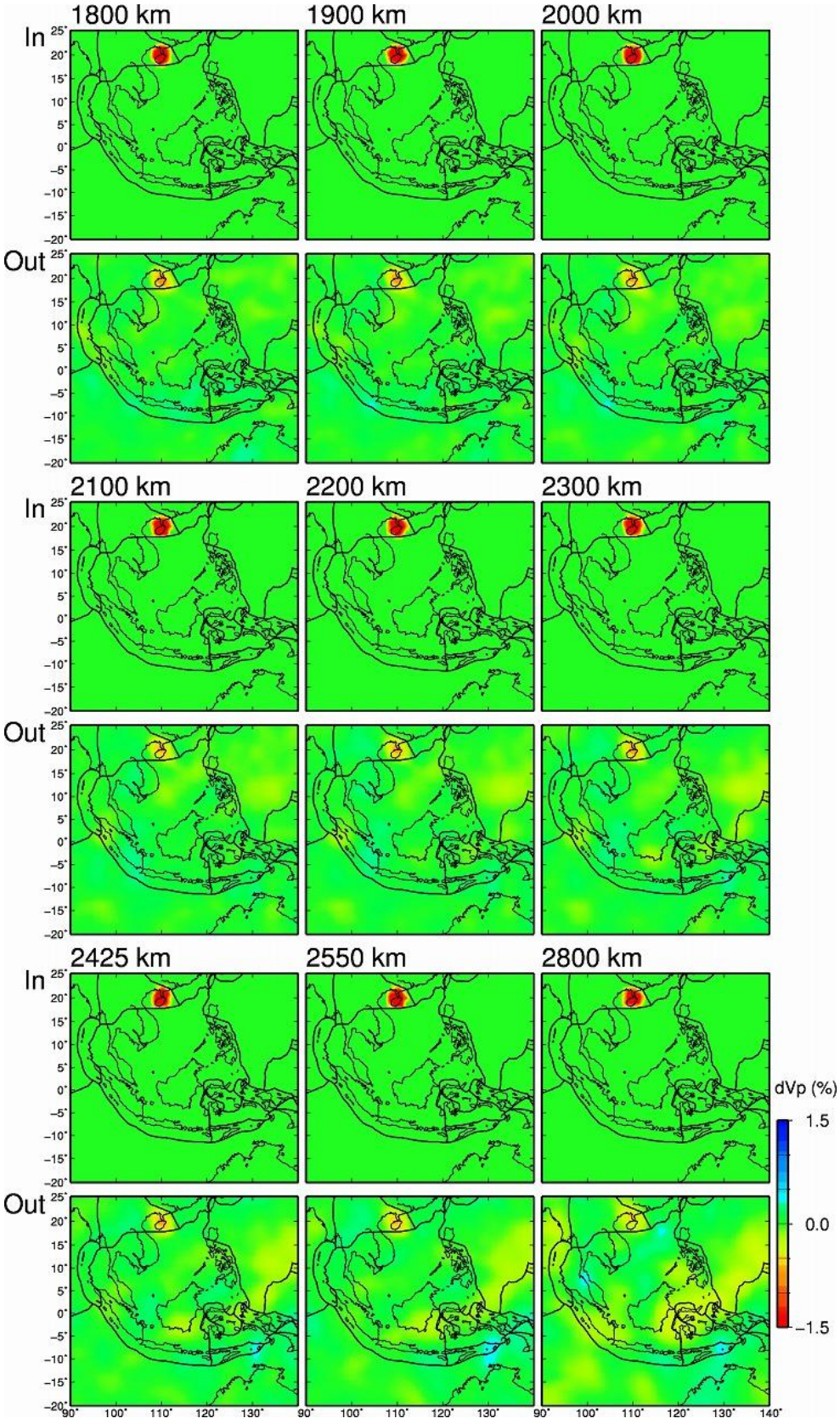

Figure S28. (continued).

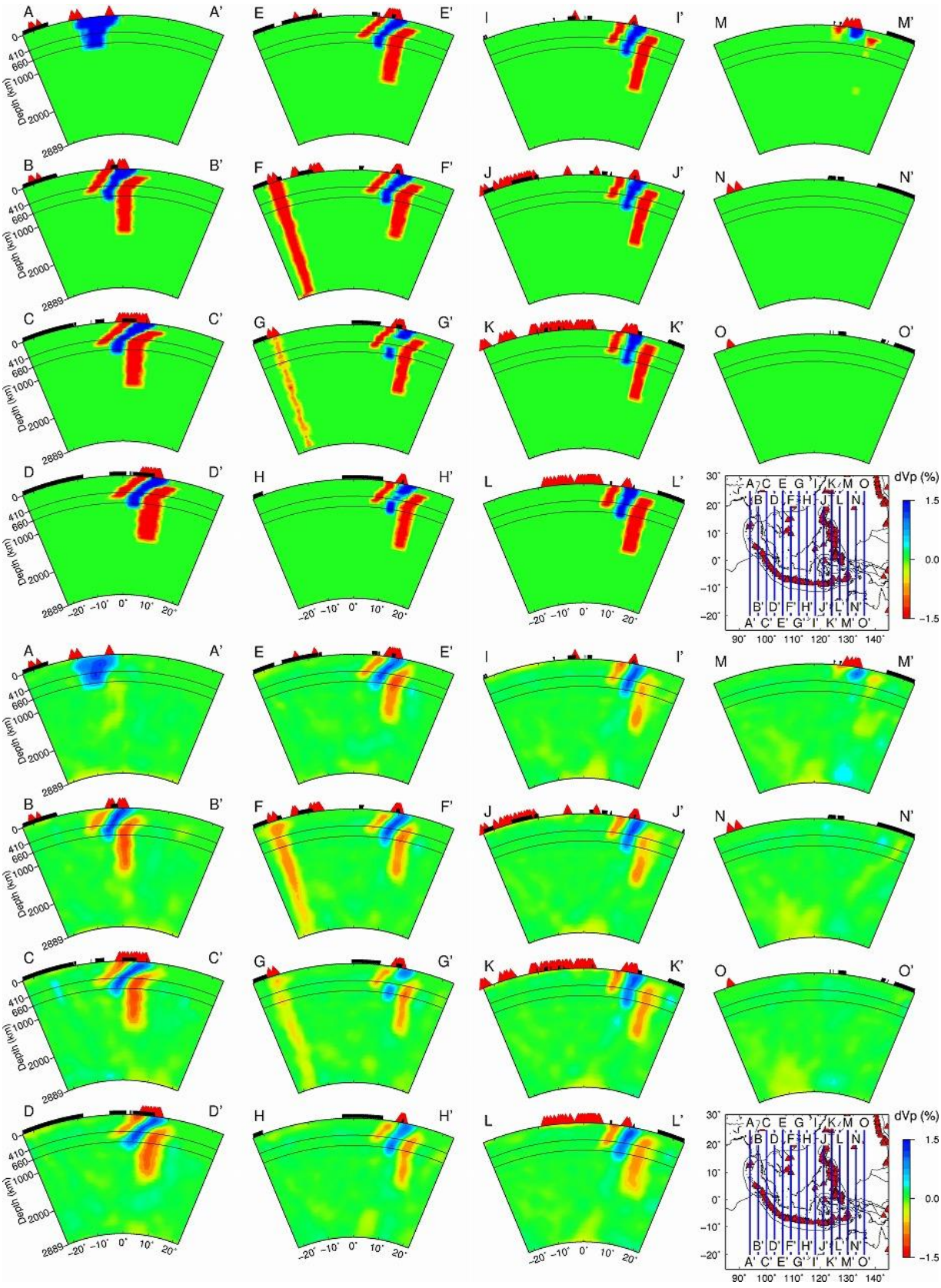

211 **Figure S29.**

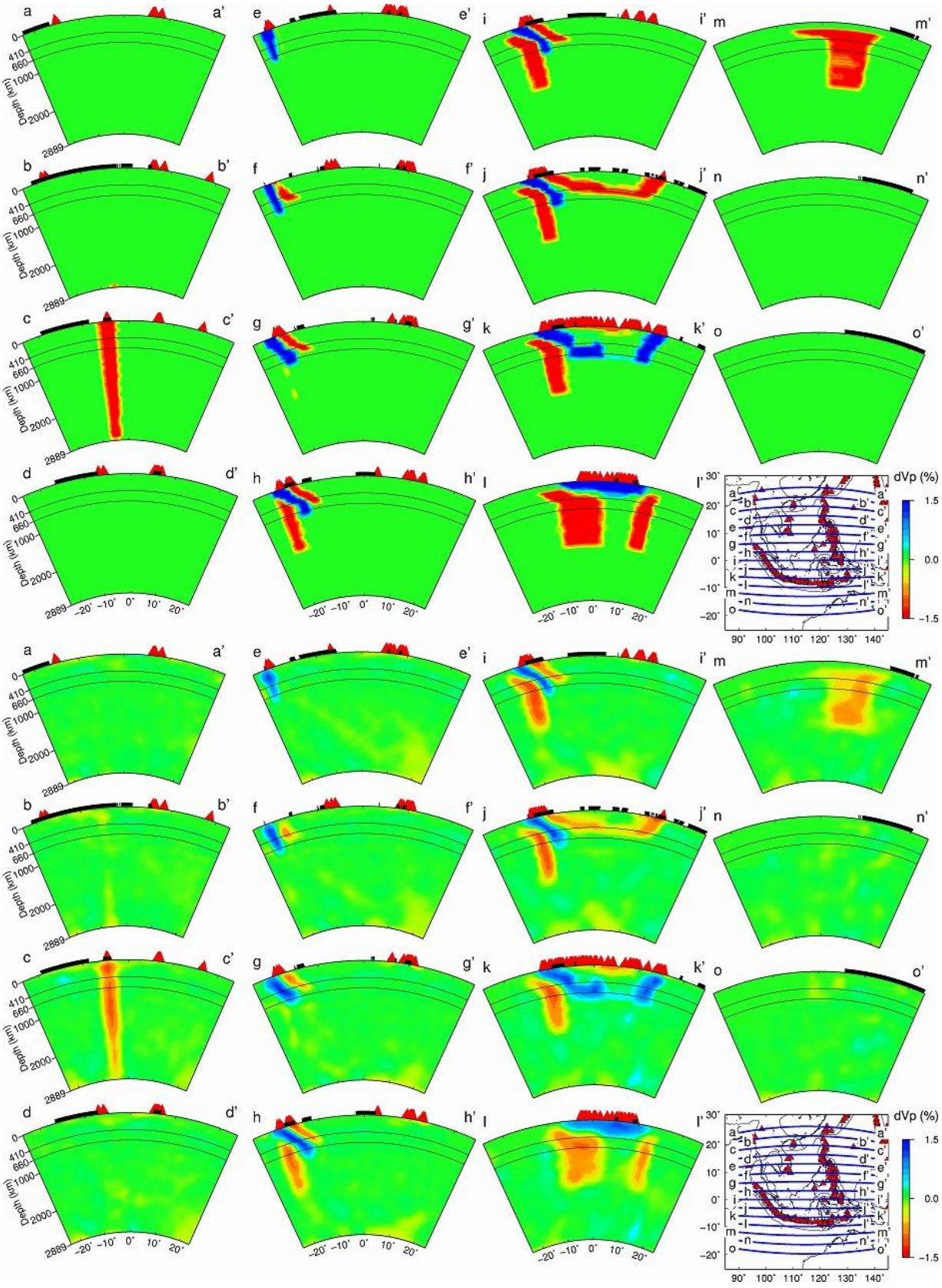

212 **Figure S30.**

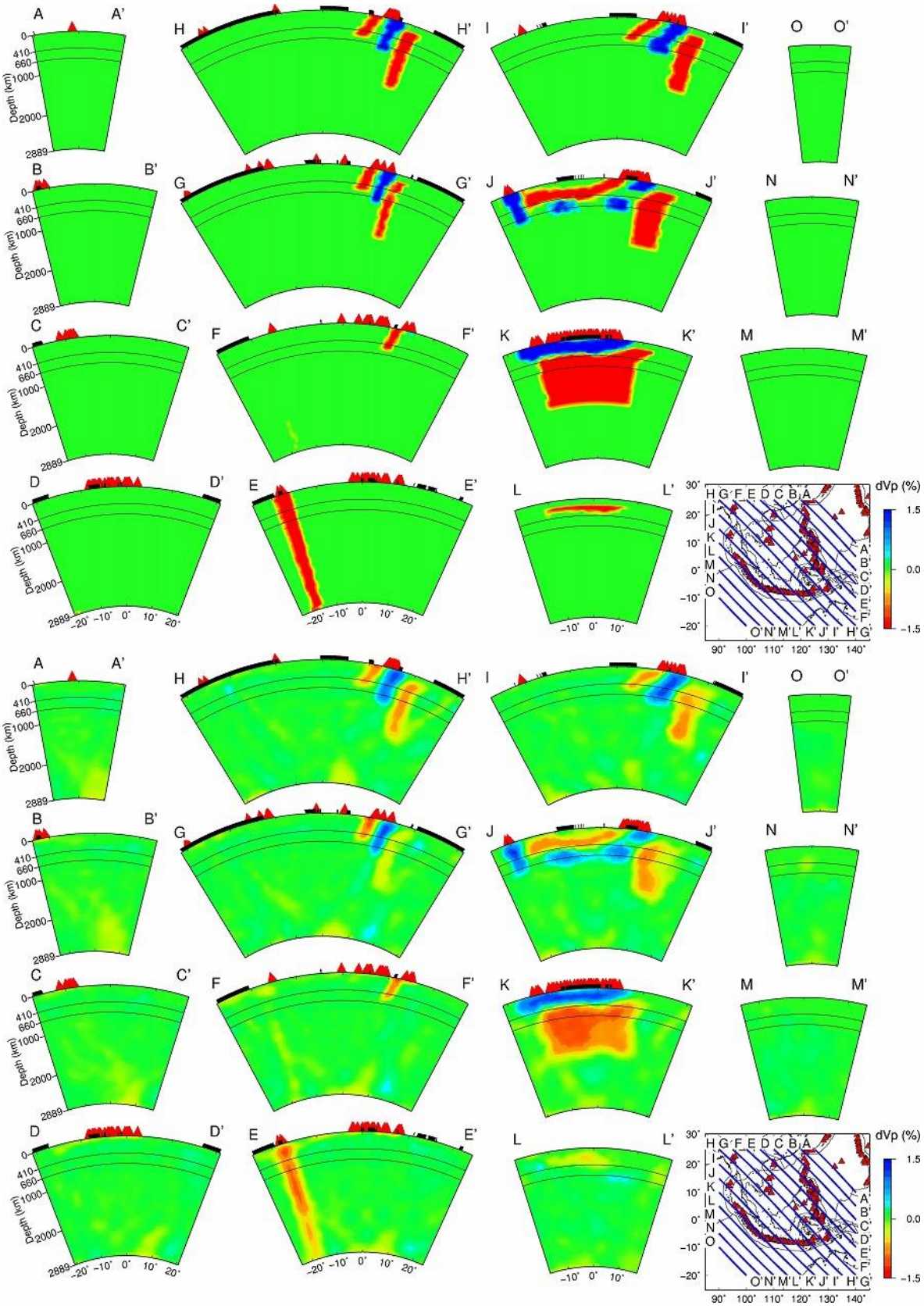

213 **Figure S31.**

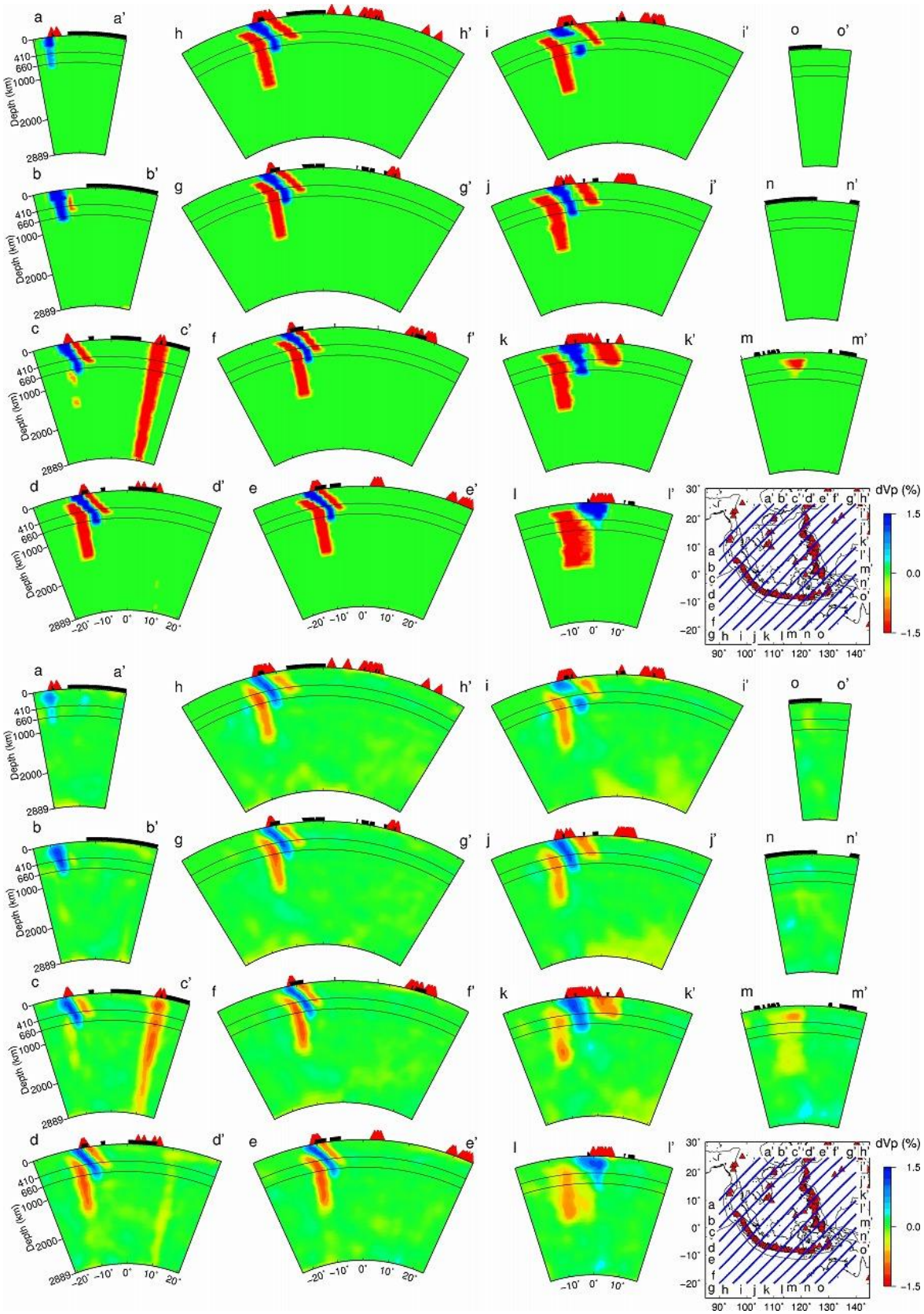

Figure S32.

Figure S28. The same as Figure S23 but for the synthetic resolution test without a low-Vp bridge through the slab hole (SRT2).

Figure S29. Vertical cross-sections showing **(top)** the input model and **(bottom)** output results of the SRT2 along 15 profiles in the N-S direction. Locations of the profiles are shown on the inset map. The 410-km and the 660-km discontinuities are shown in black solid lines. The thick black lines on the surface denote land areas. The red triangles denote active volcanoes. The thin black lines on the inset map denote the plate boundaries.

Figure S30. The same as Figure S29 but along 15 profiles in the E-W direction.

Figure S31. The same as Figure S29 but along 15 profiles in the NW-SE direction.

Figure S32. The same as Figure S29 but along 15 profiles in the NE-SW direction.

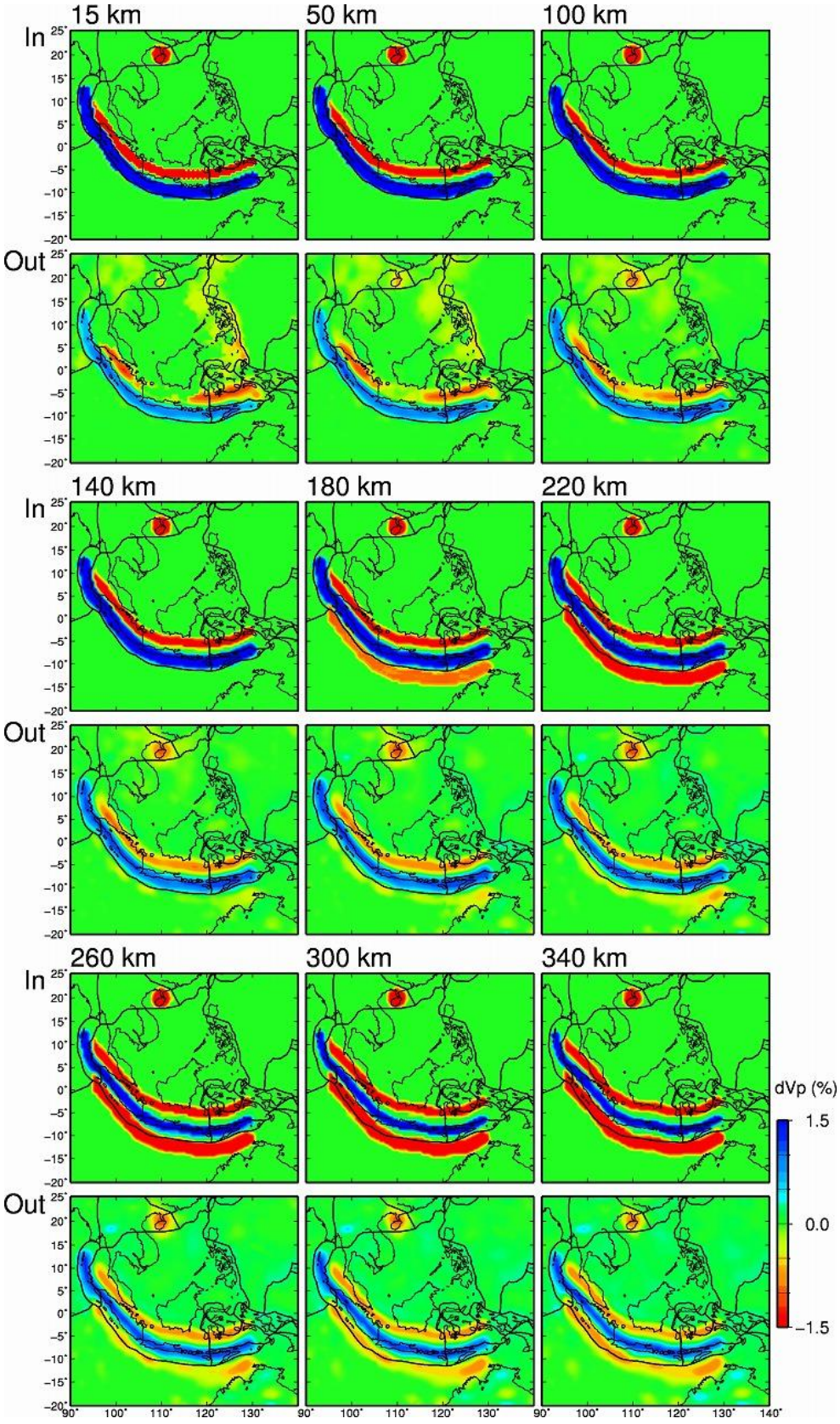
15 km
50 km
100 km
In
Out
140 km
180 km
220 km
In
Out
260 km
300 km
340 km
In
Out
dVp (%)
1.5
0.0
−1.5

Figure S33.

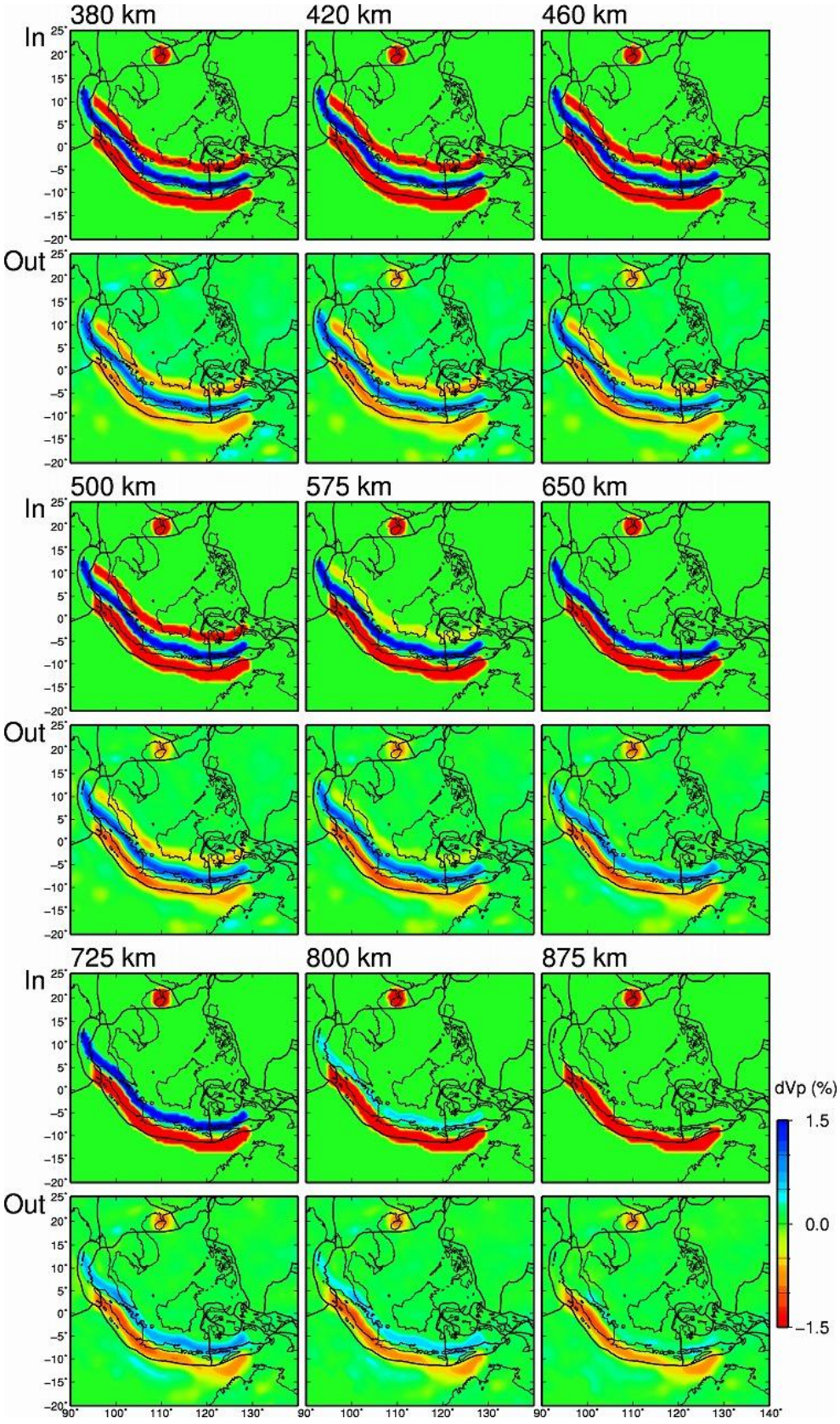

Figure S33. (continued).

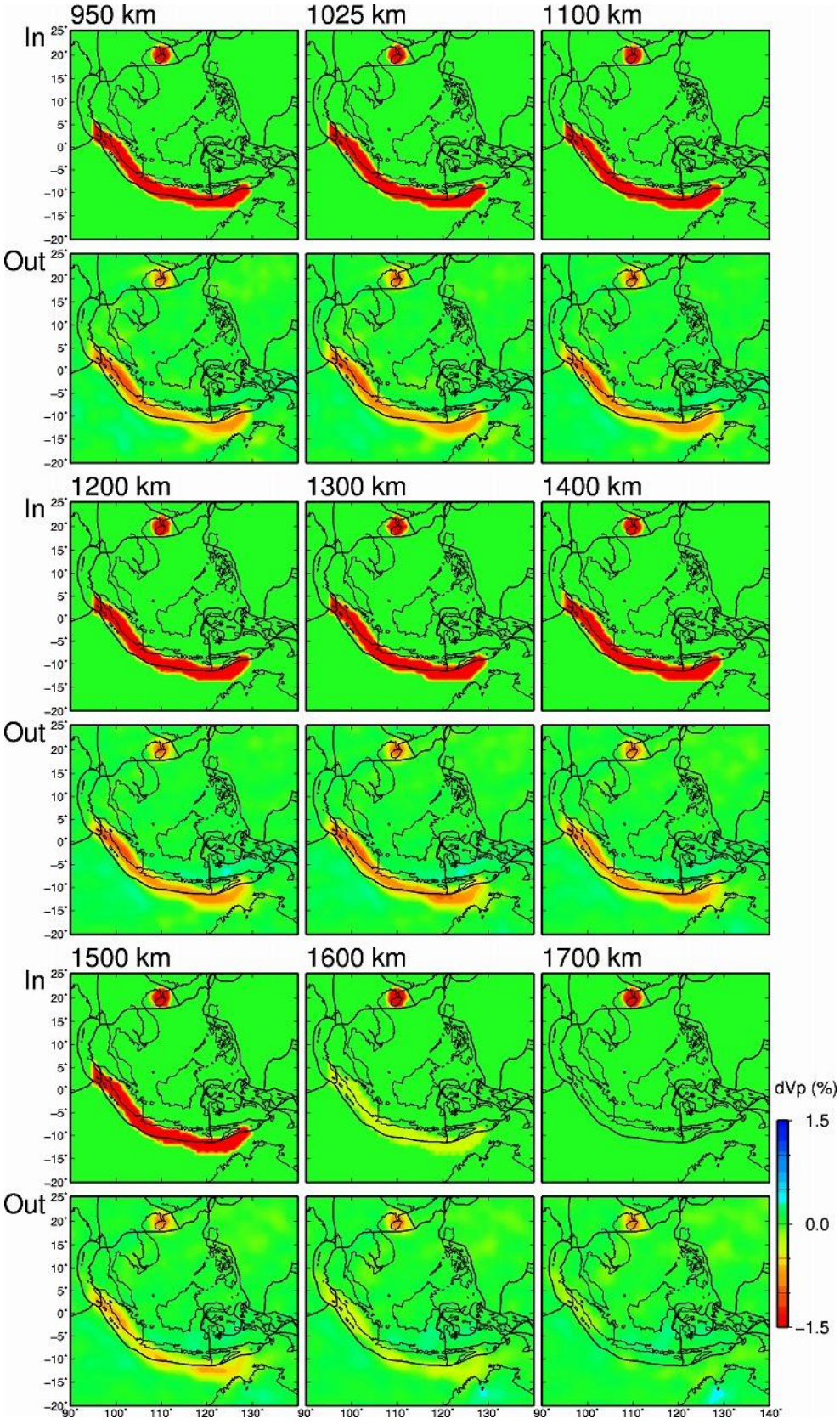

Figure S33. (continued).

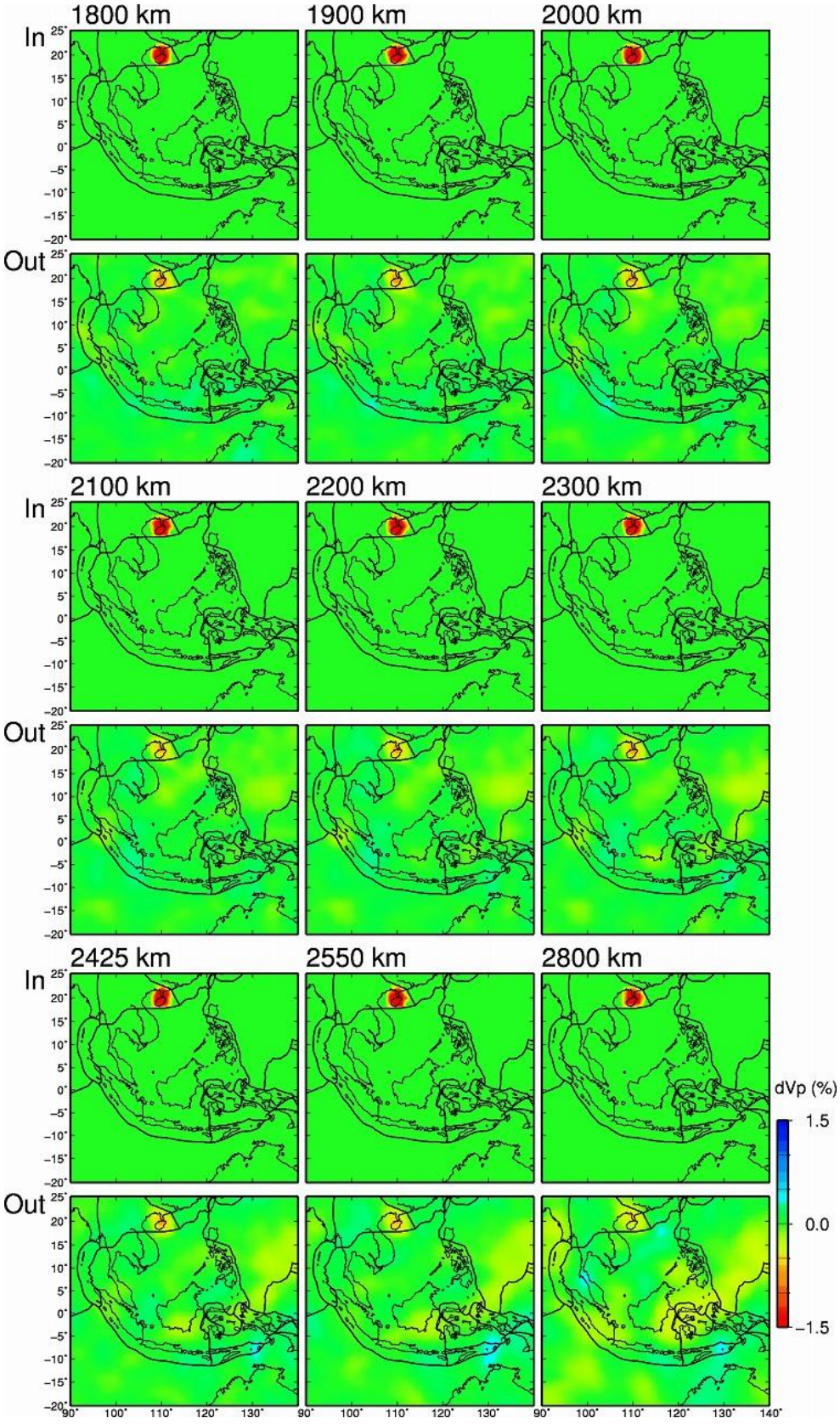

Figure S33. (continued).

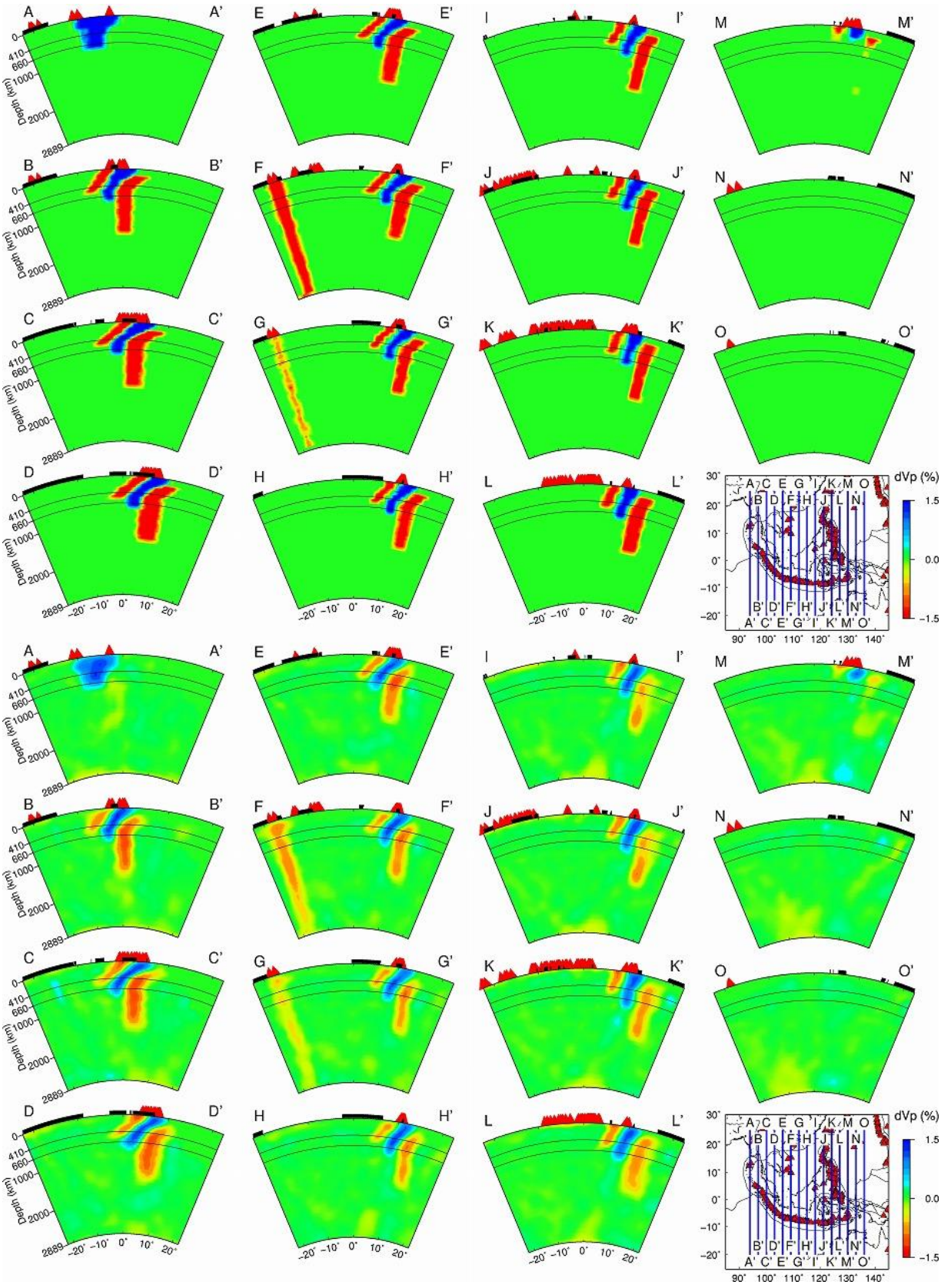
A
A'
E
E'
I
I'
M
M'
B
B'
F
F'
J
J'
N
N'
C
C'
G
G'
K
K'
O
O'
D
D'
H
H'
L
L'
0
410
660
1000
2000
2889
Depth (km)
-20° -10° 0° 10° 20°
dVp (%)
1.5
0.0
-1.5
30°
20°
10°
0°
-10°
-20°
90° 100° 110° 120° 130° 140°

Figure S34.

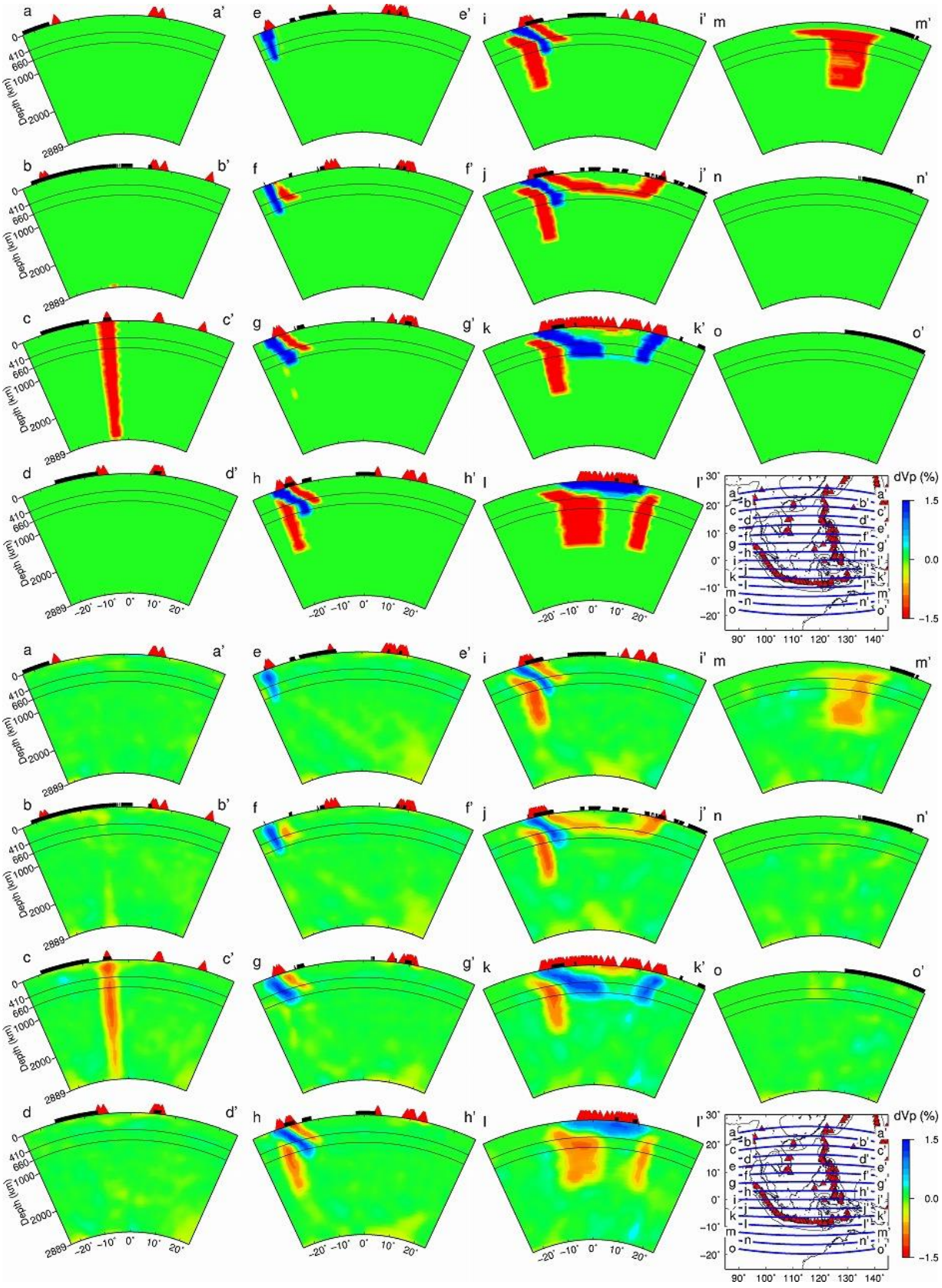

Figure S35.

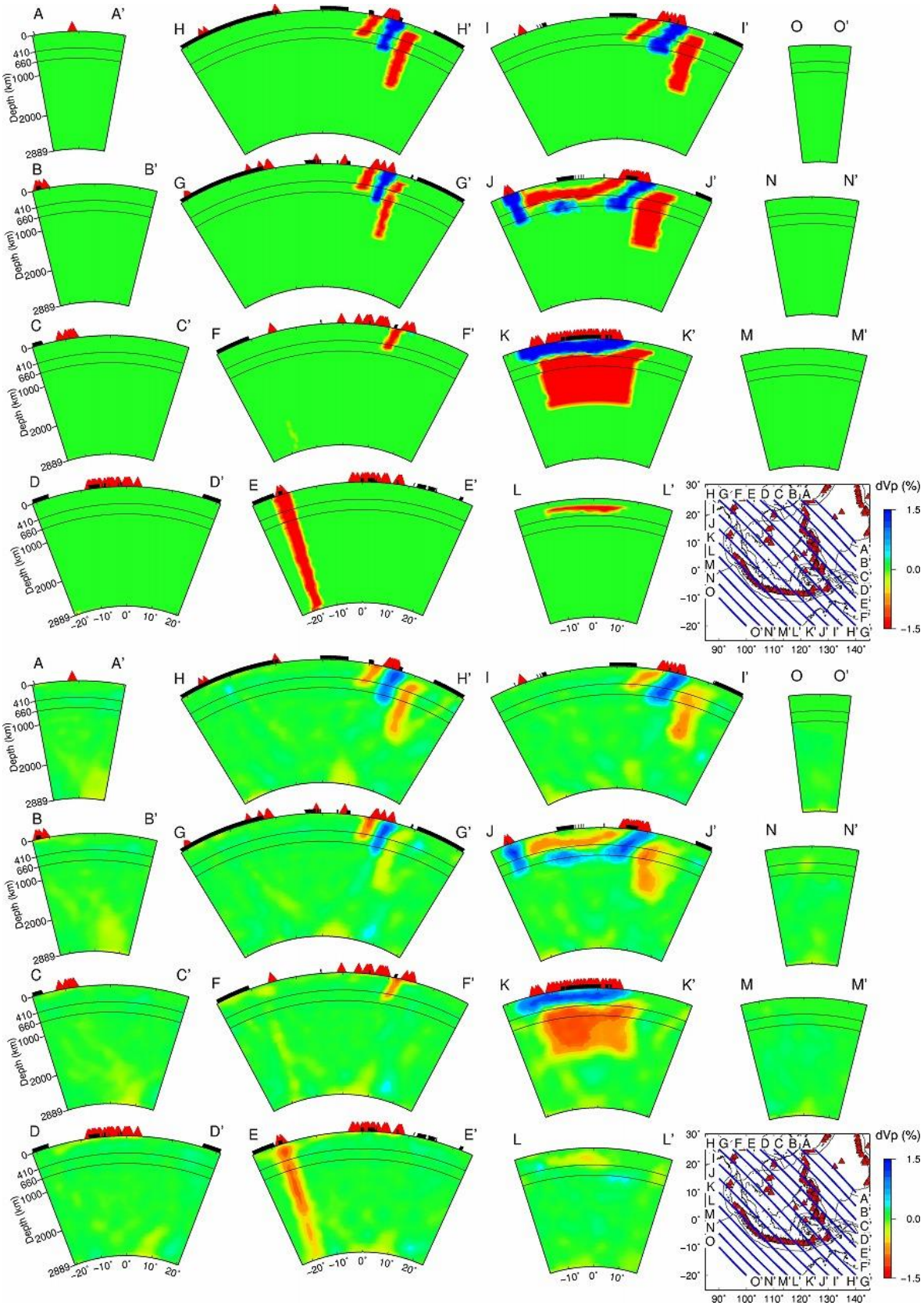

236 **Figure S36.**

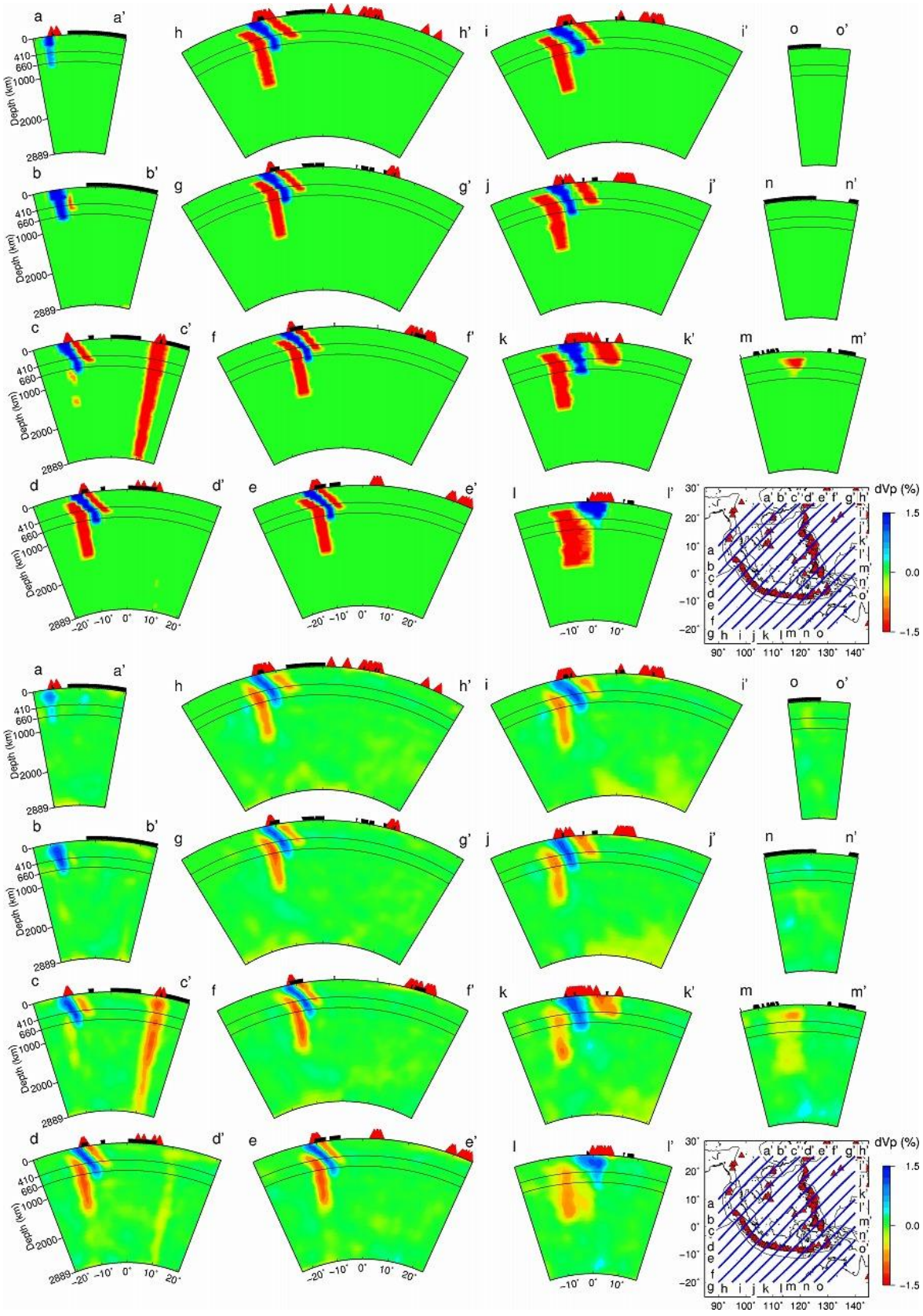

Figure S37.

238

239 **Figure S33.** The same as Figure S23 but for the synthetic resolution test without a hole in the
240 Australian slab and a low-Vp bridge through the slab hole (SRT3).

241

242 **Figure S34.** Vertical cross-sections showing **(top)** the input model and **(bottom)** output results
243 of the SRT3 along 15 profiles in the N-S direction. Locations of the profiles are shown on the
244 inset map. The 410-km and the 660-km discontinuities are shown in black solid lines. The thick
245 black lines on the surface denote land areas. The red triangles denote active volcanoes. The thin
246 black lines on the inset map denote the plate boundaries.

247

248 **Figure S35.** The same as Figure S34 but along 15 profiles in the E-W direction.

249

250 **Figure S36**. The same as Figure S34 but along 15 profiles in the NW-SE direction.

251

252 **Figure S37**. The same as Figure S34 but along 15 profiles in the NE-SW direction.

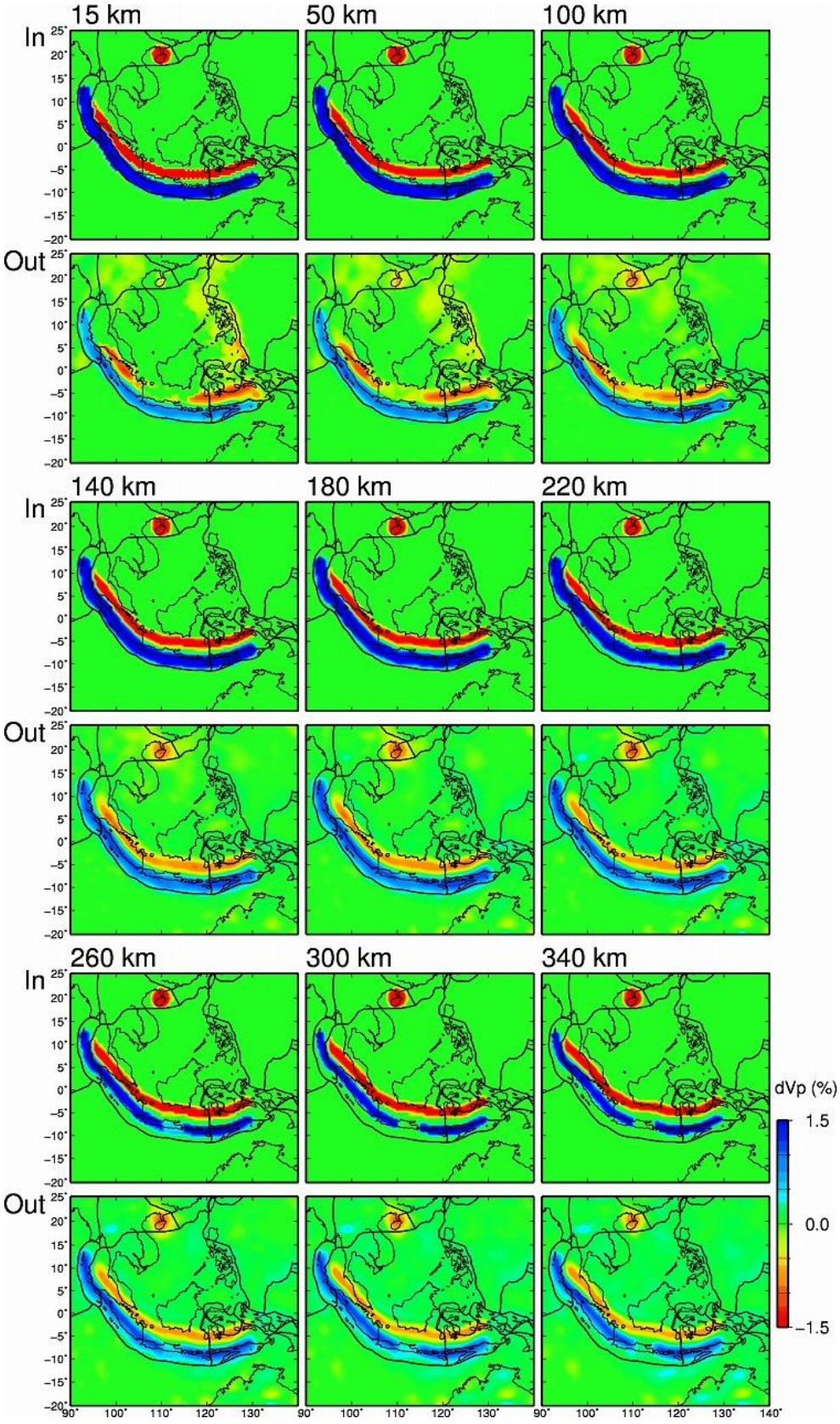
15 km
50 km
100 km
In
Out
140 km
180 km
220 km
In
Out
260 km
300 km
340 km
In
Out
dVp (%)
1.5
0.0
−1.5

Figure S38.

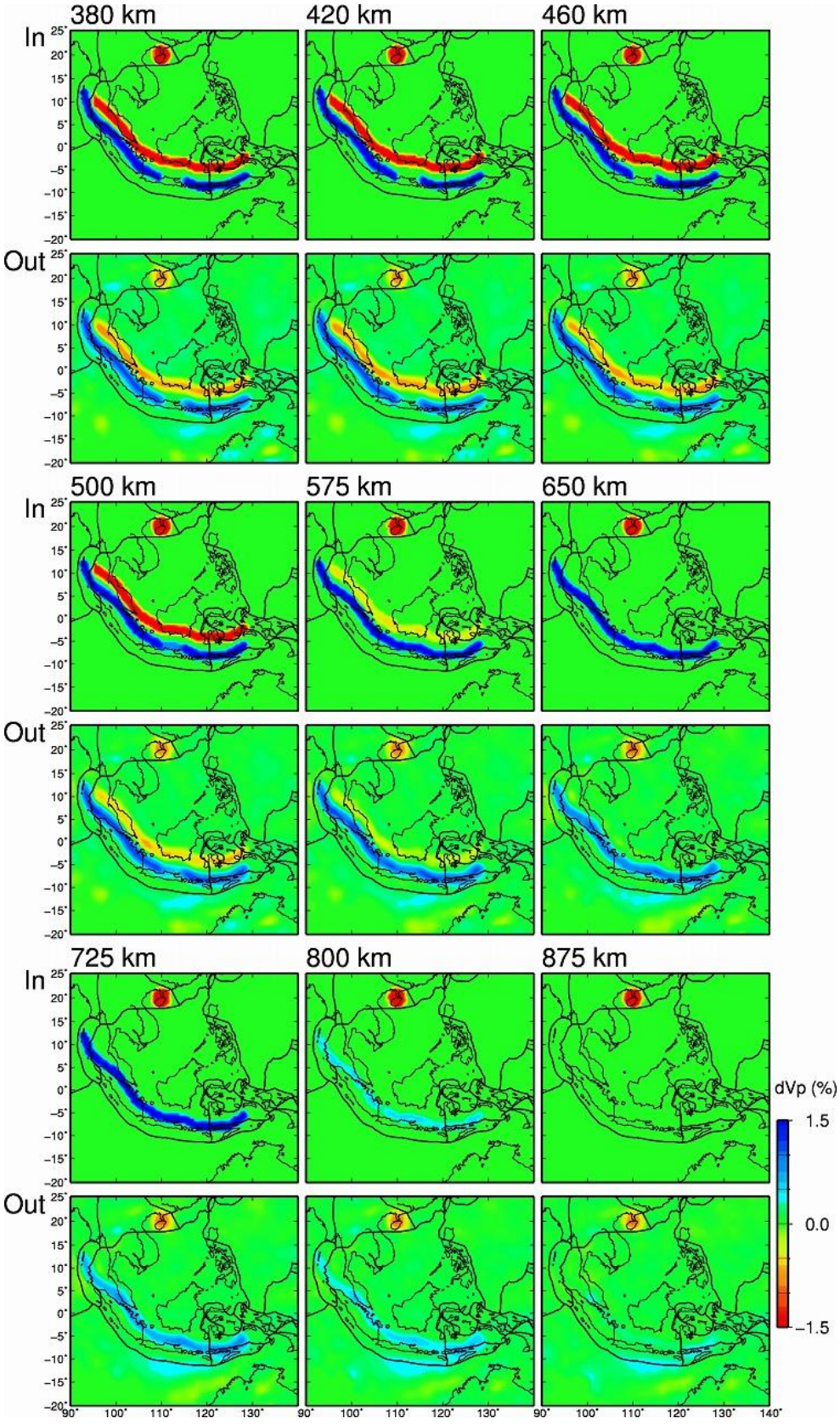

Figure S38. (continued).

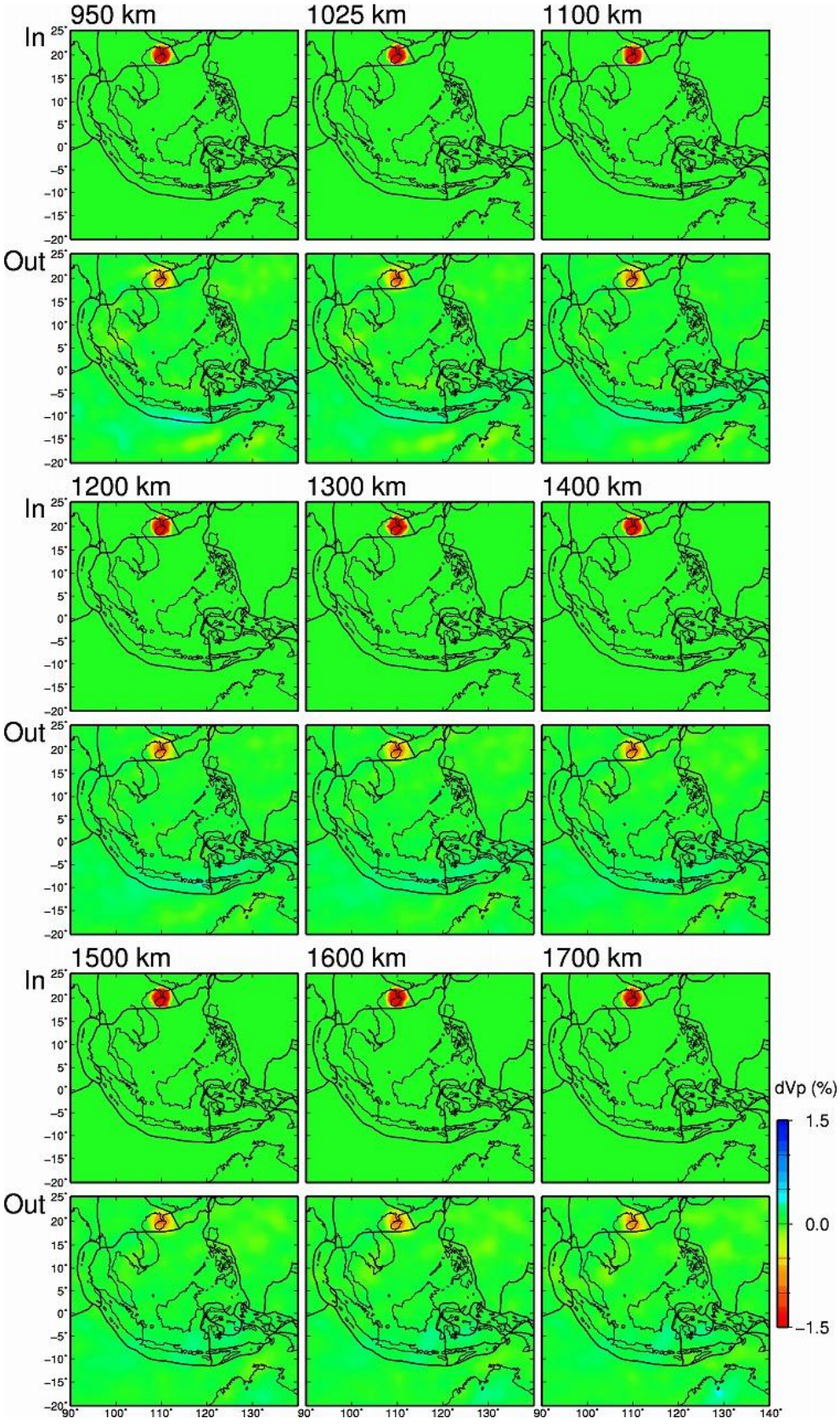

Figure S38. (continued).

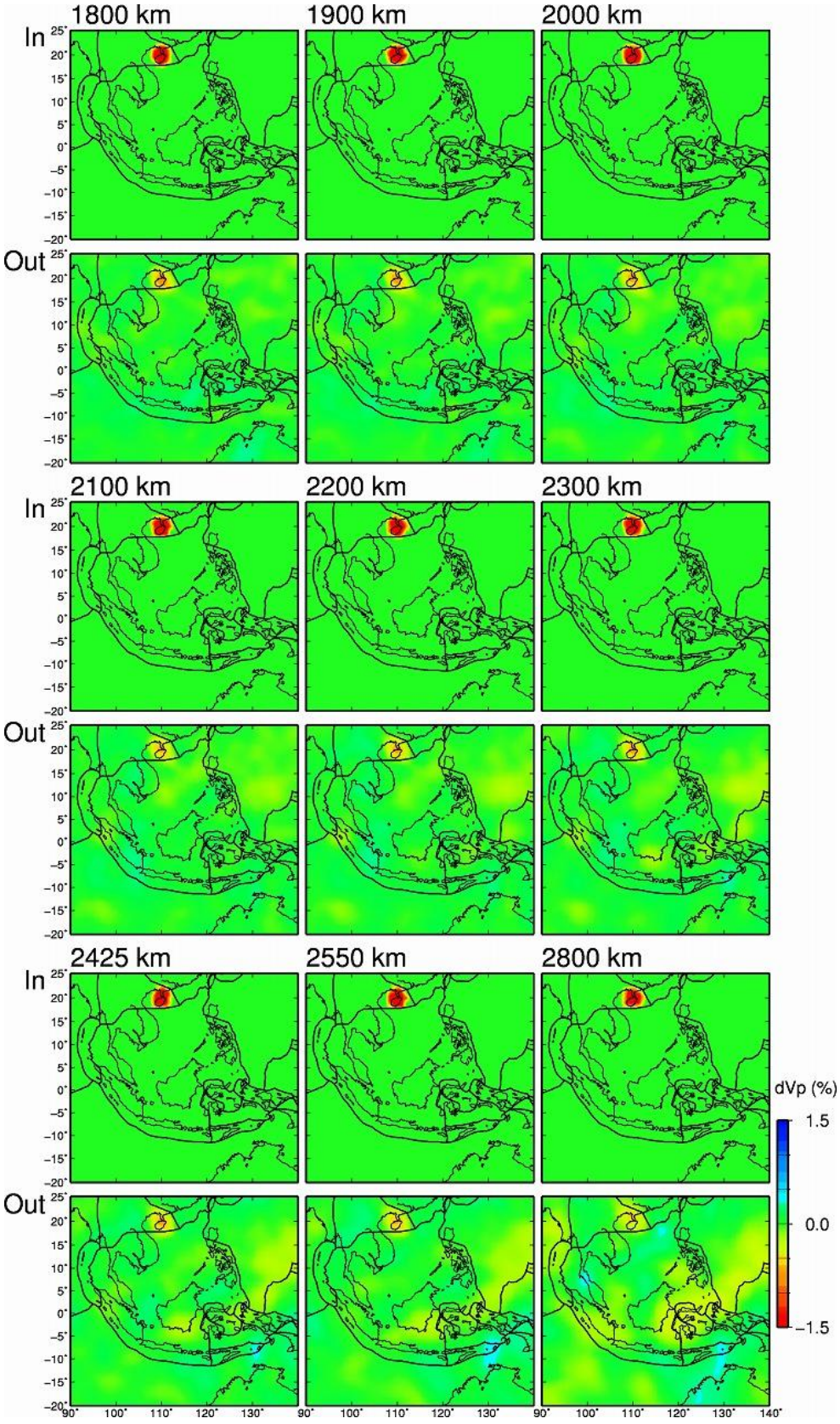

Figure S38. (continued).

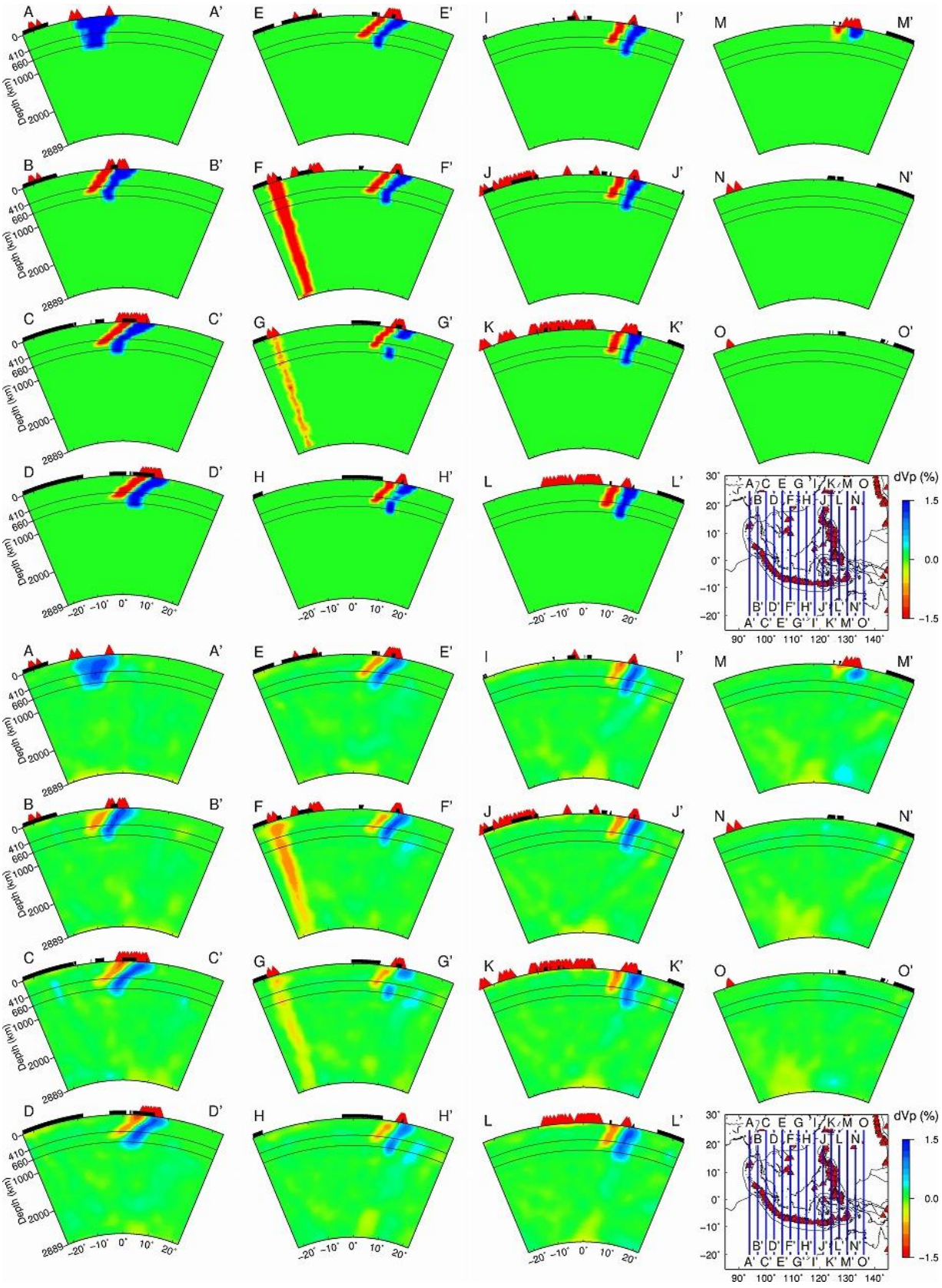

257 **Figure S39.**

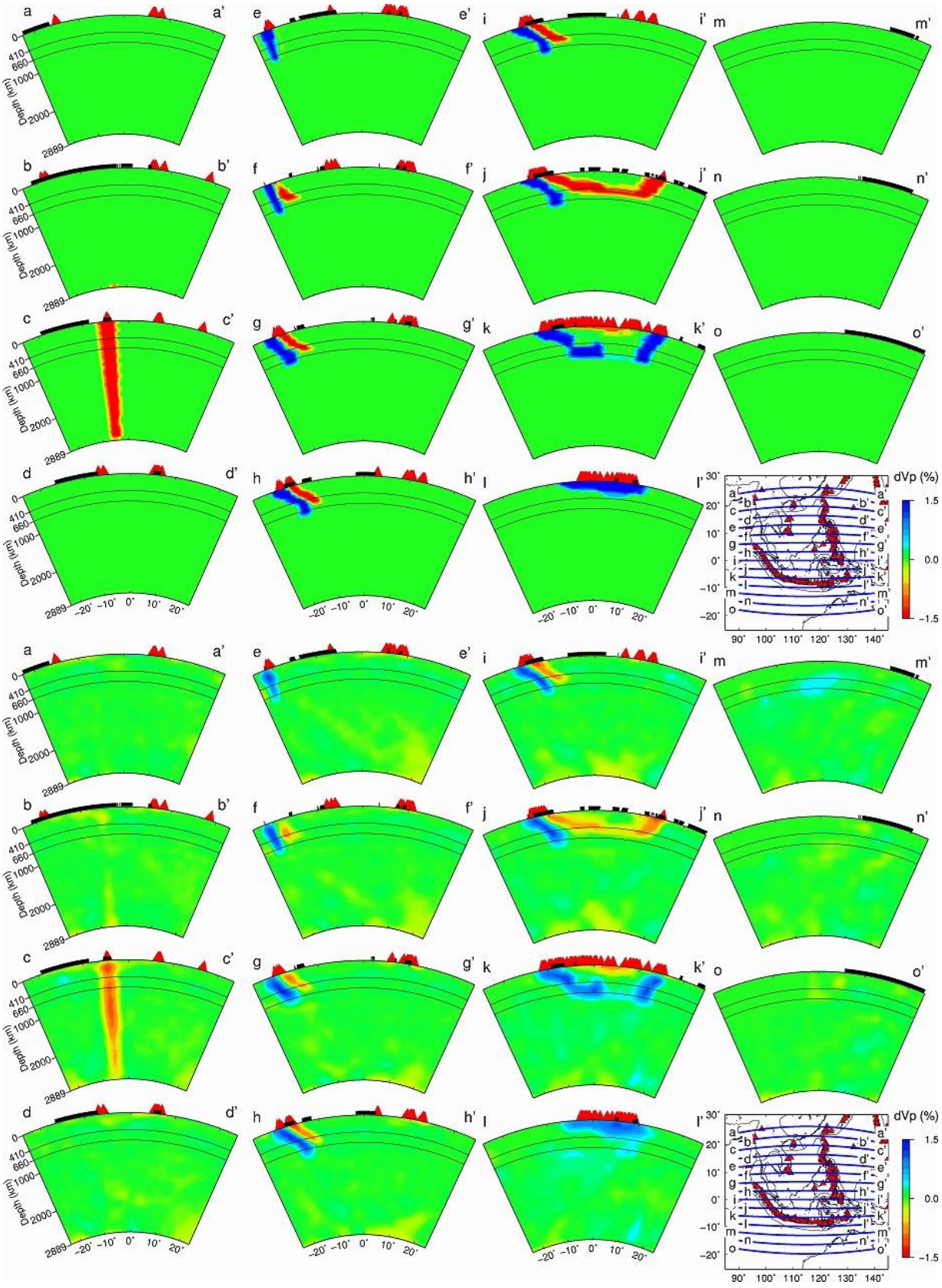
a
a'
b
b'
c
c'
d
d'
e
e'
f
f'
g
g'
h
h'
i
i'
j
j'
k
k'
l
l'
m
m'
n
n'
o
o'
0
410
660
1000
2000
2889
Depth (km)
-20°
-10°
0°
10°
20°
30°
90°
100°
110°
120°
130°
140°
dVp (%)
1.5
0.0
-1.5

Figure S40.

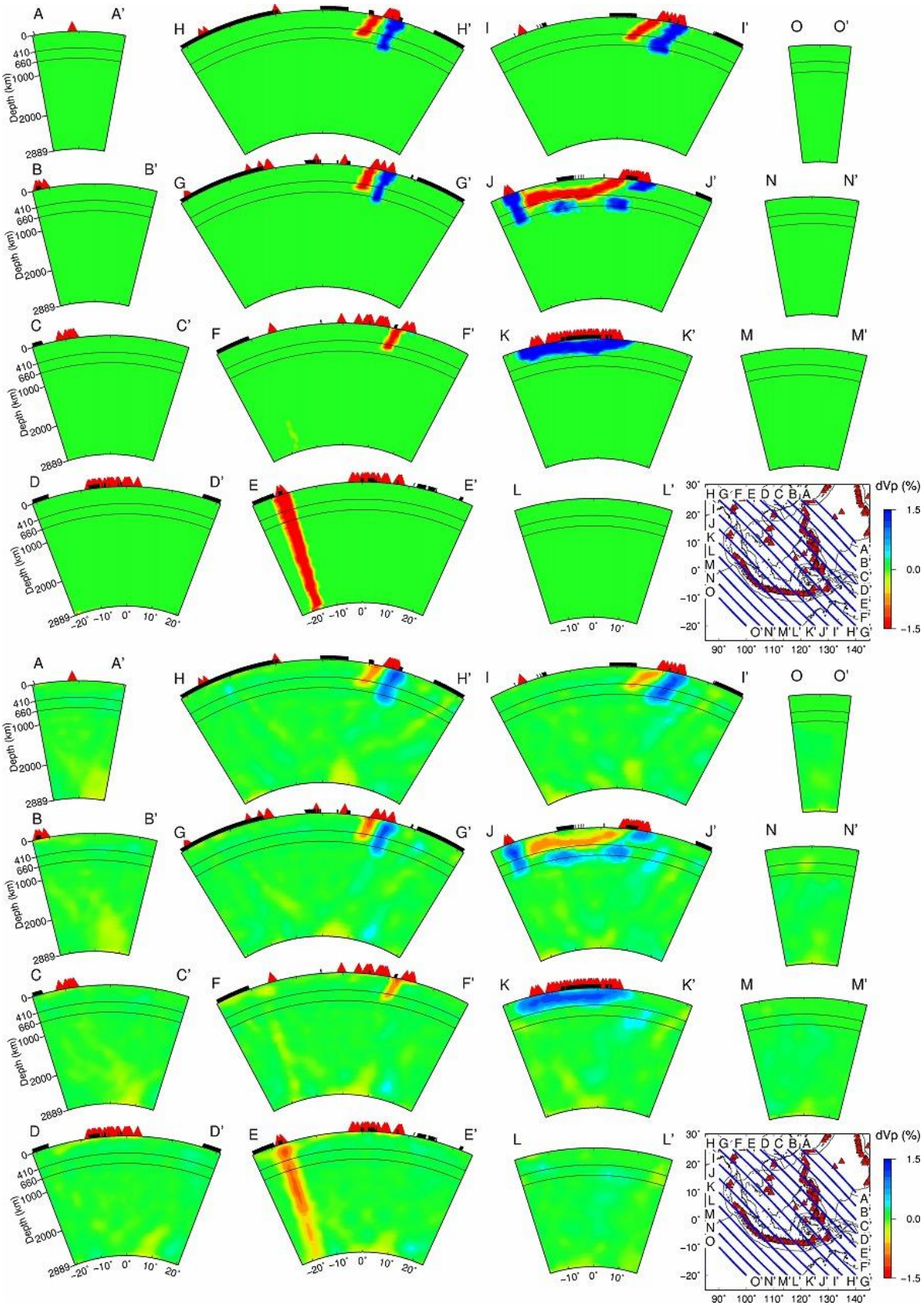
A
A'
H
H'
I
I'
O
O'
B
B'
G
G'
J
J'
N
N'
C
C'
F
F'
K
K'
M
M'
D
D'
E
E'
L
L'
Depth (km)
0
410
660
1000
2000
2889
dVp (%)
1.5
0.0
-1.5

Figure S41.

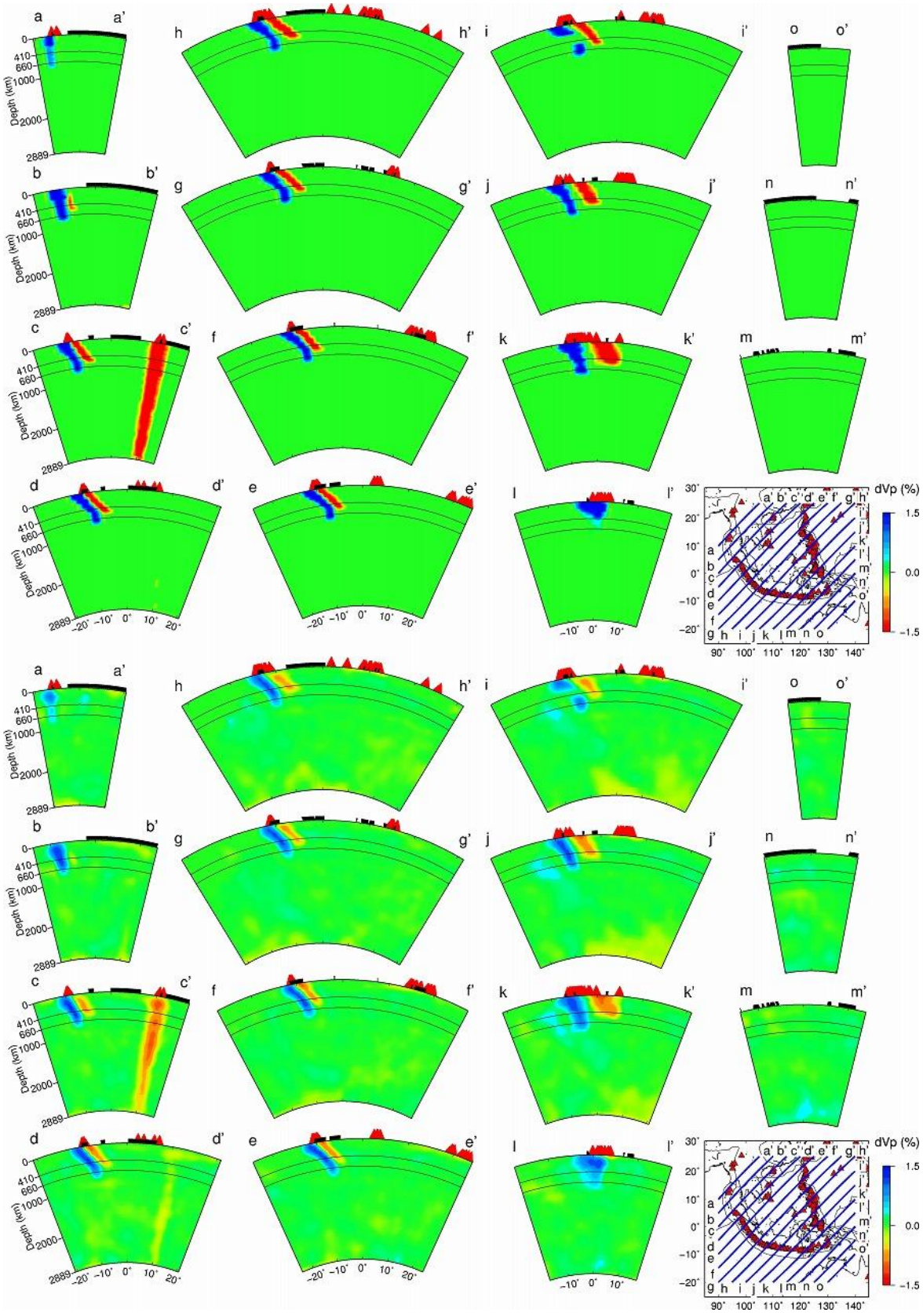

Figure S42.

Figure S38. The same as Figure S23 but for the synthetic resolution test without a low-Vp subslab hot mantle upwelling (SHMU) and a low-Vp bridge through the slab hole (SRT4).

Figure S39. Vertical cross-sections showing **(top)** the input model and **(bottom)** output results of the SRT4 along 15 profiles in the N-S direction. Locations of the profiles are shown on the inset map. The 410-km and the 660-km discontinuities are shown in black solid lines. The thick black lines on the surface denote land areas. The red triangles denote active volcanoes. The thin black lines on the inset map denote the plate boundaries.

Figure S40. The same as Figure S39 but along 15 profiles in the E-W direction.

Figure S41. The same as Figure S39 but along 15 profiles in the NW-SE direction.

Figure S42. The same as Figure S39 but along 15 profiles in the NE-SW direction.

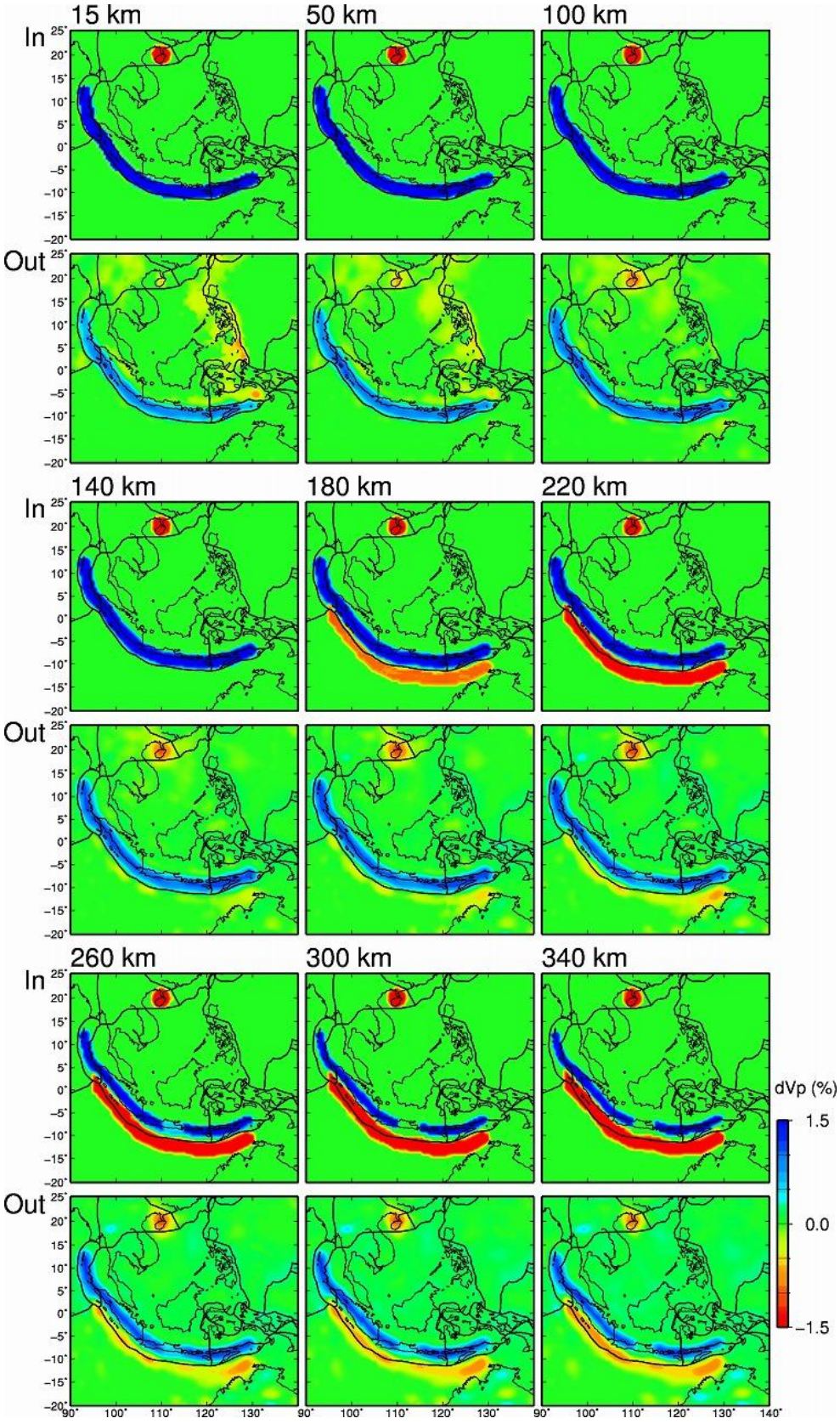
15 km
50 km
100 km
In
Out
140 km
180 km
220 km
In
Out
260 km
300 km
340 km
In
Out
dVp (%)
1.5
0.0
−1.5

Figure S43.

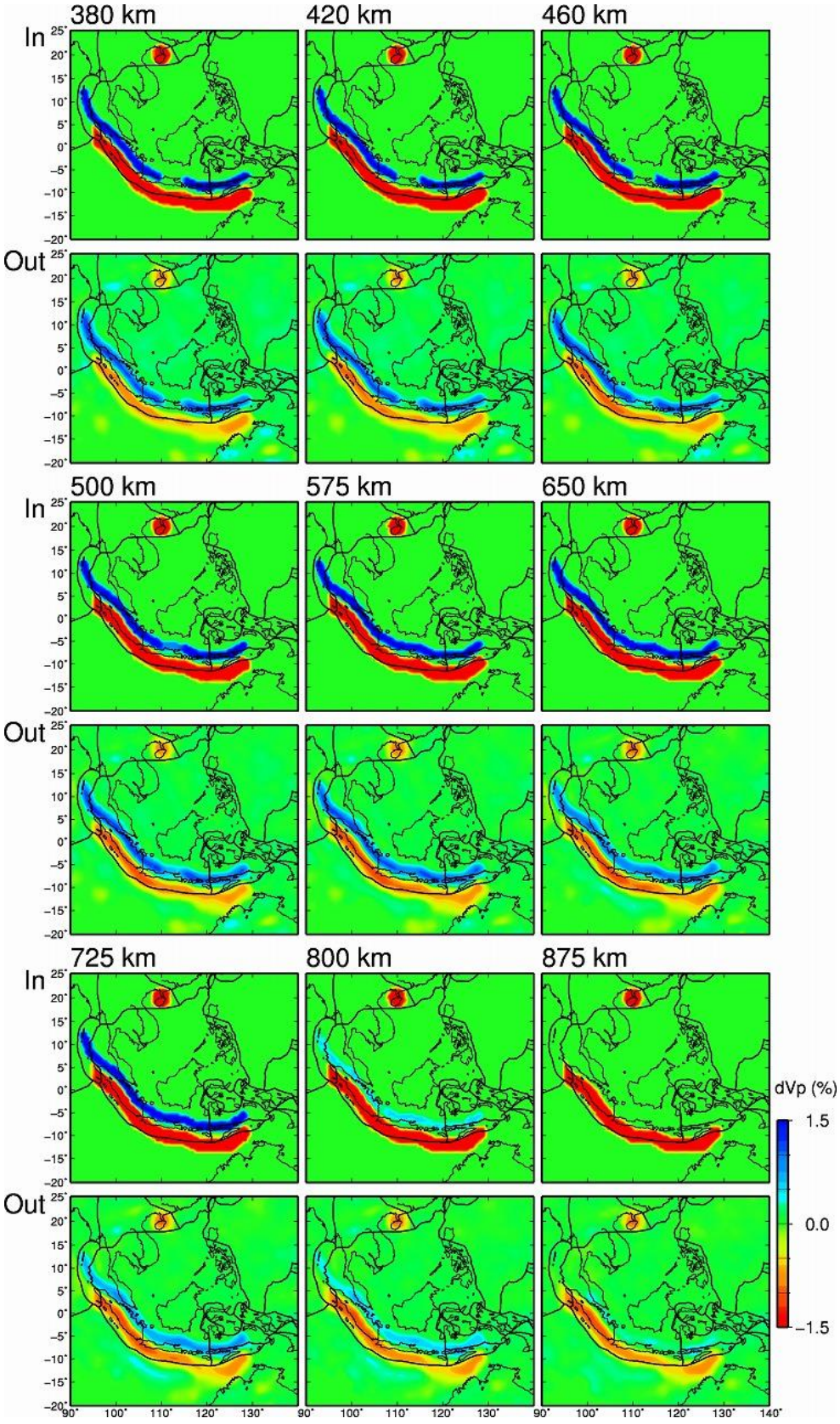

Figure S43. (continued).

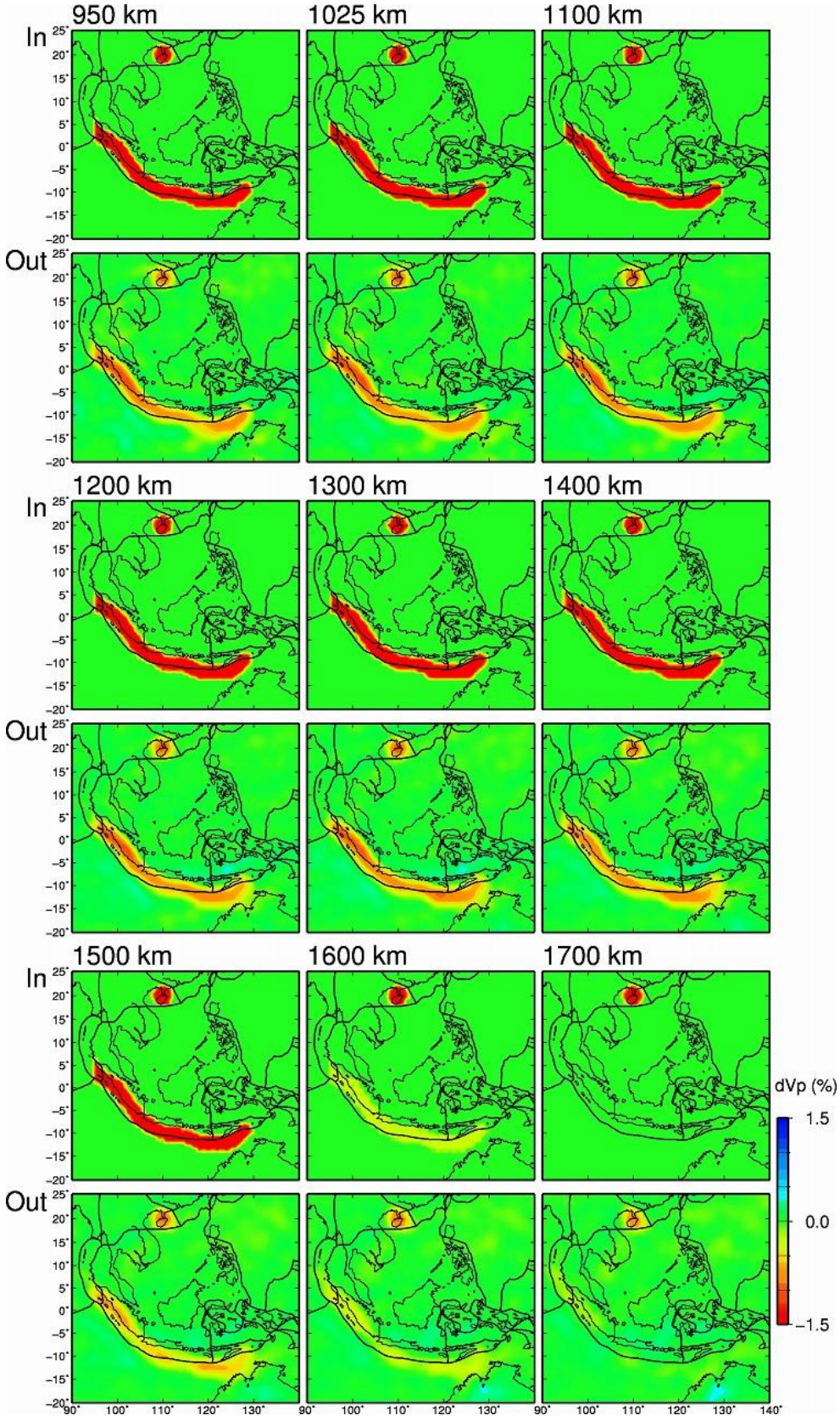

Figure S43. (continued).

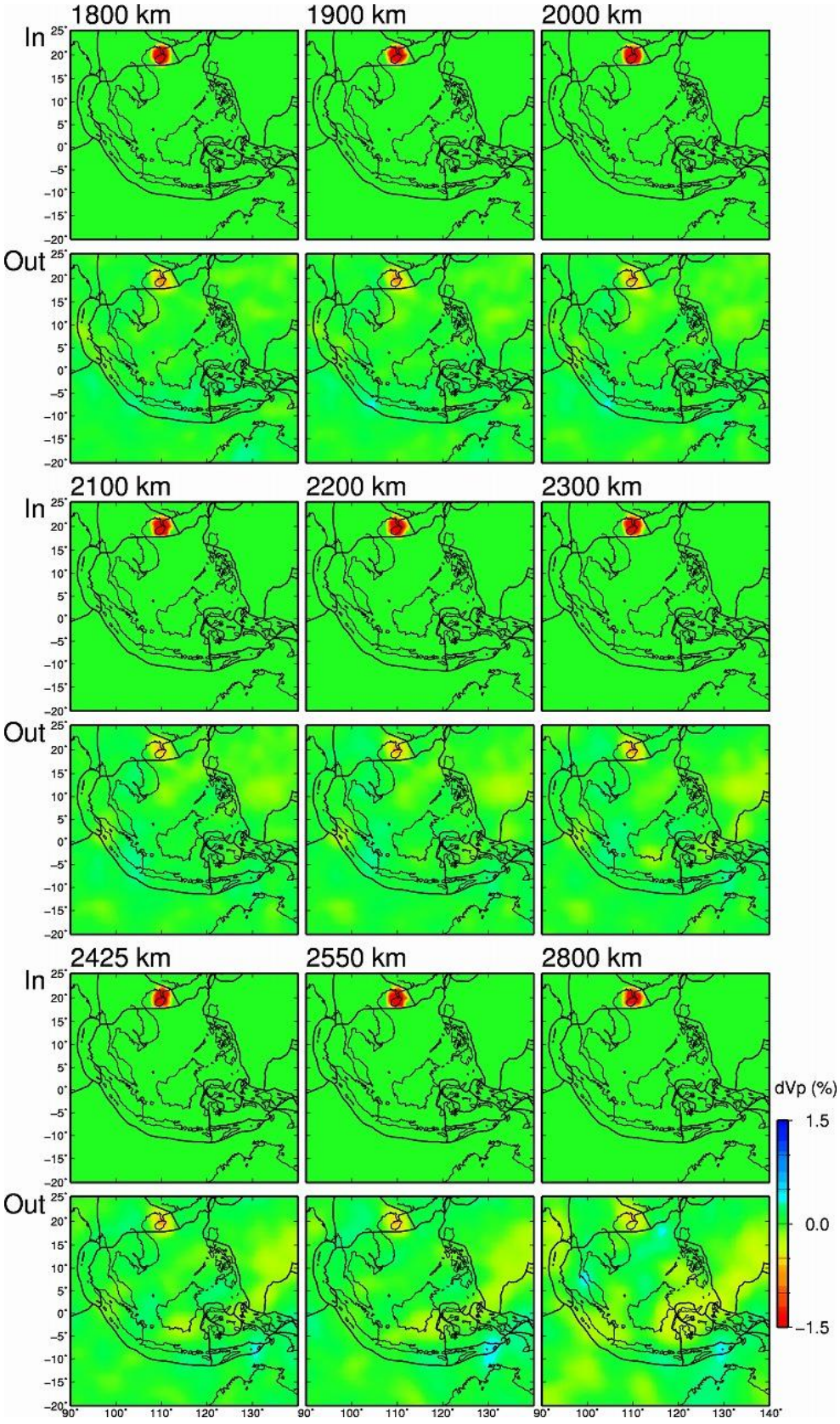

Figure S43. (continued).

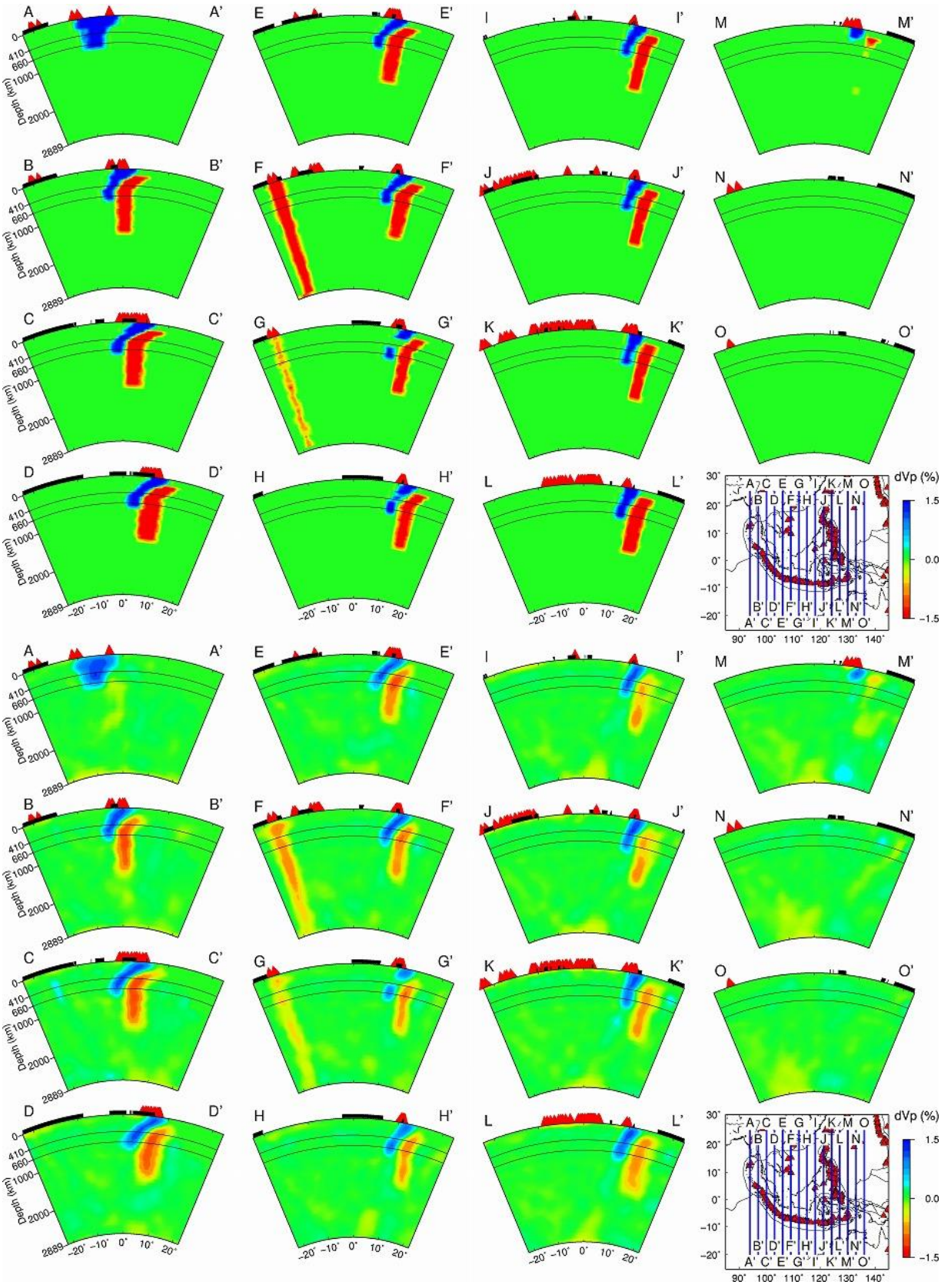
A A'
E E'
I I'
M M'
B B'
F F'
J J'
N N'
C C'
G G'
K K'
O O'
D D'
H H'
L L'
Depth (km)
0
410
660
1000
2000
2889
−20° −10° 0° 10° 20°
dVp (%)
1.5
0.0
−1.5
30°
20°
10°
0°
−10°
−20°
90° 100° 110° 120° 130° 140°

Figure S44.

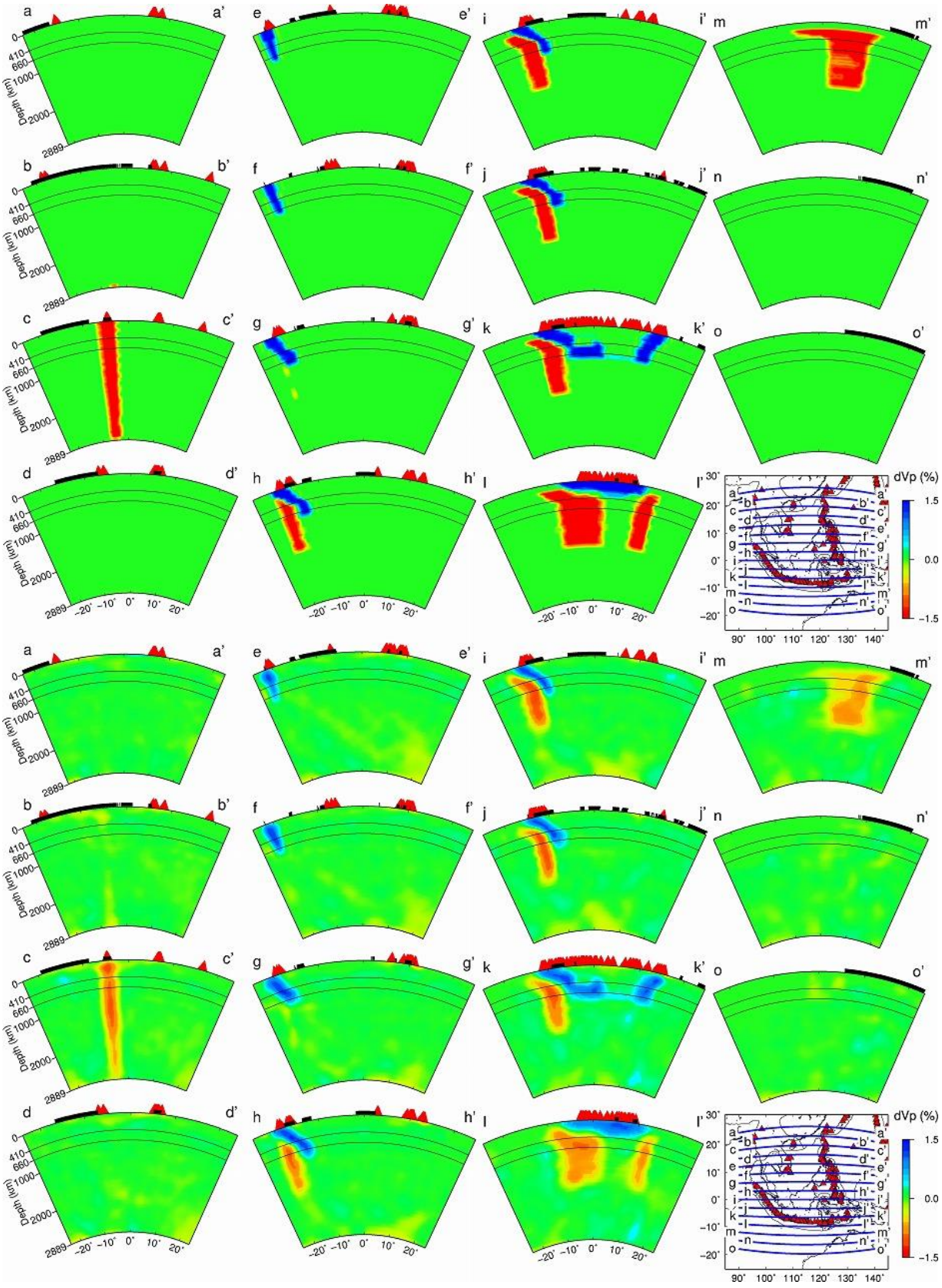

289 **Figure S45.**

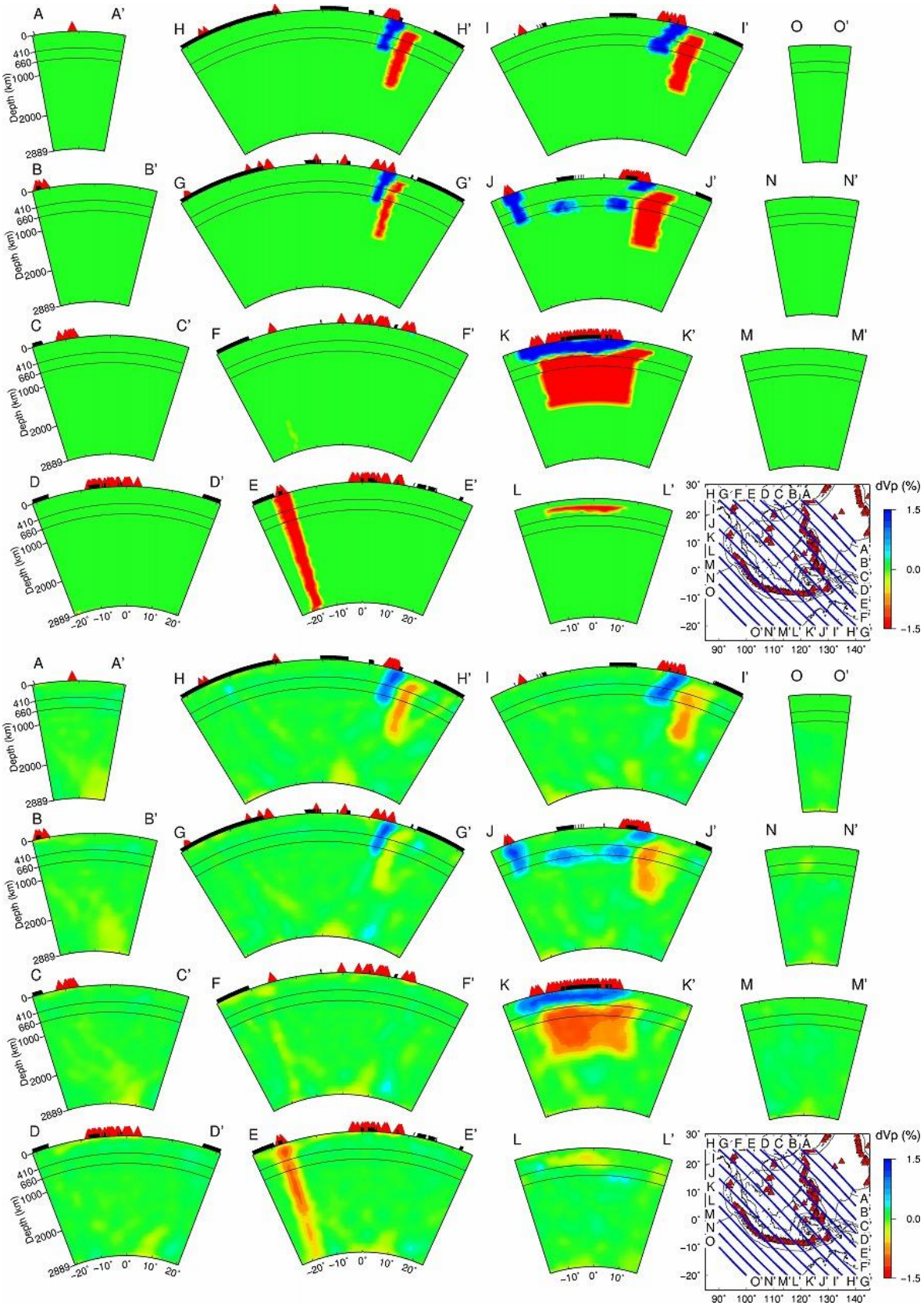
A
A'
H
H'
I
I'
O
O'
B
B'
G
G'
J
J'
N
N'
C
C'
F
F'
K
K'
M
M'
D
D'
E
E'
L
L'
Depth (km)
0
410
660
1000
2000
2889
dVp (%)
1.5
0.0
-1.5
90° 100° 110° 120° 130° 140°
30° 20° 10° 0° -10° -20°
-20° -10° 0° 10° 20°
-10° 0° 10°

Figure S46.

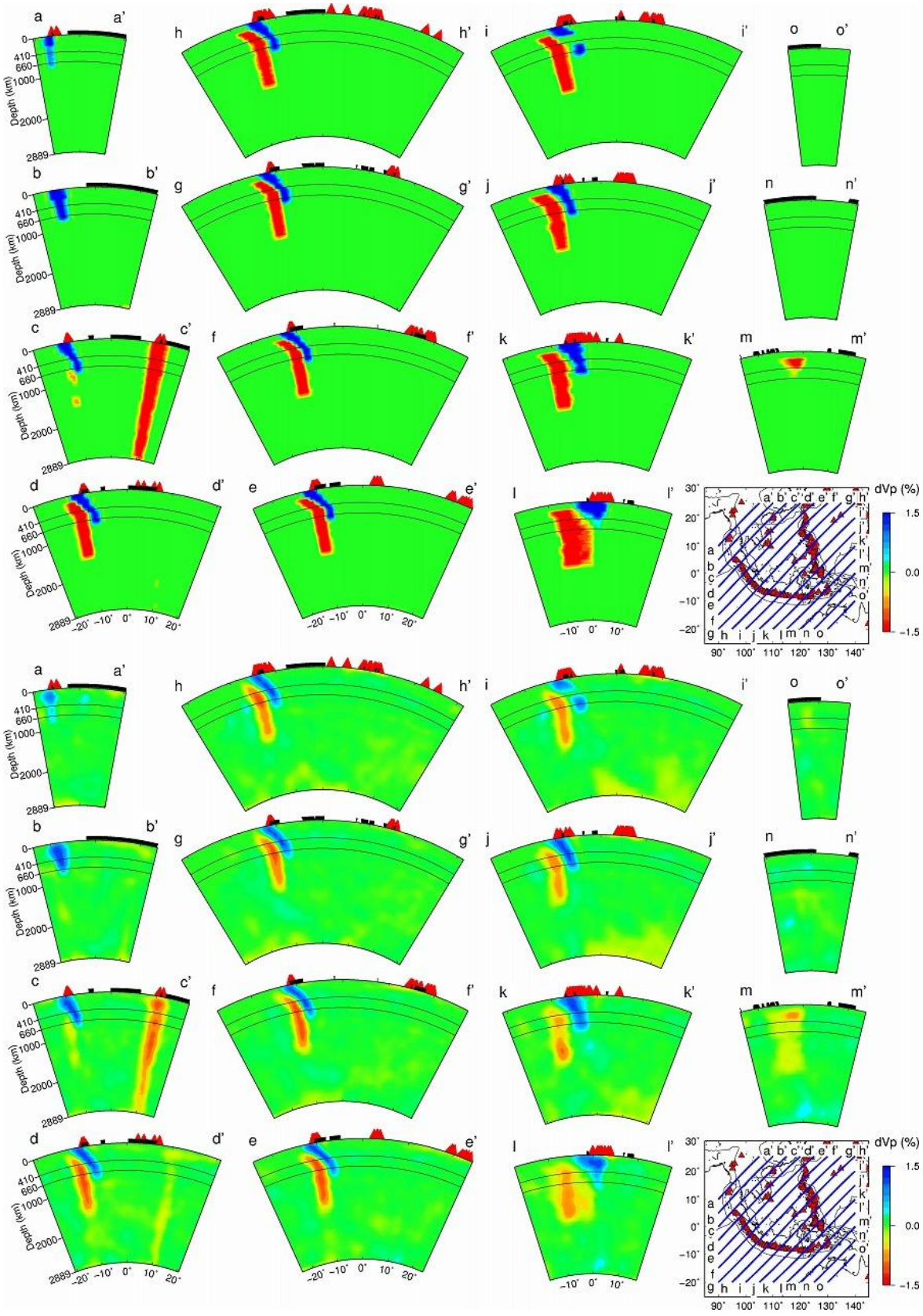

Figure S47.

Figure S43. The same as Figure S23 but for the synthetic resolution test without a low-Vp hot mantle upwelling in the mantle wedge and a low-Vp bridge through the slab hole (SRT5).

Figure S44. Vertical cross-sections showing **(top)** the input model and **(bottom)** output results of the SRT5 along 15 profiles in the N-S direction. Locations of the profiles are shown on the inset map. The 410-km and the 660-km discontinuities are shown in black solid lines. The thick black lines on the surface denote land areas. The red triangles denote active volcanoes. The thin black lines on the inset map denote the plate boundaries.

Figure S45. The same as Figure S44 but along 15 profiles in the E-W direction.

Figure S46. The same as Figure S44 but along 15 profiles in the NW-SE direction.

Figure S47. The same as Figure S44 but along 15 profiles in the NE-SW direction.

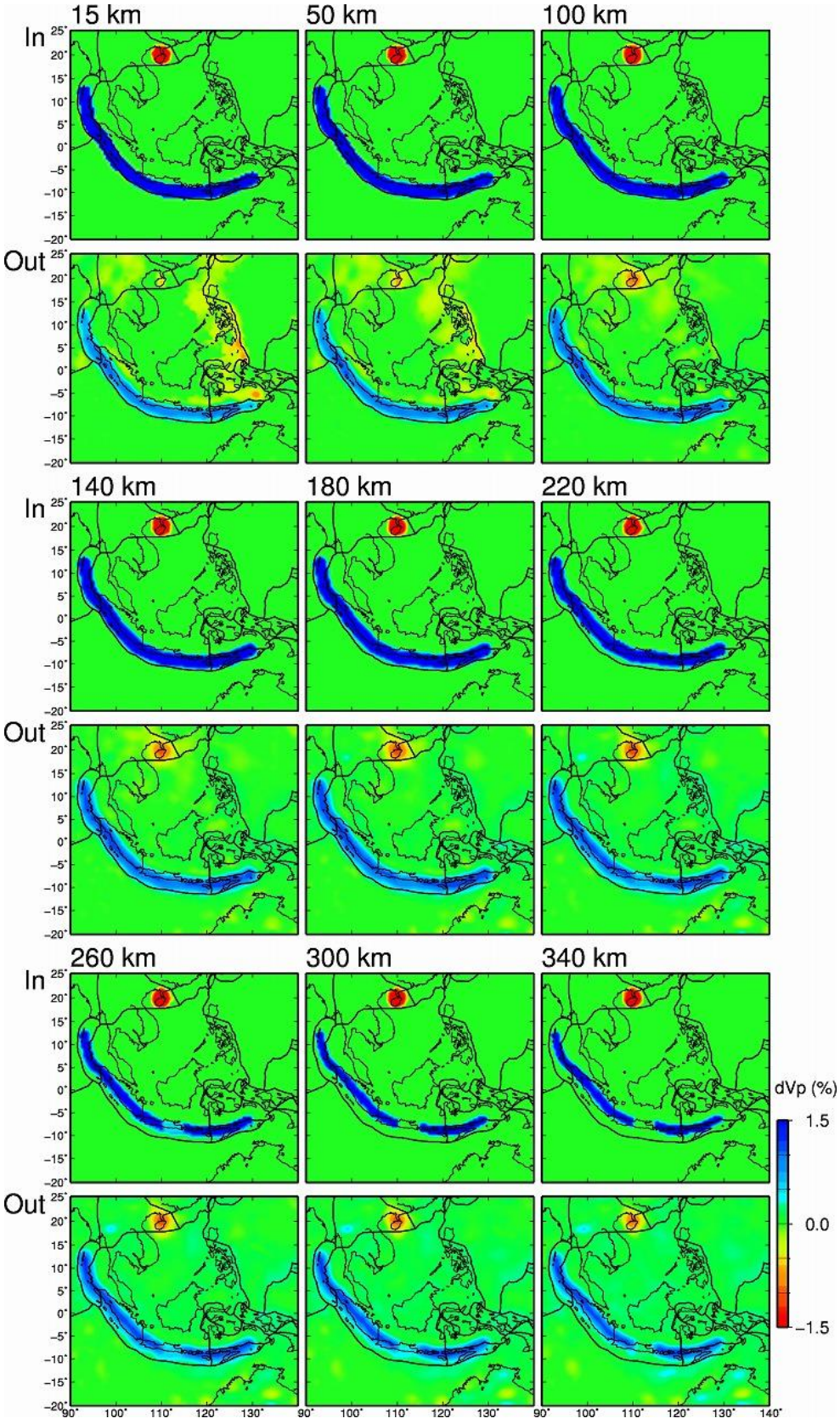
15 km
50 km
100 km
In
Out
140 km
180 km
220 km
In
Out
260 km
300 km
340 km
In
Out
dVp (%)
1.5
0.0
−1.5

Figure S48.

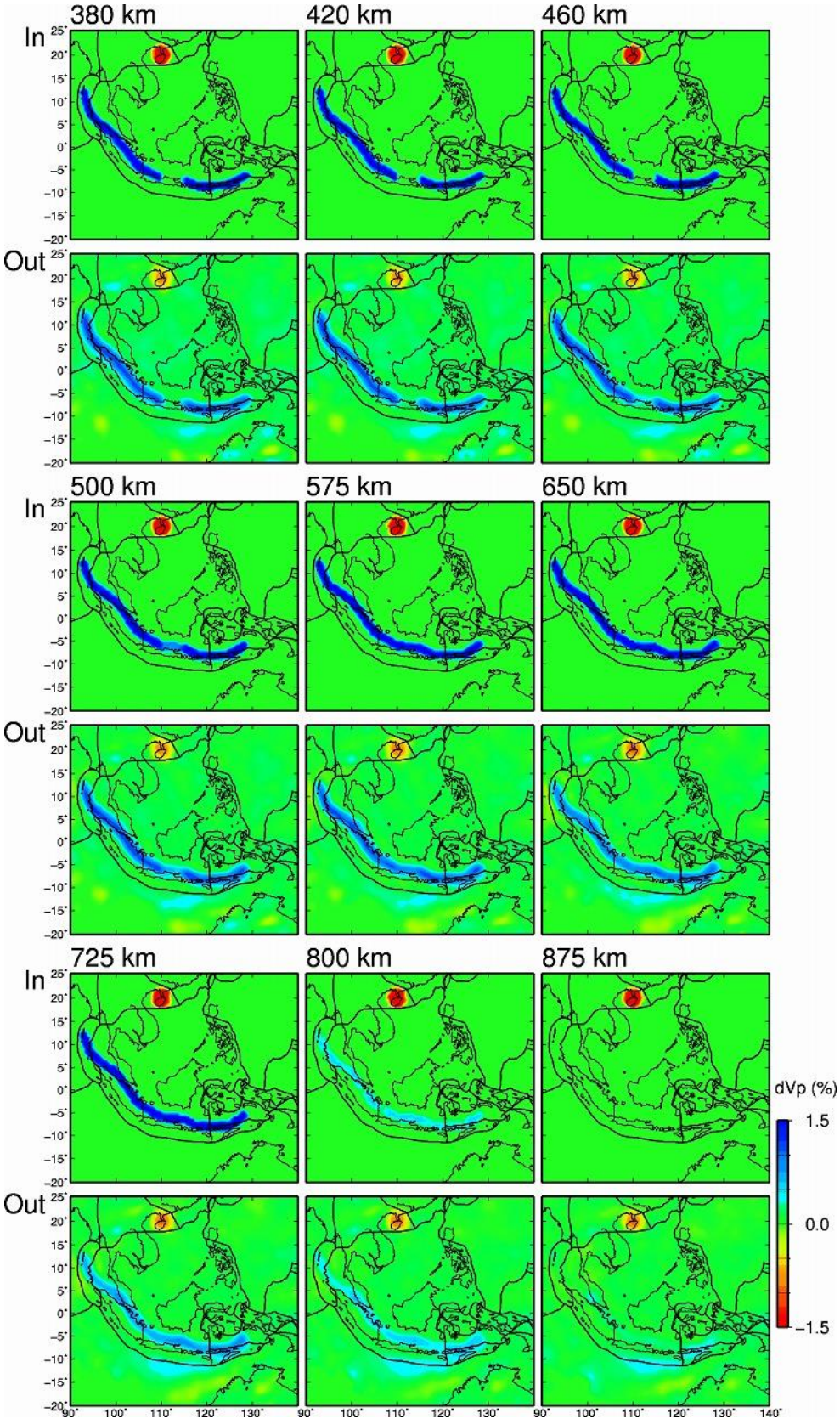

Figure S48. (continued).

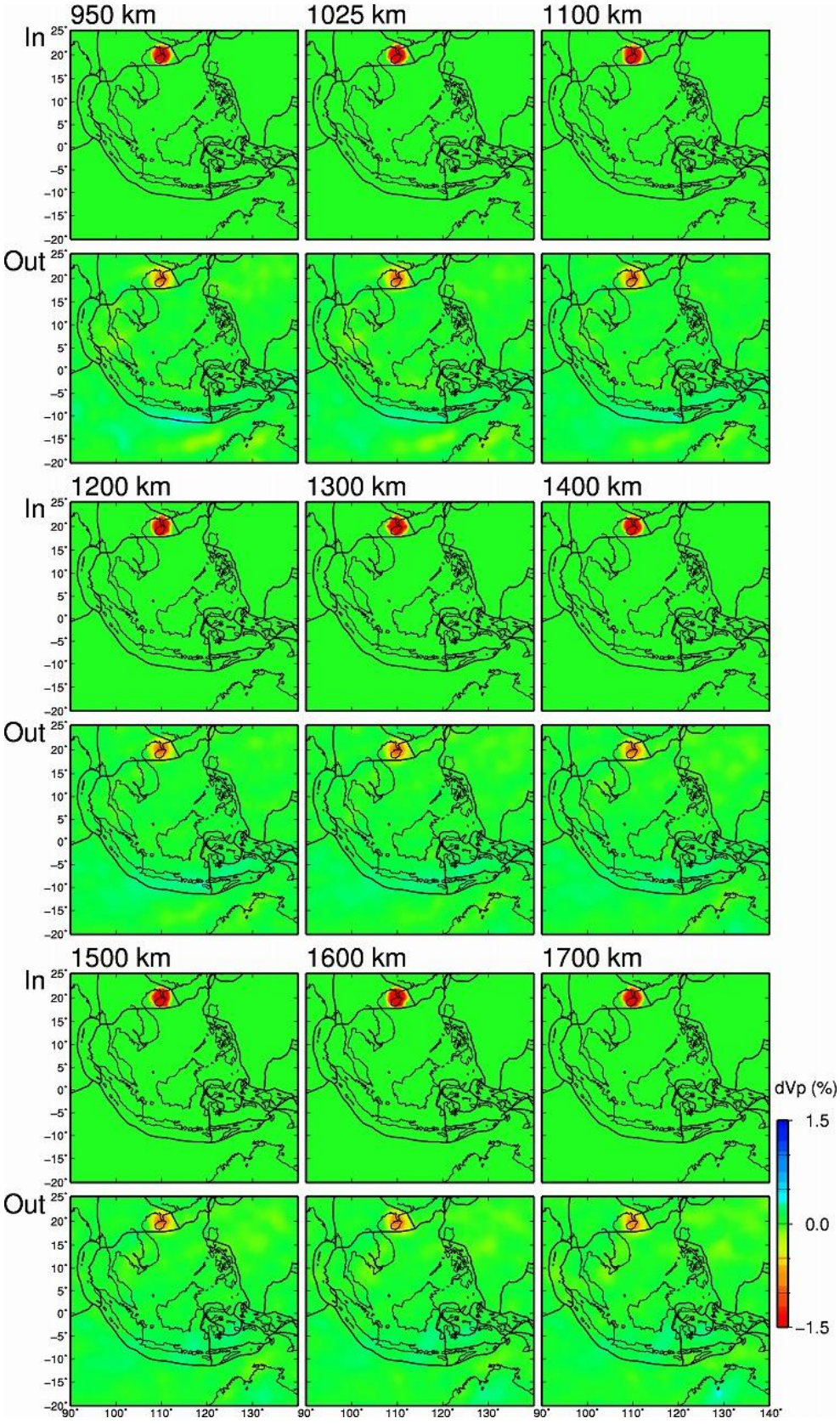

Figure S48. (continued).

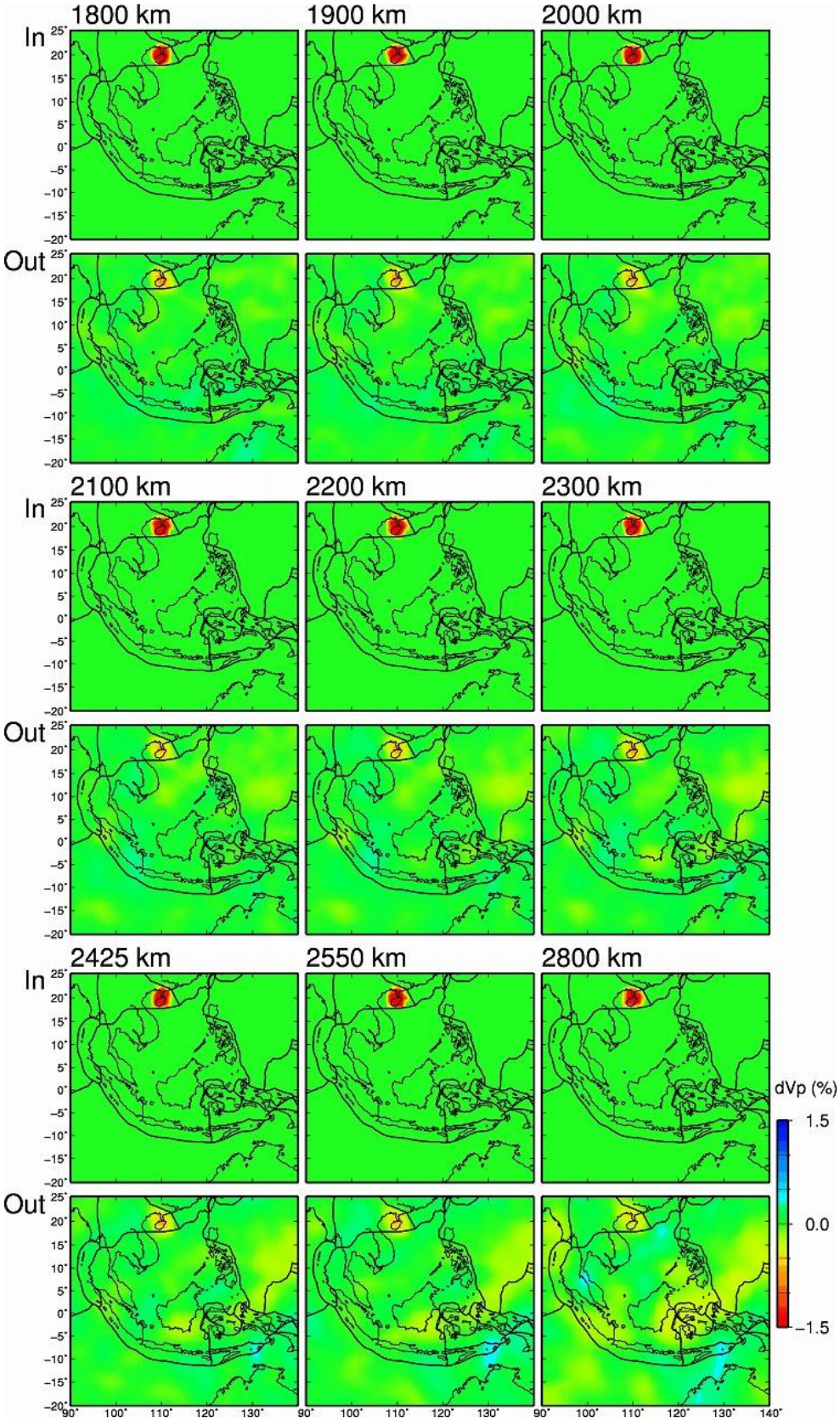

Figure S48. (continued).

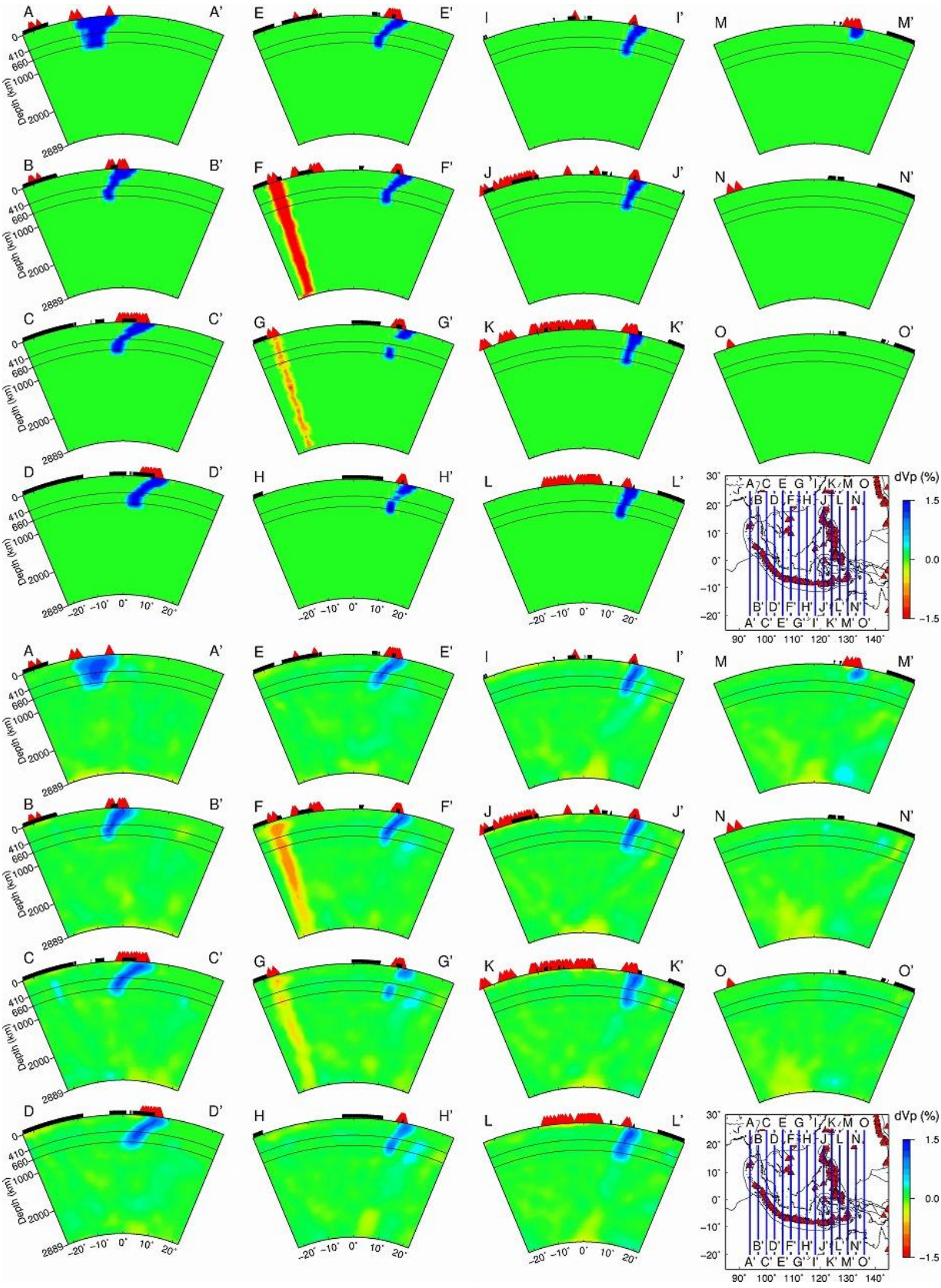
A
A'
E
E'
I
I'
M
M'
B
B'
F
F'
J
J'
N
N'
C
C'
G
G'
K
K'
O
O'
D
D'
H
H'
L
L'
0
410
660
1000
2000
2889
Depth (km)
-20° -10° 0° 10° 20°
dVp (%)
1.5
0.0
-1.5
30°
20°
10°
0°
-10°
-20°
90° 100° 110° 120° 130° 140°

Figure S49.

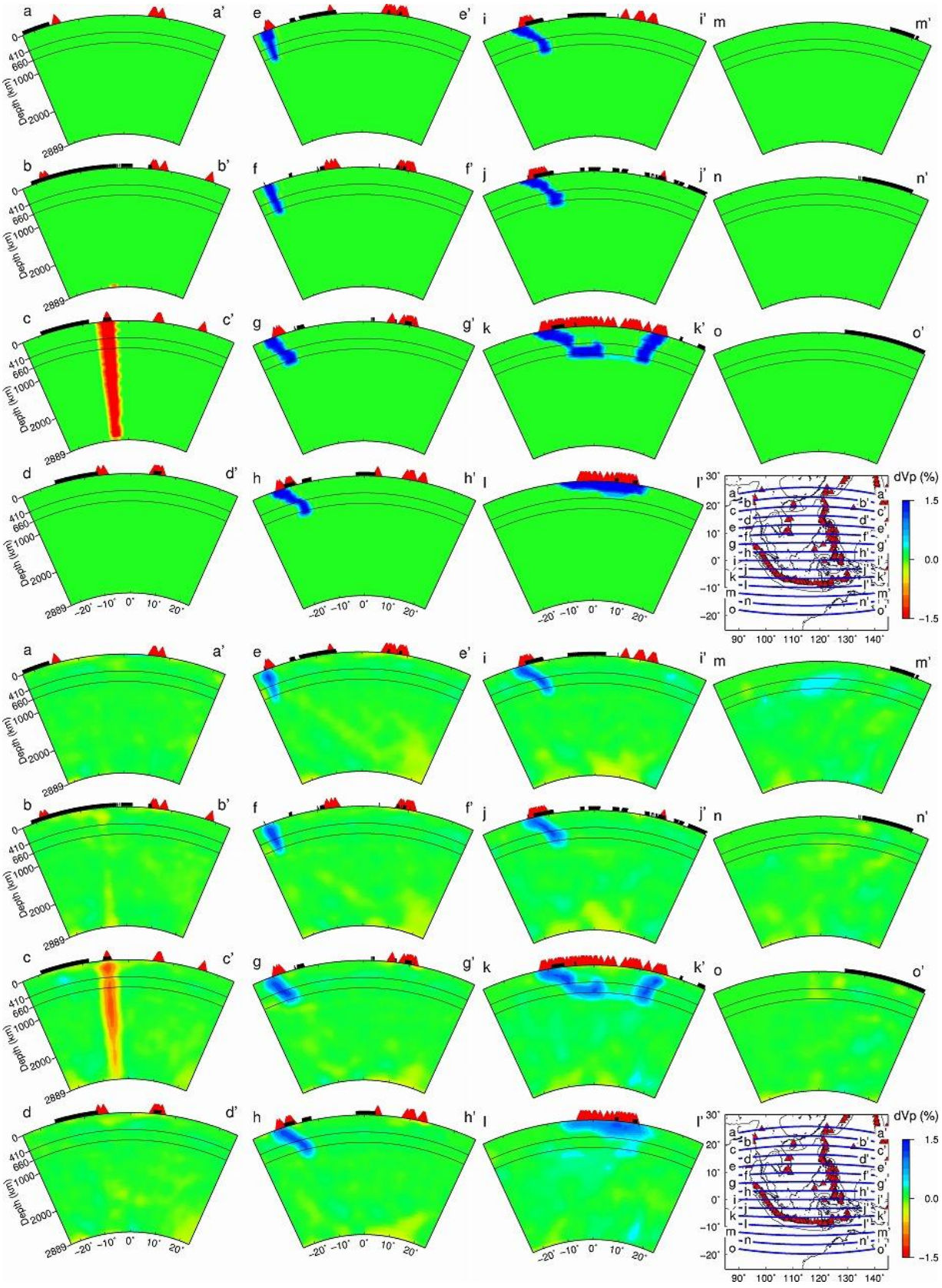

312 **Figure S50.**

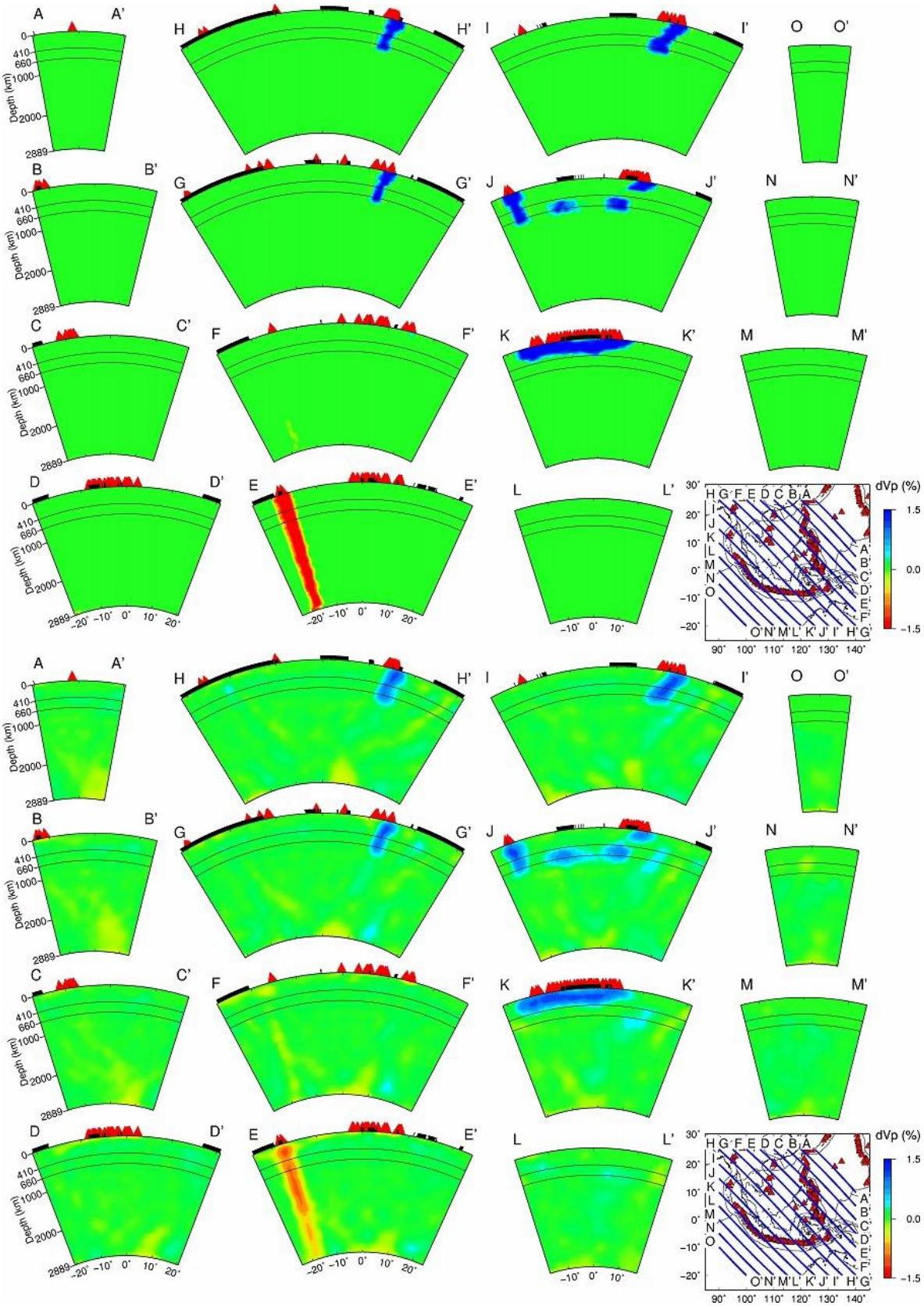

313 **Figure S51.**

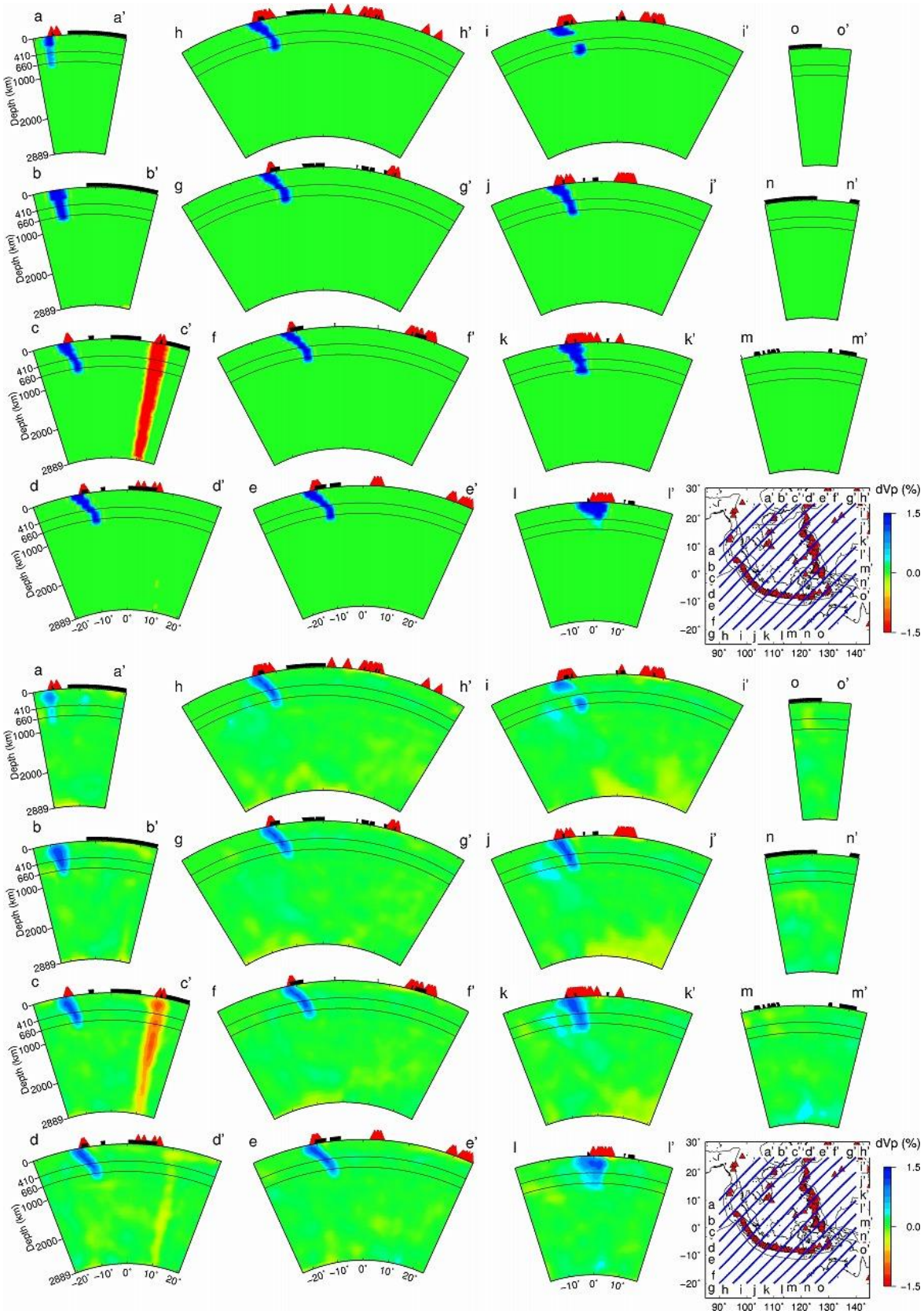
a
a'
b
b'
c
c'
d
d'
e
e'
f
f'
g
g'
h
h'
i
i'
j
j'
k
k'
l
l'
m
m'
n
n'
o
o'
Depth (km)
0
410
660
1000
2000
2889
−20°
−10°
0°
10°
20°
30°
90°
100°
110°
120°
130°
140°
dVp (%)
1.5
0.0
−1.5

Figure S52.

Figure S48. The same as Figure S23 but for the synthetic resolution test without a low-Vp hot mantle upwelling in the mantle wedge, a low-Vp subslab hot mantle upwelling (SHMU), and a low-Vp bridge through the slab hole (SRT6).

Figure S49. Vertical cross-sections showing **(top)** the input model and **(bottom)** output results of the SRT6 along 15 profiles in the N-S direction. Locations of the profiles are shown on the inset map. The 410-km and the 660-km discontinuities are shown in black solid lines. The thick black lines on the surface denote land areas. The red triangles denote active volcanoes. The thin black lines on the inset map denote the plate boundaries.

Figure S50. The same as Figure S49 but along 15 profiles in the E-W direction.

Figure S51. The same as Figure S49 but along 15 profiles in the NW-SE direction.

Figure S52. The same as Figure S49 but along 15 profiles in the NE-SW direction.

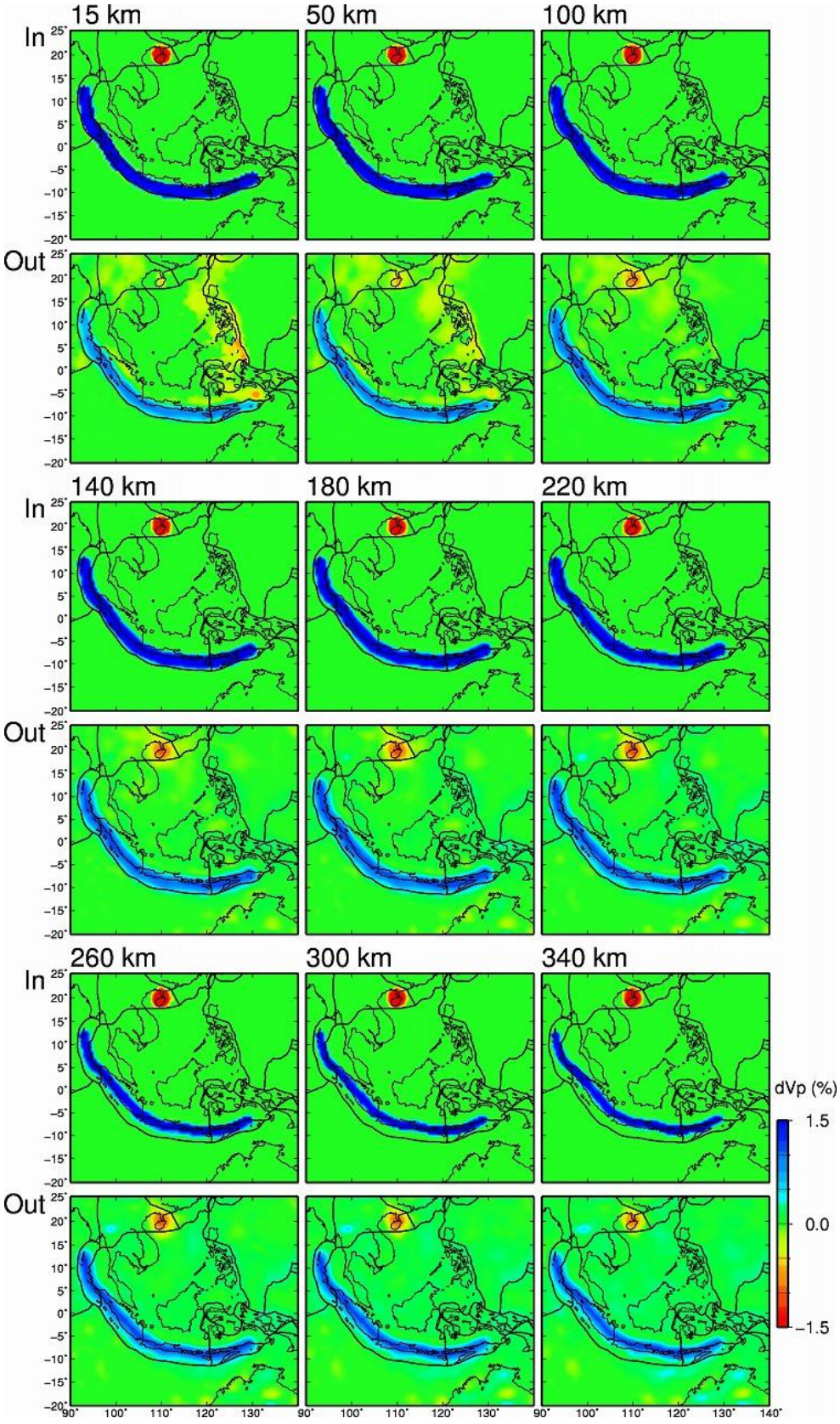
15 km
50 km
100 km
In
Out
140 km
180 km
220 km
In
Out
260 km
300 km
340 km
In
Out
dVp (%)
1.5
0.0
−1.5

Figure S53.

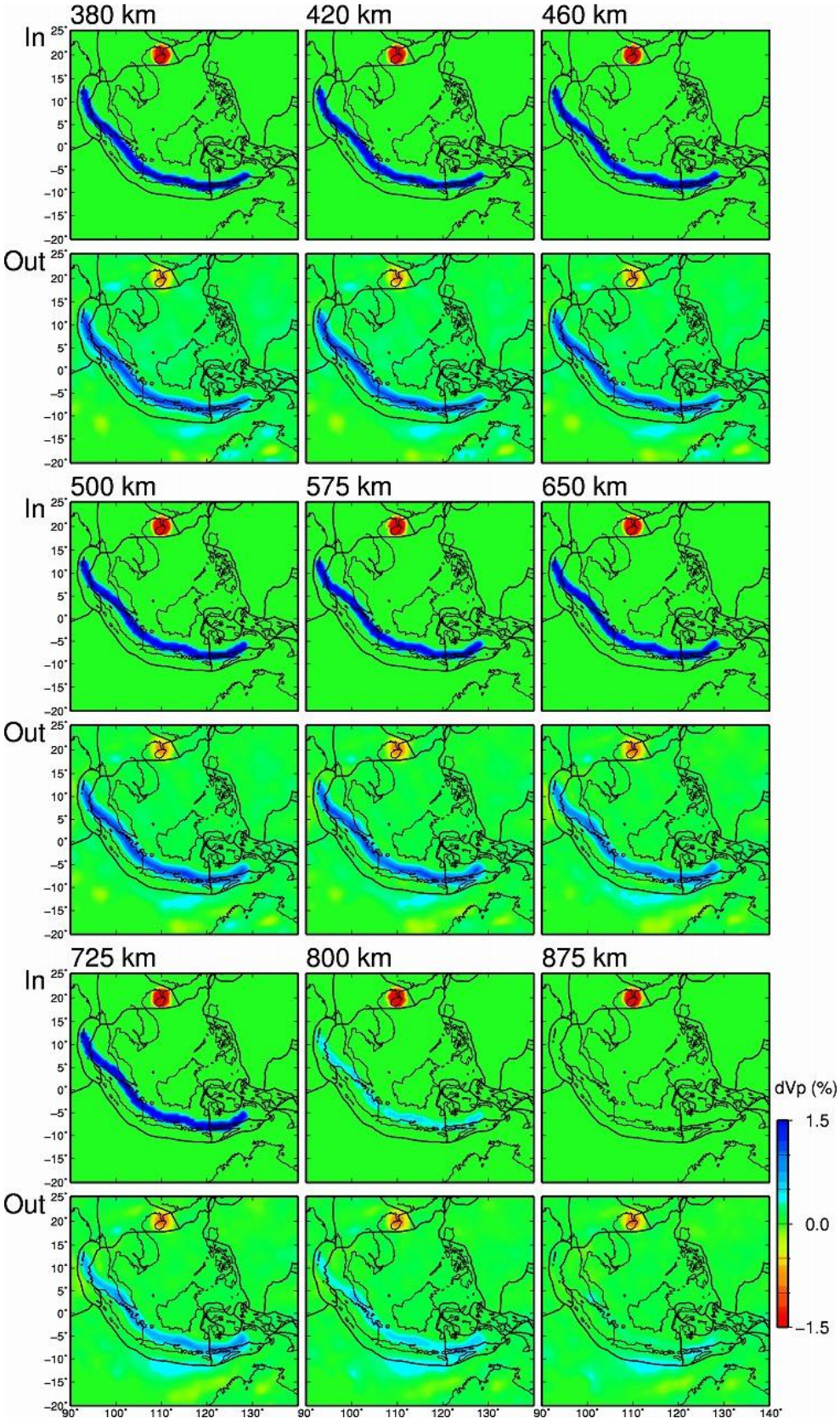

Figure S53. (continued).

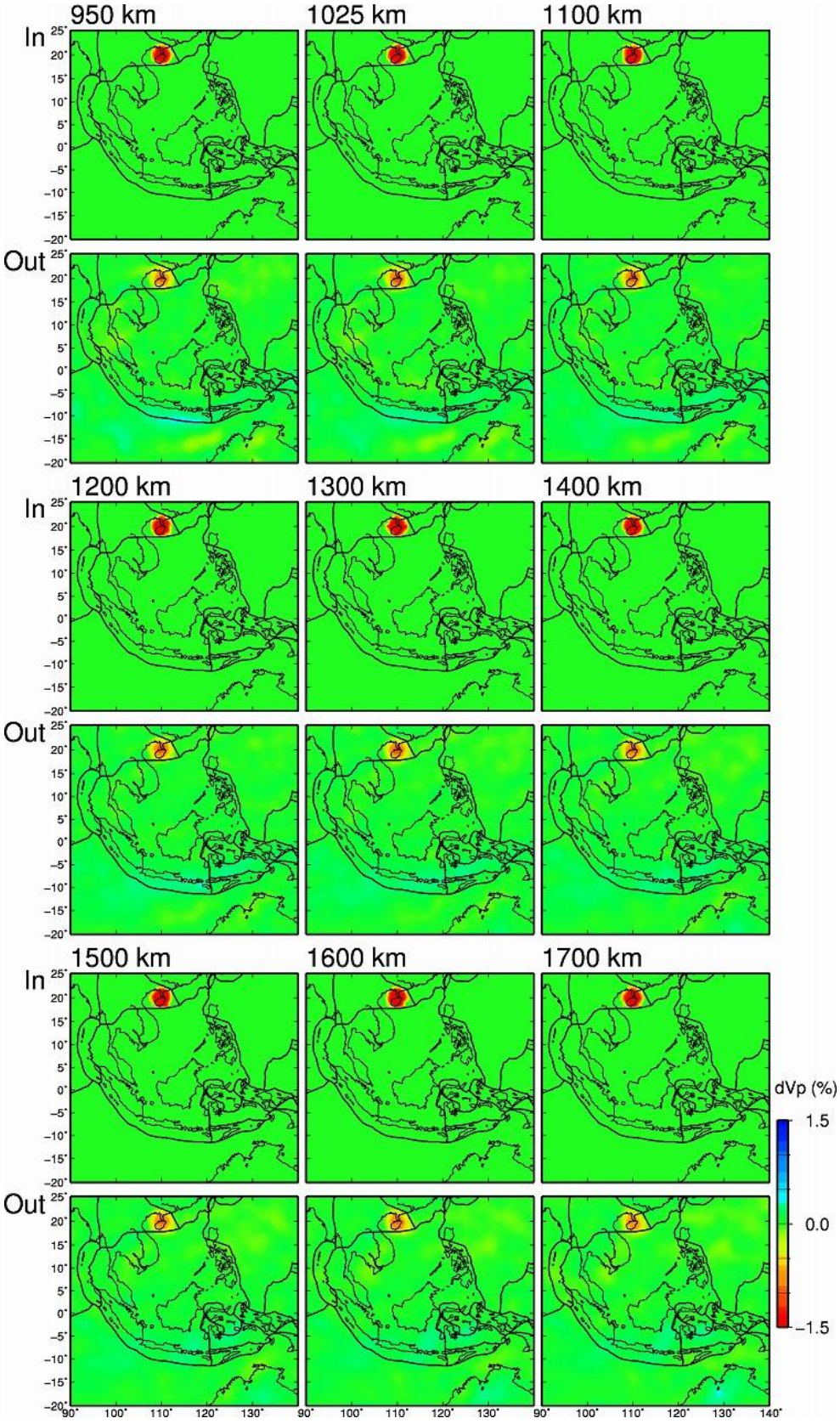

Figure S53. (continued).

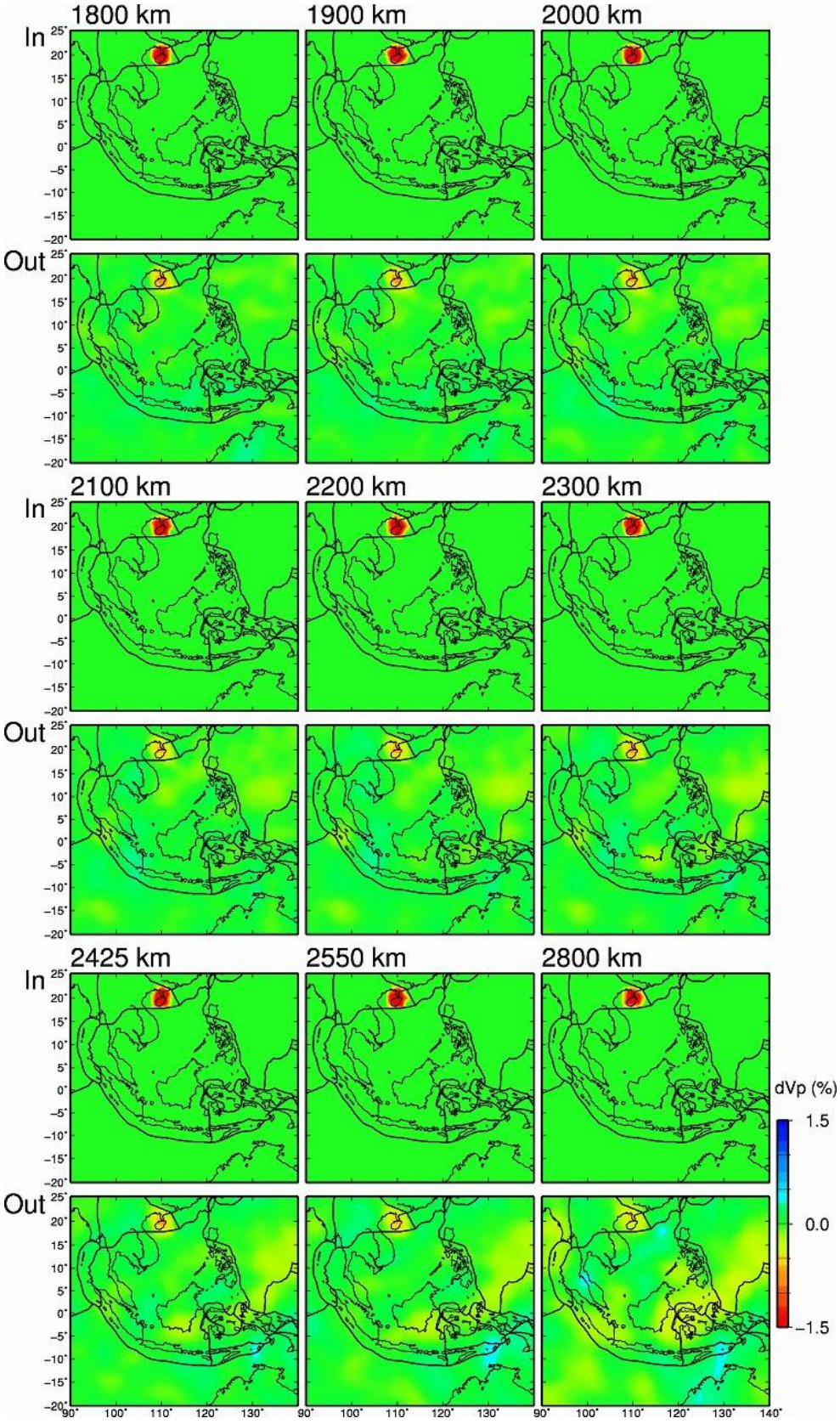

Figure S53. (continued).

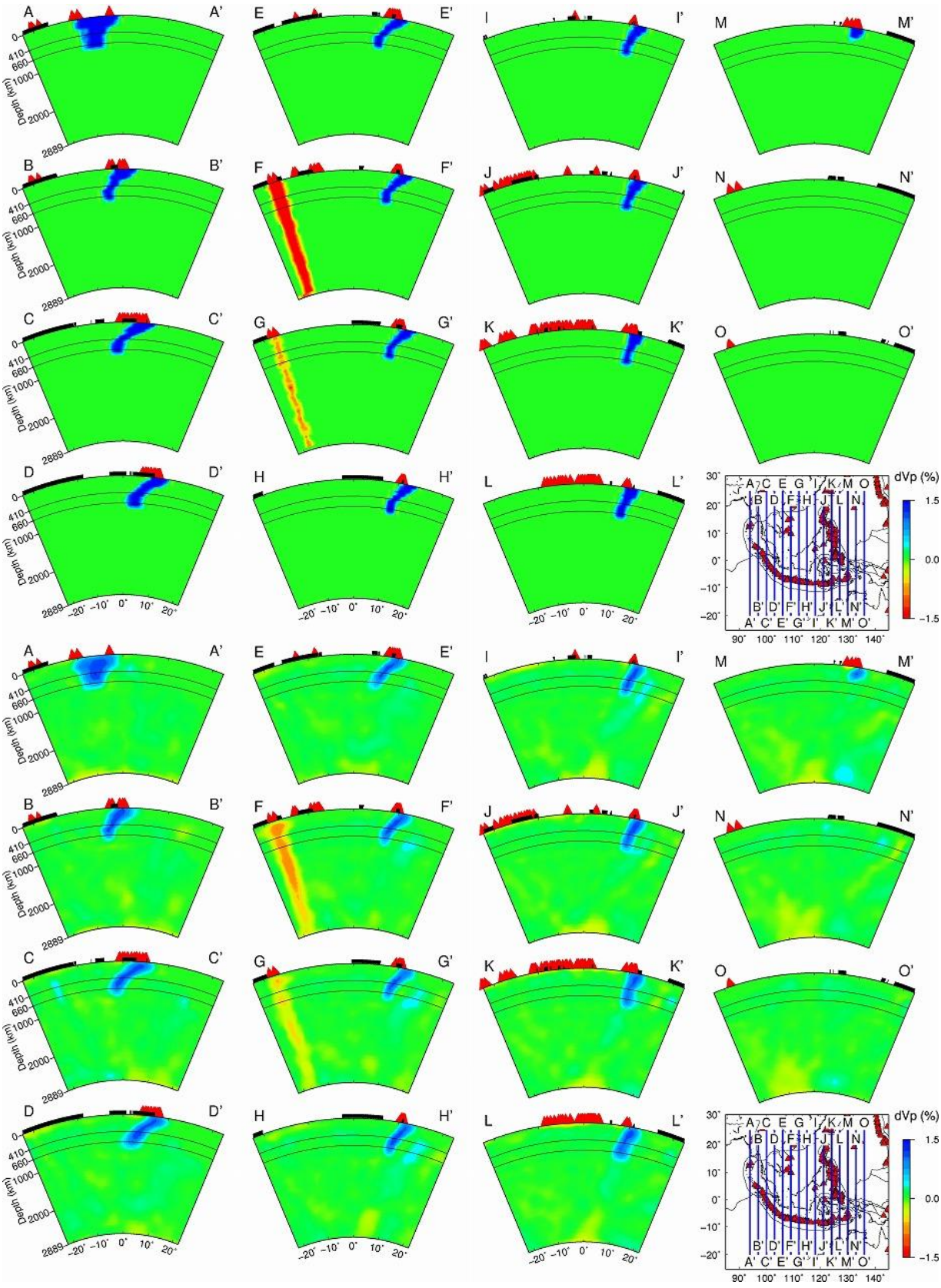

335 **Figure S54.**

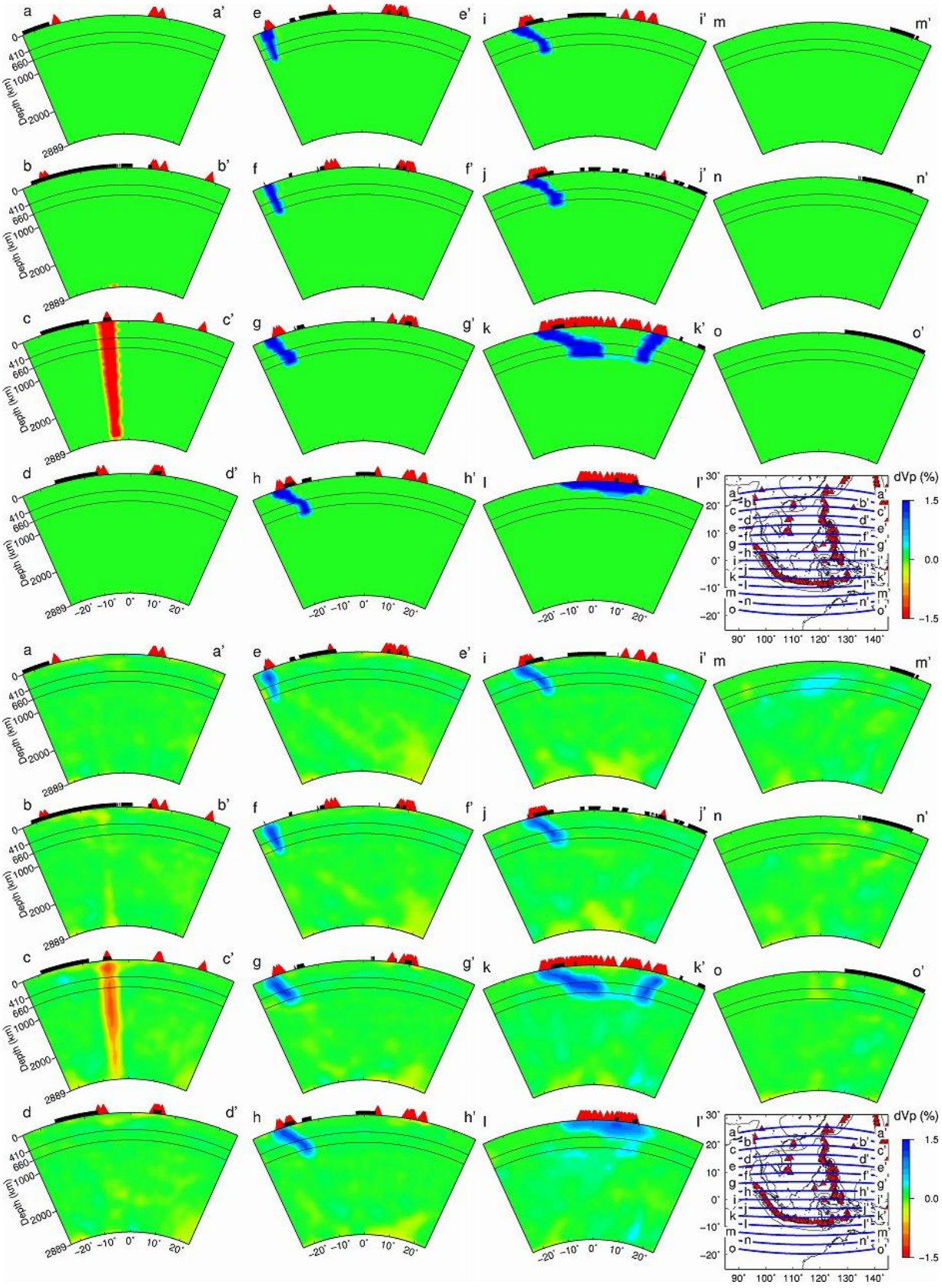

Figure S55.

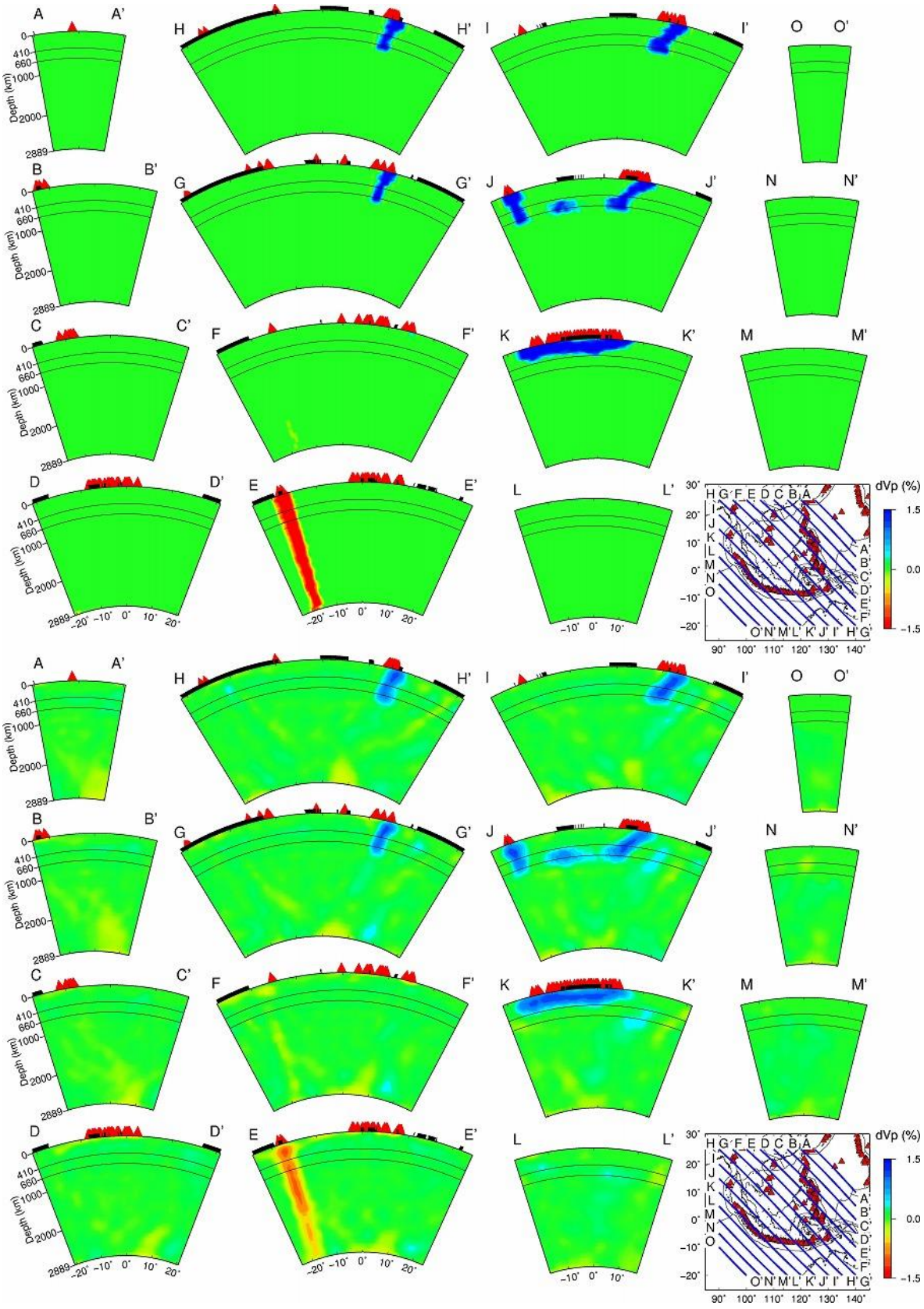

337 **Figure S56.**

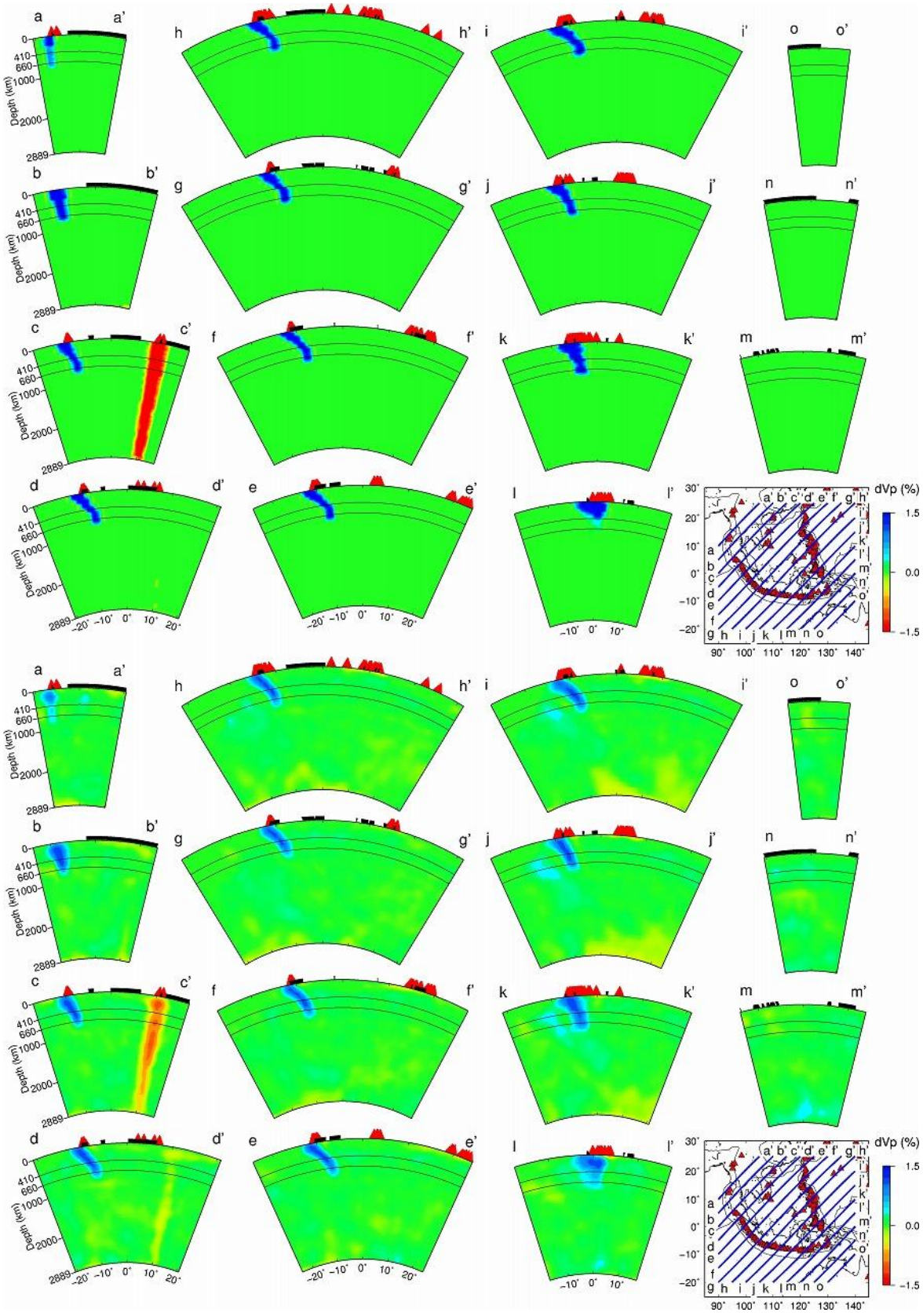
a
a'
h
h'
i
i'
o
o'
b
b'
g
g'
j
j'
n
n'
c
c'
f
f'
k
k'
m
m'
d
d'
e
e'
l
l'
Depth (km)
0
410
660
1000
2000
2889
dVp (%)
1.5
0.0
-1.5

Figure S57.

Figure S53. The same as Figure S23 but for the synthetic resolution test without a low-Vp hot mantle upwelling in the mantle wedge, a low-Vp subslab hot mantle upwelling (SHMU), a hole in the Australian slab between depths 260−460 km and latitudes 110°−115°, and a low-Vp bridge through the slab hole (SRT7).

Figure S54. Vertical cross-sections showing **(top)** the input model and **(bottom)** output results of the SRT7 along 15 profiles in the N-S direction. Locations of the profiles are shown on the inset map. The 410-km and the 660-km discontinuities are shown in black solid lines. The thick black lines on the surface denote land areas. The red triangles denote active volcanoes. The thin black lines on the inset map denote the plate boundaries.

Figure S55. The same as Figure S54 but along 15 profiles in the E-W direction.

Figure S56. The same as Figure S54 but along 15 profiles in the NW-SE direction.

Figure S57. The same as Figure S54 but along 15 profiles in the NE-SW direction.

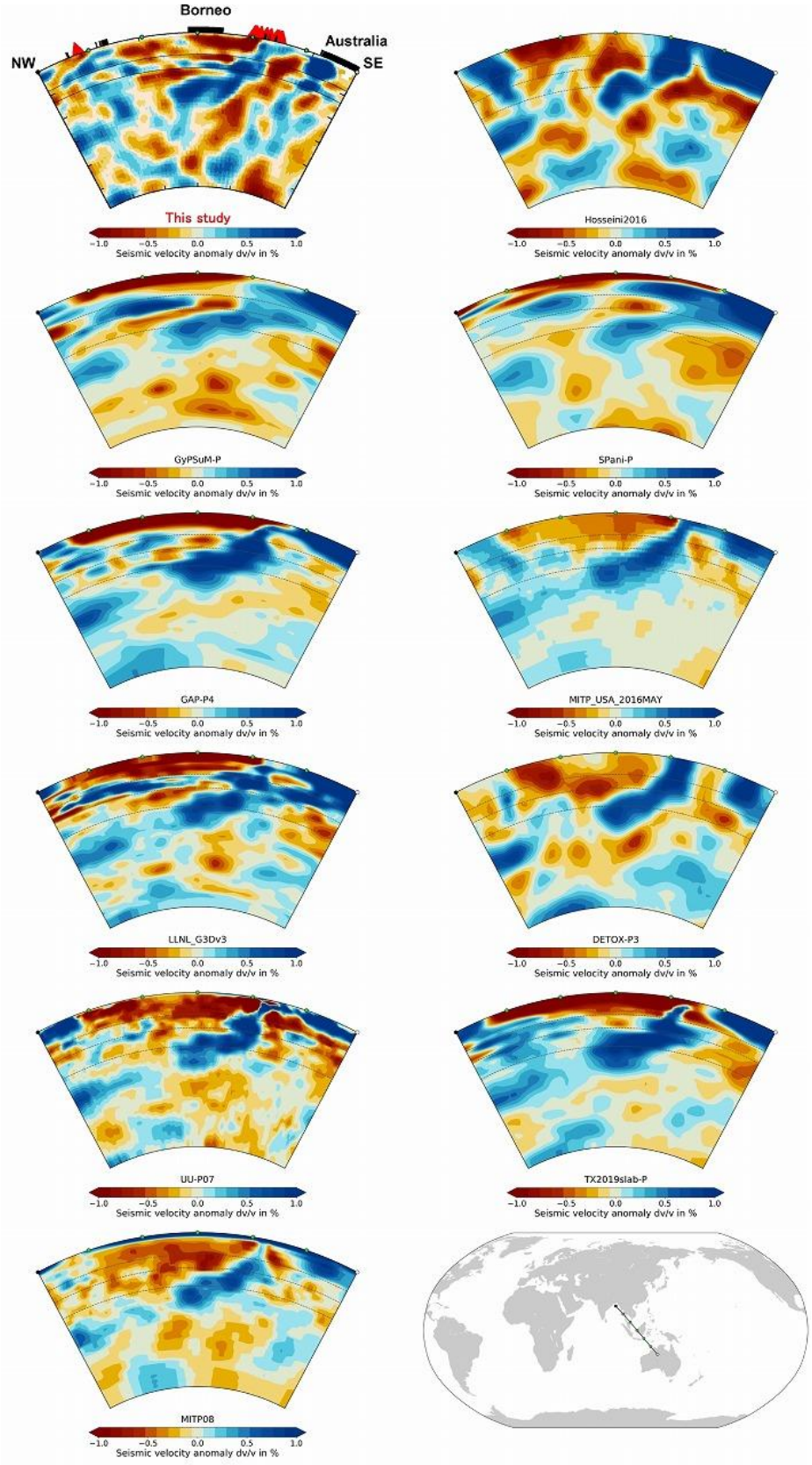
Borneo
NW
Australia
SE
This study
Hosseini2016
GyPSuM-P
SPani-P
GAP-P4
MITP_USA_2016MAY
LLNL_G3Dv3
DETOX-P3
UU-P07
TX2019slab-P
MITP08
−1.0 −0.5 0.0 0.5 1.0
Seismic velocity anomaly dv/v in %

Figure S58.

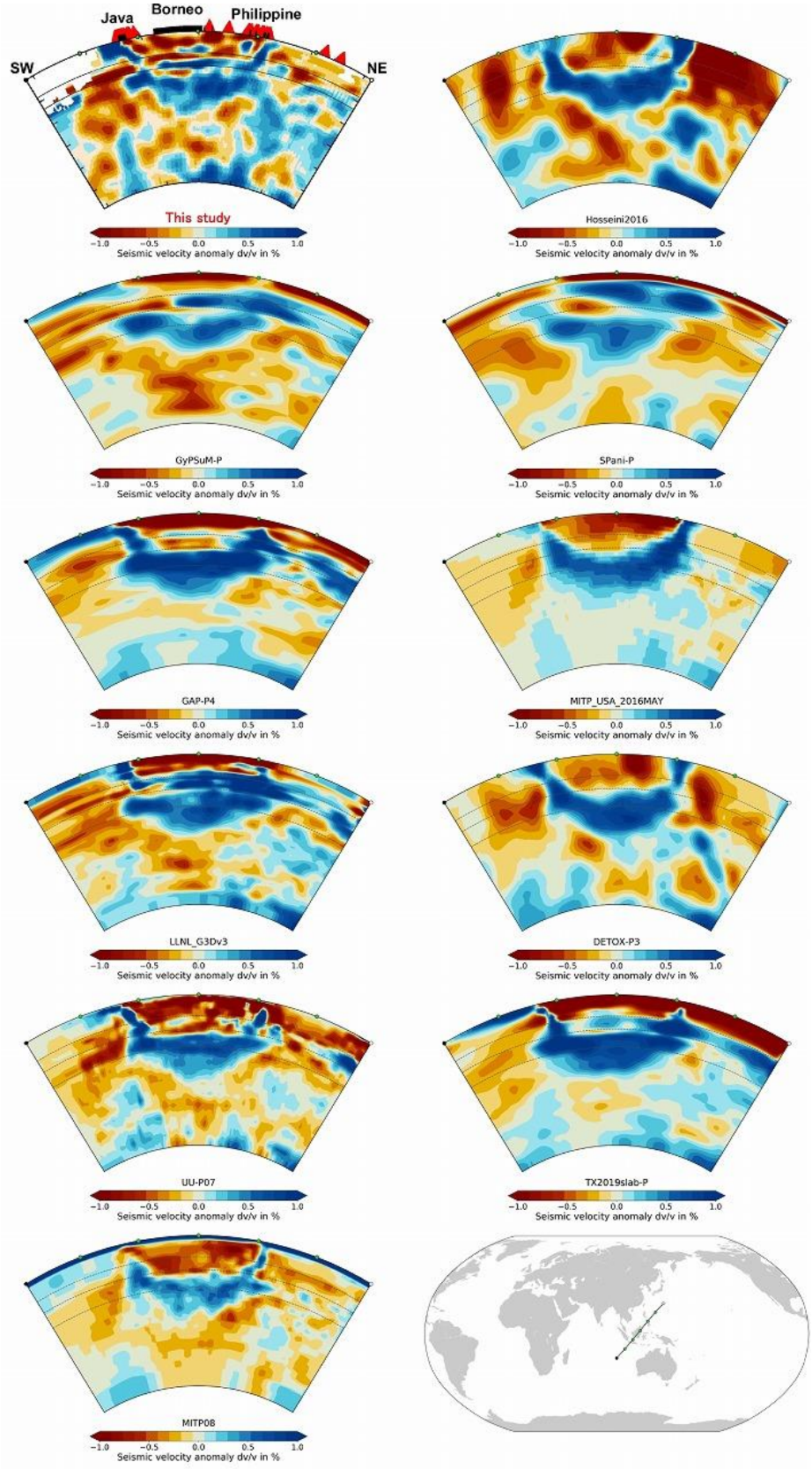

363 **Figure S59**.

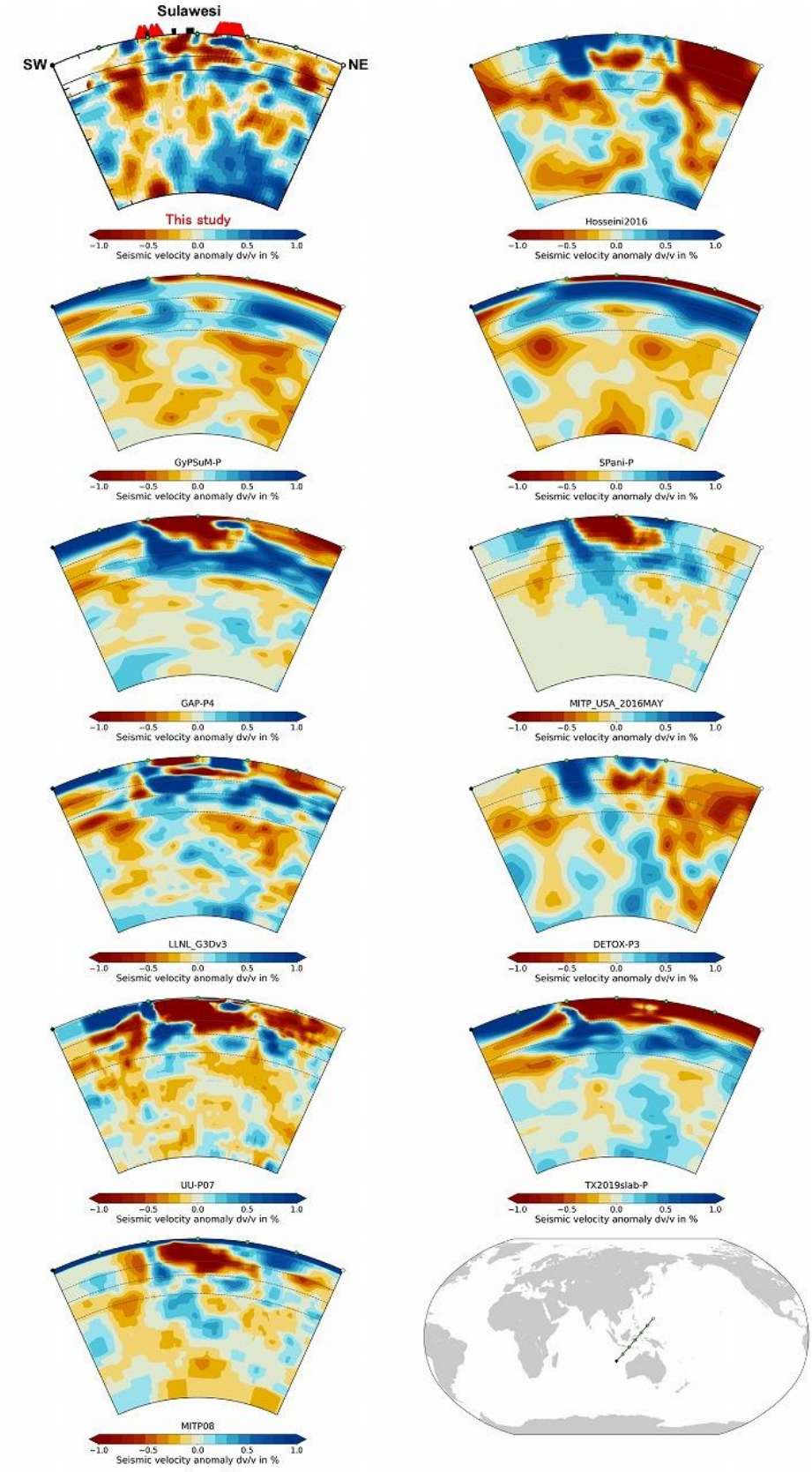
Sulawesi
SW
NE
This study
Hosseini2016
GyPSuM-P
SPani-P
GAP-P4
MITP_USA_2016MAY
LLNL_G3Dv3
DETOX-P3
UU-P07
TX2019slab-P
MITP08
−1.0 −0.5 0.0 0.5 1.0
Seismic velocity anomaly dv/v in %

Figure S60.

Figure S58. Comparison of a Vp cross-section oriented in the NW-SE direction through Borneo and Australia obtained by this study (upper left) with 10 existing models, i.e., UU-P07 (Amaru, 2007), MITP08 (Li et al., 2008), GyPSuM-P (Simmons et al., 2010), LLNL_G3Dv3 (Simmons et al., 2012), GAP-P4 (Fukao & Obayashi, 2013; Obayashi et al., 2013), SPani-P (Tesoniero et al., 2015), Hosseini2016 (Hosseini, 2016), MITP_USA_2016MAY (Burdick et al., 2017), TX2019slab-P (Lu et al., 2019), and DETOX-P3 (Hosseini et al., 2020). All the images are shown with the same color scale. The blue and red colors denote high and low Vp perturbations, respectively, whose scale (in %) is shown below each panel.

Figure S59. The same as Figure S58 but for a Vp cross-section oriented in the NE-SW direction through Java, Borneo, and Philippines.

Figure S60. The same as Figure S58 but for a Vp cross-section oriented in the NE-SW direction through Sulawesi.

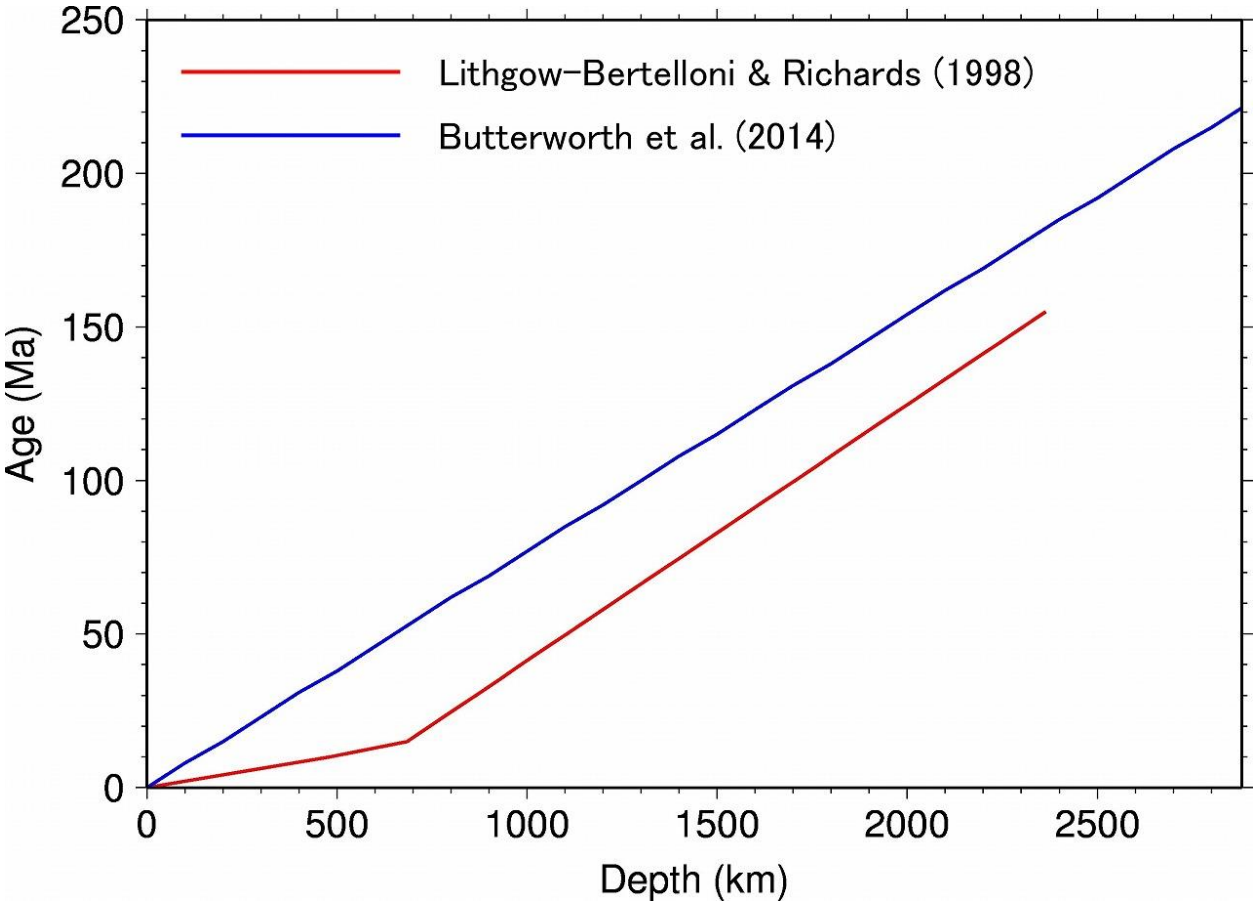

Figure S61. The age-depth relationships of a subducted slab obtained by (red) Lithgow-Bertelloni & Richards (1998) and (blue) Butterworth et al. (2014). We note that the relationship by Butterworth et al. (2014) only holds for the lower mantle.

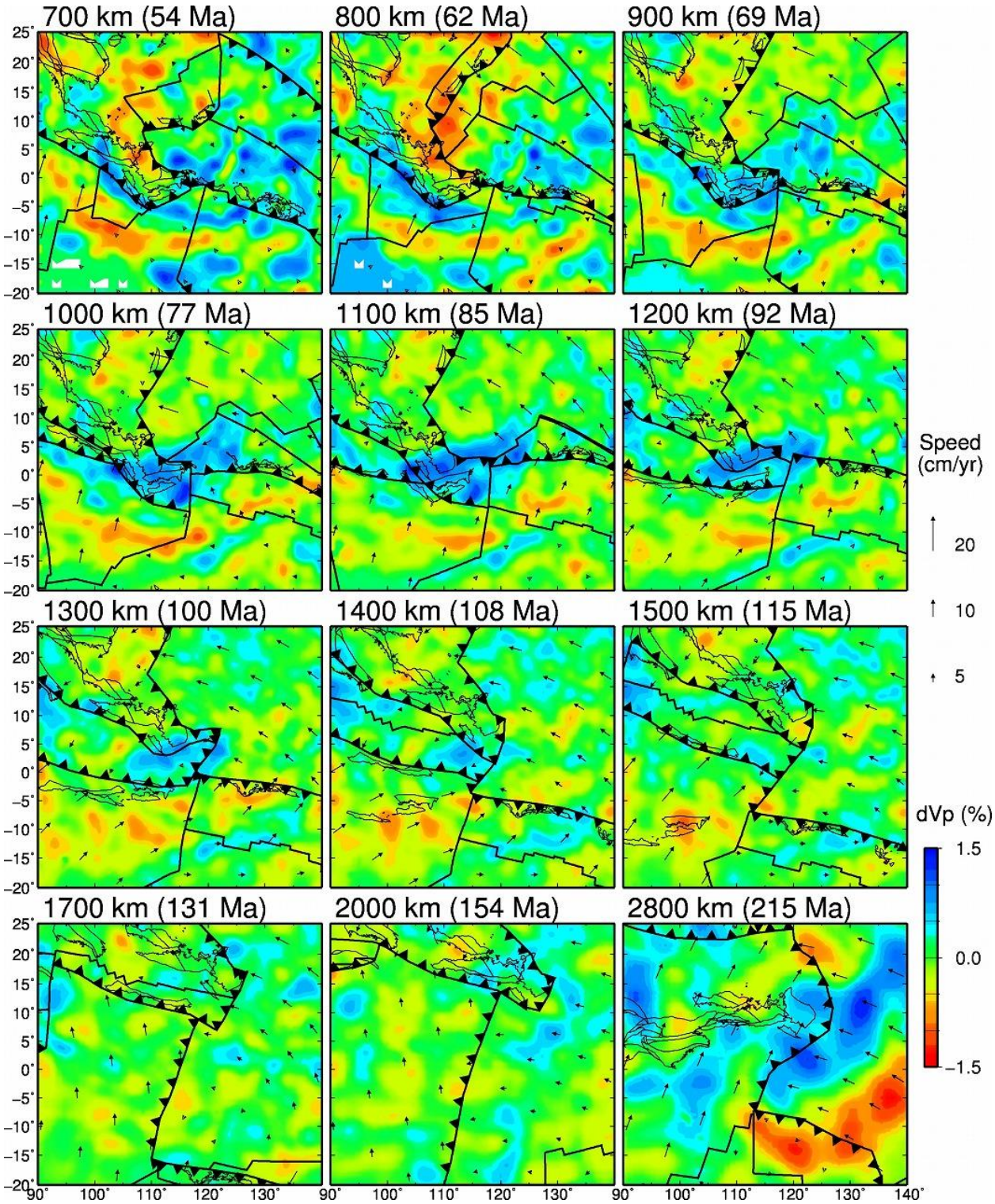

Figure S62. The same as Figure 14 but for the age-depth relationship by Butterworth et al. (2014).

Table S1. Number of grid nodes at each depth, which are arranged for conducting the tomographic inversion.

Depth (km)	The number of grids
15.0	18,717
32.5	8,929
50.0	18,612
75.0	8,751
100.0	18,284
140.0	8,679
180.0	17,848
220.0	8,370
260.0	17,388
300.0	8,185
340.0	16,992
380.0	7,976
420.0	16,580
460.0	7,786
500.0	15,961
575.0	7,451
650.0	15,101
725.0	7,093
800.0	14,425
875.0	6,741
950.0	13,711
1025.0	6,389
1100.0	12,989
1200.0	6,015
1300.0	12,001
1400.0	5,570
1500.0	11,055
1600.0	5,124
1700.0	10,158
1800.0	4,700
1900.0	9,434
2000.0	4,300
2100.0	8,597
2200.0	3,913
2300.0	7,796
2425.0	3,509
2550.0	6,794
2675.0	3,117
2800.0	6,018
Total	391,059

406 **Table S2**. Number of grid nodes at each depth for the checkerboard resolution test with a lateral
407 grid interval of 278 km inside the target region (CRT1).

Depth (km)	The number of grids
15.0	1,964
32.5	393
50.0	1,954
75.0	391
100.0	1,946
140.0	389
180.0	1,887
220.0	383
260.0	1,866
300.0	376
340.0	1,841
380.0	351
420.0	1,724
460.0	346
500.0	1,703
575.0	339
650.0	1,642
725.0	313
800.0	1,533
875.0	306
950.0	1,466
1025.0	300
1100.0	1,366
1200.0	272
1300.0	1,300
1400.0	265
1500.0	1,183
1600.0	231
1700.0	1,107
1800.0	214
1900.0	1,003
2000.0	203
2100.0	948
2200.0	185
2300.0	853
2425.0	175
2550.0	732
2675.0	148
2800.0	666
Total	34,264

408

409

Table S3. Number of grid nodes at each depth for the checkerboard resolution test with a lateral grid interval of 167 km inside the target region (CRT2).

Depth (km)	The number of grids
15.0	5,404
32.5	1,048
50.0	5,373
75.0	1,035
100.0	5,328
140.0	1,029
180.0	5,217
220.0	982
260.0	5,013
300.0	969
340.0	4,883
380.0	959
420.0	4,822
460.0	908
500.0	4,659
575.0	897
650.0	4,366
725.0	839
800.0	4,224
875.0	794
950.0	3,976
1025.0	770
1100.0	3,745
1200.0	722
1300.0	3,466
1400.0	667
1500.0	3,185
1600.0	614
1700.0	2,921
1800.0	566
1900.0	2,774
2000.0	520
2100.0	2,527
2200.0	475
2300.0	2,288
2425.0	431
2550.0	1,968
2675.0	385
2800.0	1,724
Total	92,473